UNIVERSIDAD DE MURCIA

ESCUELA INTERNACIONAL DE DOCTORADO

TESIS DOCTORAL

ROLE OF OXIDATIVE STRESS IN MELANOMA AND STEATOHEPATITIS/RELEVANCIA DEL ESTRÉS OXIDATIVO EN EL MELANOMA Y LA ESTEATOHEPATITIS

D.ª Irene Pardo Sánchez

2023

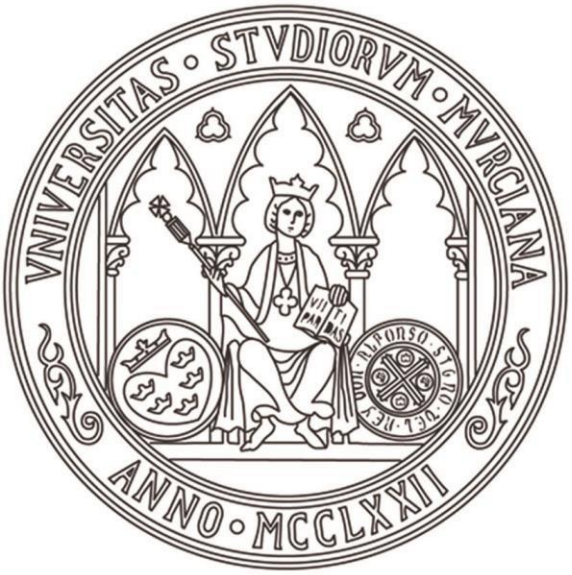

UNIVERSIDAD DE MURCIA

ESCUELA INTERNACIONAL DE DOCTORADO

TESIS DOCTORAL

ROLE OF OXIDATIVE STRESS IN MELANOMA AND STEATOHEPATITIS/RELEVANCIA DEL ESTRÉS OXIDATIVO EN EL MELANOMA Y LA ESTEATOHEPATITIS

Autor: D.ª Irene Pardo Sánchez

Director/es: D. Victoriano Mulero Méndez y D.ª Diana García Moreno

UNIVERSIDAD DE MURCIA

DECLARACIÓN DE AUTORÍA Y ORIGINALIDAD DE LA TESIS PRESENTADA PARA OBTENER EL TÍTULO DE DOCTOR

Aprobado por la Comisión General de Doctorado el 19-10-2022

D./Dña. Irene Pardo Sánchez

doctorando del Programa de Doctorado en

Biología Molecular y Biotecnología

de la Escuela Internacional de Doctorado de la Universidad Murcia, como autor/a de la tesis presentada para la obtención del título de Doctor y titulada:

ROLE OF OXIDATIVE STRESS IN MELANOMA AND STEATOHEPATITIS (RELEVANCIA DEL ESTRÉS OXIDATIVO EN EL MELANOMA Y LA ESTEATOHEPATITIS)

y dirigida por,

D./Dña. Victoriano Mulero Méndez

D./Dña. Diana García Moreno

D./Dña.

DECLARO QUE:

La tesis es una obra original que no infringe los derechos de propiedad intelectual ni los derechos de propiedad industrial u otros, de acuerdo con el ordenamiento jurídico vigente, en particular, la Ley de Propiedad Intelectual (R.D. legislativo 1/1996, de 12 de abril, por el que se aprueba el texto refundido de la Ley de Propiedad Intelectual, modificado por la Ley 2/2019, de 1 de marzo, regularizando, aclarando y armonizando las disposiciones legales vigentes sobre la materia), en particular, las disposiciones referidas al derecho de cita, cuando se han utilizado sus resultados o publicaciones.

Si la tesis hubiera sido autorizada como tesis por compendio de publicaciones o incluyese 1 o 2 publicaciones (como prevé el artículo 29.8 del reglamento), declarar que cuenta con:

- *La aceptación por escrito de los coautores de las publicaciones de que el doctorando las presente como parte de la tesis.*
- *En su caso, la renuncia por escrito de los coautores no doctores de dichos trabajos a presentarlos como parte de otras tesis doctorales en la Universidad de Murcia o en cualquier otra universidad.*

Del mismo modo, asumo ante la Universidad cualquier responsabilidad que pudiera derivarse de la autoría o falta de originalidad del contenido de la tesis presentada, en caso de plagio, de conformidad con el ordenamiento jurídico vigente.

En Murcia, a 20 de febrero de 2023

Fdo.: Irene Pardo Sánchez

Esta DECLARACIÓN DE AUTORÍA Y ORIGINALIDAD debe ser insertada en la primera página de la tesis presentada para la obtención del título de Doctor.

Información básica sobre protección de sus datos personales aportados	
Responsable:	Universidad de Murcia. Avenida teniente Flomesta, 5. Edificio de la Convalecencia. 30003; Murcia. Delegado de Protección de Datos: dpd@um.es
Legitimación:	La Universidad de Murcia se encuentra legitimada para el tratamiento de sus datos por ser necesario para el cumplimiento de una obligación legal aplicable al responsable del tratamiento. art. 6.1.c) del Reglamento General de Protección de Datos
Finalidad:	Gestionar su declaración de autoría y originalidad
Destinatarios:	No se prevén comunicaciones de datos
Derechos:	Los interesados pueden ejercer sus derechos de acceso, rectificación, cancelación, oposición, limitación del tratamiento, olvido y portabilidad a través del procedimiento establecido a tal efecto en el Registro Electrónico o mediante la presentación de la correspondiente solicitud en las Oficinas de Asistencia en Materia de Registro de la Universidad de Murcia

La realización del presente trabajo ha sido posible gracias a la adjudicación de un Contrato Predoctoral de la Asociación Española Contra el Cáncer 2018 y los fondos adjudicados al proyecto del Ministerio de Ciencia e Innovación BIO2017-84702-R.

TABLE OF CONTENTS

ABBREVIATIONS

α-MSH – Alpha Melanocyte Stimulating Hormone

µg – Microgram

µl – Microliter

µm – Micrometer

µM – Micromolar

a.u. – Arbitrary Units

AASLD – American Association for the Study of Liver Diseases

AGC – Automatic Gain Control

Aifm2 – Apoptosis Inducing Factor Mitochondria Associated 2

AKT – AKT serine/threonine kinase 1

ANOVA – Analysis of Variance

ApoB – Apolipoprotein B

Apoeb – Apolipoprotein Eb zebrafish

ATP – Adenosine Triphosphate

BCA – Bradford Protein Assay

BCAA – Branched-Chain Amino Acids

bp – Base Pairs

BRAF – B-Raf proto-oncogene

CAID – Centro de Apoyo a la Investigación y Desarrollo

CARM – Comunidad Autónoma de la Región de Murcia

CCL – C-C motif Chemokine Ligand

cm – Centimeters

COX-2 – Ciclooxygenase2

CRISPR – Clustered Regularly Interspaced Short Palindromic Repeats

crRNA – CRISPR RNA

CXCL – CXC motif Chemokine Ligand

CXCR – CXC motif Chemokine Receptor

Cyp51 – Cytochrome P450 Family 51

Da – Dalton

DAMPs – Damage-Associated Molecular Patterns

DDA – Data-Dependent Acquisition

DEP – Differentially Expressed Proteins

Dhcr7 – 7-dehydrocholesterol reductase

DHE – Dihydroethidium

DMEM/F12 – Dulbecco's Modified Eagle Medium/Nutrient Mixture F-12

DN – Dominant Negative

DNA – Deoxyribonucleic Acid

dpf – Days Post Fertilization

DRG – Dorsal Root Ganglia

DTT – Dithiothreitol

DUOX1 – Dual Oxidase 1

DUOXA1 – DUOX1 Activator factor

E.g. – for example

ERK – Extracellular Signal-Related Kinase

F – Forward Primer

F1 – Filial 1 (first filial generation)

F2 – Filial 2 (second filial generation)

FAD – Flavin Adenine Dinucleotide

Fas – FS-7-Associated Surface antigen

FBS – Fetal Bovine Serum

Fdft1 – Farnesyl Diphosphate Farnesyltransferase 1 (squalene synthase)

Fdps – Farnesyl Diphosphate Synthase

FFAs – Free Fatty Acids

Fn1 – Fibronectin 1

g – g forze

G-CSF – Granulocyte Colony-Stimulating Factor

GFP – Green Fluorescent Protein

GO – Gene Ontology

GOI – Gene of Interest

GPX – Glutathione Peroxidase

Gy – Gray

h – Hours

HA – Hemagglutinin tag

V5 – V5 tag

HCC – Hepatocellular Carcinoma

HCD – High Cholesterol Diet

HCD – Higher Energy Collision Dissociation

HIF-1 – Hypoxia-Inducible Factor-1

Hmgcs – 3-Hydroxy-3-Methylglutaryl-CoA Synthase

hpf – Hours Post-Fertilization

HPLC-MS – Mass Spectrometry

HRAS – HRas protooncogen

HRP – Horseradish Peroxidase

mM – Milimolar

HSCs – Hepatic Stellate Cells

Hsd17b7 – Hydroxysteroid 17-Beta Dehydrogenase 7

Hsf1 – Heat Shock transcription Factor 1

i.e – *id est*, in other words

ID-1 – DNA binding 1

IDT – Integrated DNA Technologies

IFNγ – Interferon Gamma

Igfsp1 – Insulin-like Growth Factor Binding Protein

IL – Interleukin

IR – Insulin Resistance

IRF8 – Interferon Regulatory Factor

KCs – Kupffer Cells

Lck – Lymphocyte-Specific Protein Tyrosine Kinase

LC-MS/MS – Liquid Chromatography Mass Spectrometry

L-DOPA – 3-4-dihydroxyphenylalanine

LSECs – Liver Sinusoidal Endothelial Cells

m/z – mass/charge number of ions

mA – Miliamperes

MAPK – Mitogen-Activated Protein Kinase

MC1R – Melanocortin 1 Receptor

mcr – MiniCoopR

MEK – MAP Kinase Kinase

mg – Milligrams

min – Minutes

MITF - Microphthalmia-Associated Transcription Factor

Mk – Molecular Weight Markers

ml – Millilitres

mm – Millimeters

MoMFs – Monocyte-derived Macrophages

MPO – Myeloperoxidase

mRNA – Messenger Ribonucleic Acid

Mvd – Mevalonate Decarboxylase

Mvk – Mevalonate Kinase

NAD^+ – Nicotinamide Adenine Dinucleotide

NADPH – Nicotinamide Adenine Dinucleotide Phosphate

NAFL – Non-Alcoholic Fatty Liver

NAFLD –Non-Alcoholic Fatty Liver Disease

NASH –Non-Alcoholic Steatohepatitis

ND –Normal Diet

NF-κB – Nuclear factor kappa-light-chain-enhancer of activated B cells

NF1 – Neurofibromatosis type 1

NHANES - National Health and Nutrition Examination Survey

NK – Natural Killer

nl – Nanoliters

nM – Nanomolar

nm – Nanometers

NOX – NADPH Oxidases

NRAS – NRas protooncogene

ns – non-significant

NT – Notocorde

ORO – Oil Red O

PAGE – Polyacrylamide Gel Electrophoresis

PBS – Phosphate Buffered Saline

PCA – Principal Component Analysis

PCR – Polymerase Chain Reaction

PDX – Patient-Derived Xenograft

PFA – Paraformaldehyde

pg – Picograms

PGE2 – Prostaglandin E2

PI3K – Phosphatidylinositol 3-Kinase

Pltp – Plasma Phospholipid Transfer Protein

pm – Picometers

PPAR – Peroxisome Proliferator-Activated Receptors

prkdc – DNA-dependent Protein Kinase catalytic subunit

PRX – Peroxiredoxins

PTEN – Phosphatase and Tensin homolog

Pmvk – Phosphomevalonate Kinase

R – Reverse primer

RAF – Rapidly Accelerated Fibrosarcoma

RAS – Rat Sarcoma virus

RNS – Reactive Nitrogen Species

ROI – Region Of Interest

ROS – Reactive Oxygen Species

RT – Room Temperature

SDS – Sodium Dodecyl Sulfate

SEER – Surveillance, Epidemiology, and End Results

SEM – Standard Error of Mean

SG – Sympathetic Ganglia

SKCM – Skin Cutaneous Melanoma

Soat2 – Sterol-O-Acetyltransferase

Spint1a – Serine Peptidase Inhibitor Kunitz Type 1a

SPRED1 – Sprouty Related EVH1 Domain Containing 1

SULT2B1b – Sulfotransferase

TAMs – Tumor Associated Macrophages

TANs – Tumor Associated Neutrophils

TCGA – The Cancer Genome Atlas

TEAB – Triethylammonium Bicarbonate Buffer

TFA – Trifluoroacetic Acid

TG – Tryglicerides

TGF – Transforming Growth Factor

TNF – Tumor Necrosis Factor

TNFR1 – Tumor Necrosis Factor Receptor 1

TP53 – Tumor Protein 53

tracrRNA – trans-activating CRISPR RNA

TRAIL-R1 – TNF-Related Apoptosis-Inducing Ligand Receptor 1

TRAIL-R2 – TNF-Related Apoptosis-Inducing Ligand Receptor 2

Tregs – T regulatory cells

TRP – Tyrosinase-related protein

TRX – Thioredoxin

U – Units

UMU – University of Murcia

UV – Ultraviolet

UVR – Ultraviolet Radiation

V – Volts

VEGF – Vascular Endothelial Growth Factor

VLCFA – Very Long Chain Fatty Acids

VLDL – Very Low-Density Lipoprotein

WHO - World Health Organization

wpt – Weeks Post Transplantation

WT – Wild Type

XDH – Xanthine dehydrogenase

XO – Xanthine Oxidase

XOR – Xanthine Oxidoreductase

ZIRC – Zebrafish International Resource Center

ZMEL1 – Zebrafish Melanoma cell line 1

zWEDGI – Wounding and Entrapment Device for Imaging Live Zebrafish Larvae

LIST OF TABLES & FIGURES

SUMMARY

During the development of this Thesis, we used zebrafish models to study the impact of Dual Oxidase 1 (Duox1) and Xanthine dehydrogenase (Xdh), two major oxidative stress contributing enzymes, during the progression of melanoma and steatohepatitis.

In the first chapter, we report a dual role of DUOX1 in melanoma. We found that high, but not low, *DUOX1* transcript levels in early melanoma are associated with poor patient survival, while no statistically significant differences in patient survival were observed in late melanoma. In addition, altered signaling pathways involved in immune system, complement activation and allograft rejection were observed in melanoma expressing low levels of *DUOX1*, suggesting the importance of oxidative stress balance in melanoma progression. Although we did not find any significant effect of this enzyme in melanocyte transformation and early melanoma progression, allotransplantation experiments in immunocompromised zebrafish recipients revealed that Duox1-deficient melanoma cells showed decreased growth but, paradoxically, generated more metastasis than control. The relevance of DUOX1 in melanoma and in skin chronic inflammatory diseases, point to DUOX1 as a pharmacological target. So, we generated a melanoma cell line that overexpresses both DUOX1 and its maturation factor DUOXA1, to perform pharmacological screening to find specific activators or inhibitors of this enzyme. Among 256 FDA/EMA-approved drugs, we identified several promising candidates that required validation.

In the second chapter, we studied the role played by Xdh in steatohepatitis development. We observed accumulation of lipids and increased reactive oxygen species (ROS) production in the liver of larvae fed with high cholesterol diet (HCD), concomitant with liver histological features related with Non-Alcoholic Fatty Liver Disease/Non-Alcoholic Steatohepatitis (NAFLD/NASH) in humans, such as accumulation of lipid droplets and ballooning of hepatocytes. Proteomic analysis of livers of wild type larvae fed with HCD showed downregulation of several enzymes which participates in the cholesterol and lipid biosynthesis pathways. Importantly, Xdh deficiency ameliorated the progression of the disease by decreasing all these pathological alterations associated to NASH progression. One of the most interesting observations of our study is that Xdh deficiency was able to ameliorate NASH

progression in larvae fed with HCD and, concomitantly, to promote the downregulation of lipid metabolic pathways, including fatty acid degradation, retinol metabolism and glycerolipid metabolism, and the upregulation of oxidative phosphorylation. Overall, all these results support that Xdh is involved in NAFLD disease progression, explaining the association found between XDH and NAFLD in several clinical studies, and point out to the relevance of the zebrafish larval model fed with HCD to identify novel signaling pathways associated with NAFLD/NASH in humans.

INTRODUCTION

1. THE SKIN

The skin is the first defensive barrier between the environment and an organism. Its main function is to protect from external factors as: temperature, pathogens or chemicals, acting as a physical and biological barrier. At the same time, it maintains internal homeostasis and prevents the loss of water. The skin could be divided into 3 layers from outside to inside: epidermis, dermis and hypodermis (Figure 1).

- Epidermis: it is the outer layer of the skin and it is formed by four main types of cells: keratinocytes, which are the most abundant cell type in the skin and produce keratin; Langerhans cells, which are involved in the epidermal immune response; Merkel cells, which contact sensitive neurons and are key in the sense of touch; and melanocytes that produce melanin and provide keratinocytes to protect the DNA from ultraviolet radiation (UVR). This layer acts as a protective barrier preventing external agents like bacteria and germs, from entering in the bloodstream and causing infections.
- Dermis: it is the middle layer and the thickest layer of the skin. It contains hair follicles, sweat glands, fibroblast, nerves, touch receptors, blood and lymph vessels. This skin layer is held by the collagen which gives flexibility and strength.
- Hypodermis: it is the bottom layer, it is also called the subcutaneous fat layer. It is formed by collagen and adipocytes. Its main function is to conserve body´s heat and protect from injury.

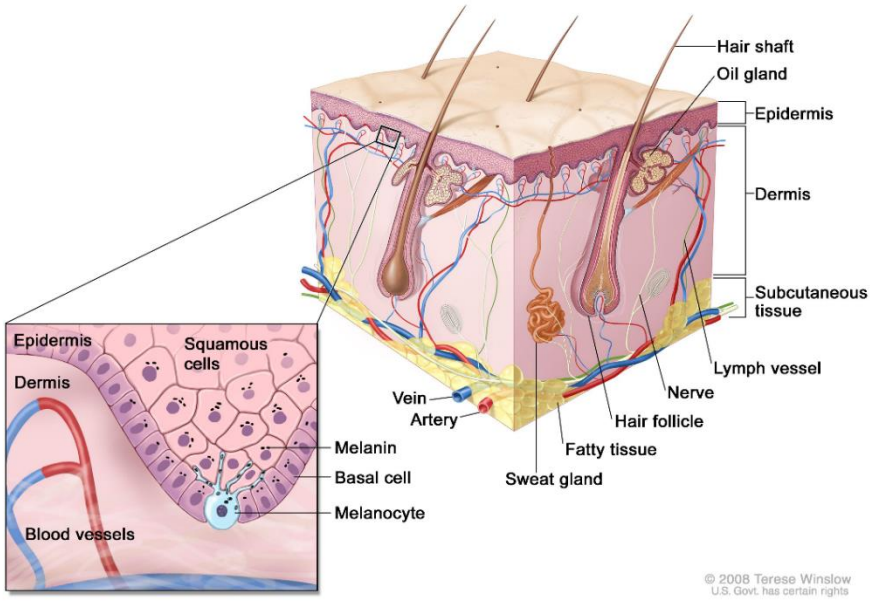

Figure 1: Representative image of the anatomy of the skin showing the three layers of the skin. Melanocytes are located in the deepest part of the epidermis. https://www.cancer.gov/publications/dictionaries/cancer-terms/def/melanocyte

1.1 MELANOCYTES & MELANIN

The skin is constantly exposed to UV light, this environmental factor could lead to damage cells and could induce mutagenesis. So, the main function of pigmentation in the skin is protection from UVR. The main pigment responsible of the protection is the melanin which is produced by melanocytes. These cells are responsible for skin and hair pigmentation, and they are located in the basal layer of the epidermis. People with more melanin have darker skin and may tan quickly (Lin & Fisher 2007).

Melanocytic development begins with the migration of the melanoblast from the neural crest during embryogenesis (Figure 2). Commitment of neural crest cells to the melanogenic lineage originate the melanoblasts. These cells can migrate to various destination sites, differentiate to melanogonia and finally to mature melanocytes (Sulaimon & Kitchell 2003).

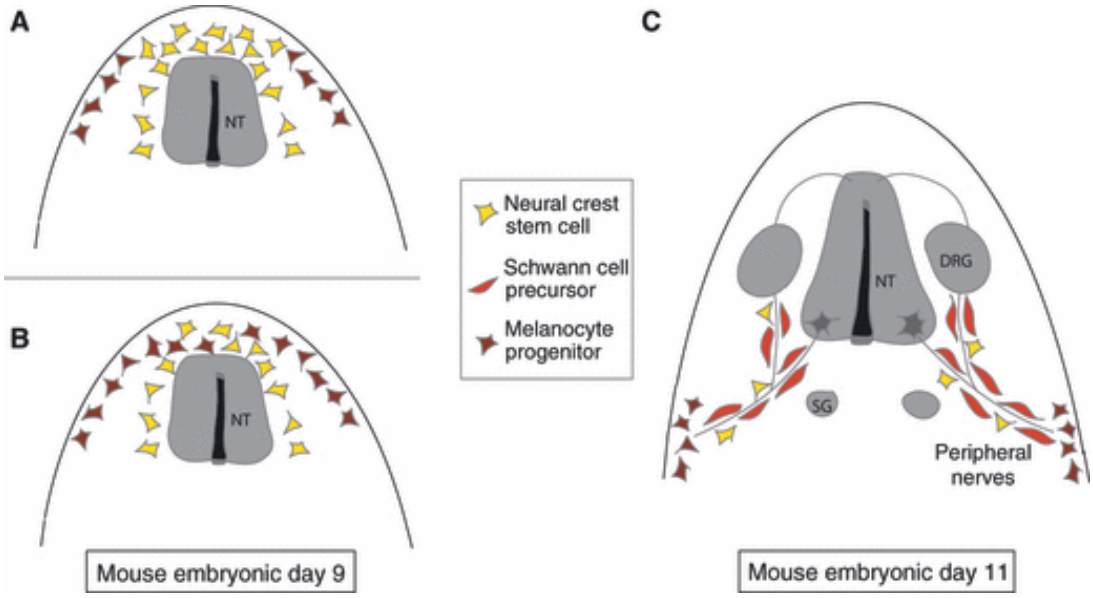

Figure 2: Melanocyte derived from neural crest cells in mouse. Melanocytes are generated either directly from the neural crest (A,B) or indirectly from nerve cells (C) (Sommer 2011). NT: notocorde, DRG: dorsal root ganglia, SG: sympathetic ganglia.

In the basal layer of the epidermis, the dendritic processes of differentiated melanocytes are combined with neighboring keratinocytes. Contact between the dendrites of melanocytes and keratinocytes is essential for the transfer of melanin-containing granules known as melanosomes. In humans, one epidermal melanocyte makes contact with approximately 30–40 keratinocytes (Scott 2014). This association enables the melanocytes to transfer melanin into the surrounding keratinocytes, where most pigmentation is shown, and helps protecting against damage from UVR. Epidermal melanocytes and keratinocytes constitute what is known as the "epidermal melanin unit" (Sulaimon & Kitchell 2003).

Synthesis of melanin in melanocytes takes place within highly specialized membrane bound intracellular organelles called melanosomes. Melanin synthesis results in the generation of hydrogen peroxide and quinone intermediates. These intermediates, if inappropriately processed, can damage cells (Meyskens et al. 2001, Nappi & Vass 1996). To avoid the interaction with other cytosolic components, the process of melanization takes place in the melanosomes, membrane delimited structures (Seiji & Fitzpatrick 1961).

Melanosome formation include four stages, which are determined by the quality, quantity, structure and arrangement of the melanin produced (Costin &

Hearing 2007). They are often separated into "early" (stage I and II) and "late" melanosomes (stage II and IV) according to lack or presence of pigment (Figure 3).

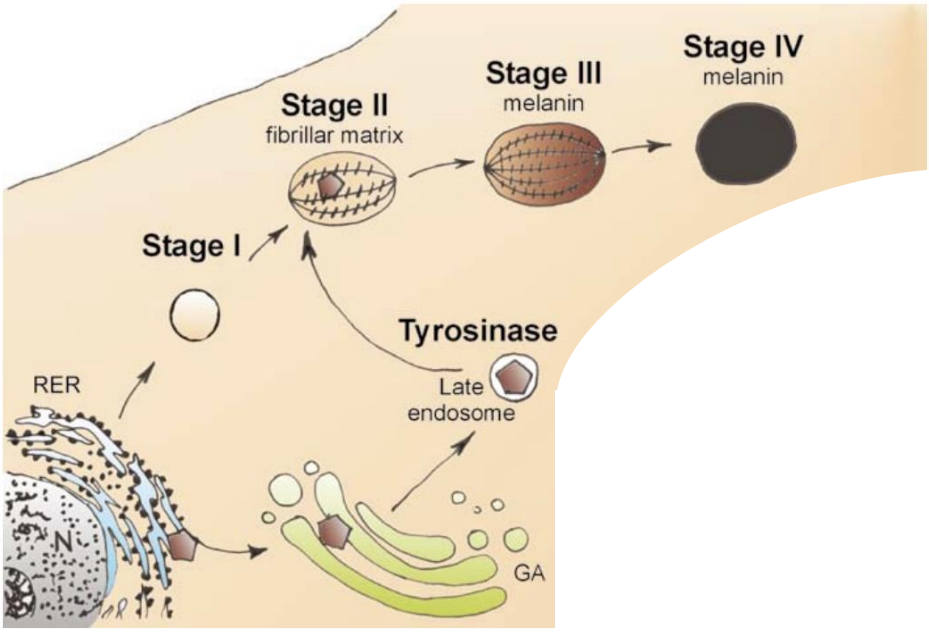

Figure 3: Melanosome formation and maturation. Figure adapted from (Cichorek et al. 2013a).

Pre-melanosomes (Stage I) show the content of proteins derived from the endoplasmic reticulum, coated vesicles, lysosomes and endosomes. These melanosomes are spherical vacuoles with no internal structural components. In stage II, the fibrillar matrix is formed by glycoproteins, melanosomes elongates and tyrosinase is present, but the synthesis of melanin is not started yet. In stage III, melanosomes produce melanin, by the Raper Mason pathway, that polymerizes and settle on the internal fibrils net. In the last stage, melanin fulfills melanosome. Each type of melanin is synthesized in separated melanosomes (Cichorek et al. 2013b, Costin & Hearing 2007).

Melanosomes produce different kinds of melanin: pheomelanin and eumelanin. Pheomelanin is red to yellow, and it is responsible for red hair. The most abundant form of melanin is eumelanin, a highly heterogenous dark brown to black (Slominski et al. 2004). Melanogenesis requires specific enzymes for melanin synthesis and structural proteins for building the fibrillar stroma for this process in the melanosomes. TYROSINASE is de main rate limiting enzyme, other critical proteins are TYROSINASE-RELATED PROTEIN 1 (TRP1) and 2 (TRP2) (Cichorek et

al. 2013a). The biosynthesis of the different types of melanin is carried out by the Raper-Mason pathway (Figure 4).

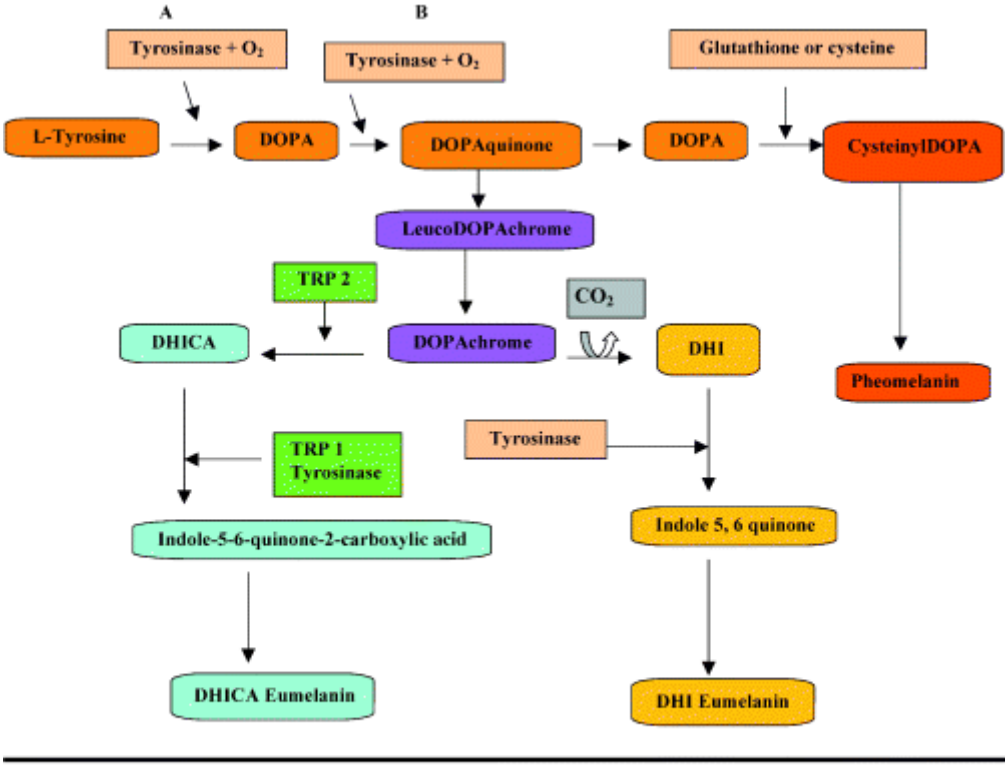

A: Tyrosine hydroxylase, **B:** Tyrosine oxidase, **TRP 1:** DHICA oxidase
TRP2: DOPAchrome tautomerase, **DHICA:** 5, 6-Dihydroxyindole-2-carboxylic acid
DHI: 5, 6-Dihydroxyindole

Figure 4: Raper-Mason pathway to synthetize eumelanin or pheomelanin (Sulaimon & Kitchell 2003).

The first step, common for all melanin types, involve hydroxilation of tyrosine to 3-4-dihydroxyphenylalanine (L-DOPA) and oxidation of L-DOPA to DOPAquinone. The synthesis of both types of melanin is catalyzed by tyrosinase (Park et al. 2009). The availability of substrates and the melanogenic enzyme function determine which type of melanin is produced. The presence of glutathione/ cysteine can induce a switch in the production of eumelanin to pheomelanin (Sonthalia et al. 2016).

The pigmentation is essentially genetically determined, but the skin melanocytes activity is under control of neighboring keratinocytes signals as well as autocrine signals and environmental factors such as UVR. UVR increase the secretion of keratinocyte-derived factors, as well as directly stimulate melanin production and melanocyte dendricity (Cichorek et al. 2013a).

The eumelanin to pheomelanin ratio contributes to the skin pigmentation differences seen in human skin. Individuals with melanocytes that make more pheomelanin tend to have lighter skin, more susceptible to sun burning. Skin with more pheomelanin also produces more reactive oxygen species, which can accelerate carcinogenesis, compared with skin that produces eumelanin or has no melanin. UVR represents the main environmental stimulus leading to intense melanocortin 1 receptor (MC1R) activation in melanocytes, primarily driven by alpha melanocyte stimulating hormone (α-MSH) secretion from keratinocytes, which controls which type of melanin is produced by melanocytes. (Lin & Fisher 2007, Schiaffino 2010). After an exposure to UVR, melanin can produce superoxide radicals that cause lethal cellular injury, but melanin is important for skin homeostasis and tanning indicative of a distress signal (D'Mello et al. 2016).

An excessive melanocyte proliferation produces freckles, nevus, lentigus and others last resort melanoma concluding in melanocytic malignization. In addition, there are others phenotypic manifestations due to the lack of melanocytes, like vitiligo, which is characterized by depigmented areas of the skin and is caused by autoimmune responses or by toxics substances that affect melanocyte development (Rashighi & Harris 2017).

1.2 MELANOMA DEVELOPMENT

Melanoma is the fifth most common cancer and the most serious skin cancer (Siegel et al. 2020). The incidence of malignant melanoma has been increasing worldwide, from being a rare skin cancer one century ago, now it is estimated that in 2021 there will be more than 100,000 new cases of melanoma in the United States and around 7,000 deaths from this disease (Siegel et al. 2021). The development of melanoma is most common in adults with a median age at diagnosis of 65, though it also affects young people (4.8% from 20 to 34 years old).

Nowadays melanoma is considered as a multifactorial disease derived from genetic susceptibility and environmental exposure (Rastrelli et al. 2014). The major environmental risk factor to develop malignant melanoma is the UV exposure and it was demonstrated that a history of sunburn in childhood could be associated with a higher risk of developing melanoma (Elwood & Jopson 1997, Gandini et al. 2005). Notably, the artificial sun exposure as tanning bed sessions may play a role in the

development of melanoma (International Agency for Research on Cancer Working Group on artificial ultraviolet & skin 2007).

Melanoma is caused by the malignant transformation of melanocytes, a type of skin cell that produces melanin to protect against exposure to UV light (Shain & Bastian 2016). In the 1960s, five levels of anatomical invasion of melanoma in the skin were described. The first step of melanoma begins as a proliferation of normal melanocytes to form a nevus, in this level the melanocytes are still confined to the epidermis. Later, the nevus can acquire an atypical growth, and a dysplastic nevus develops. Then, unlimited radial growth begins, followed by a vertical growth phase, which crosses the basement membrane forming a tumor, and finally, successfully spreads throughout the body as metastatic tumors (Amatruda & Patton 2008, Clark et al. 1991) (Figure 5).

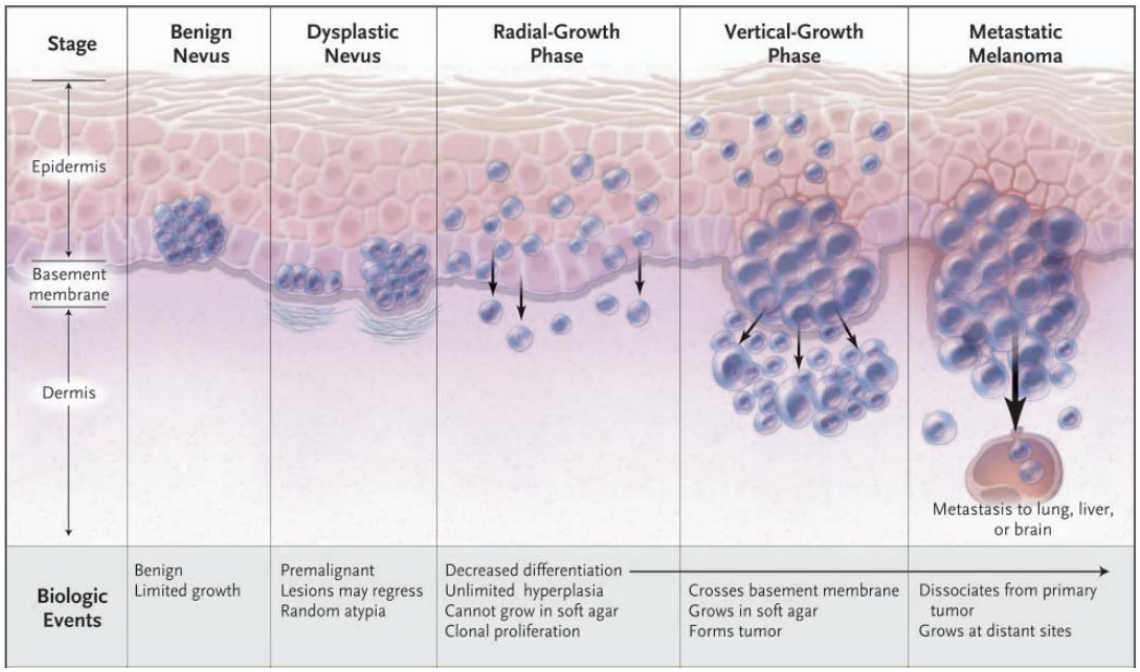

Figure 5: Melanoma progression (Miller & Mihm 2006).

During the radial-growth phase tumor cells acquire the ability to invade the dermis but they do not aggregate forming a nodule. This phase is characterized by a surface spreading of melanoma cells at the level of the basal epidermis (Ciarletta et al. 2011). This step can last for months to more than 10 years. Nodules appear when the lesion is approximately 2.5 cm in diameter (Dinulos 2021). Lesions in this step of melanoma progression are usually linked with a good prognosis (Elder 1999).

The radial growth phase is generally always curable by local excision with rare exceptions (Crowson et al. 2006).

In the vertical growth phase, the cells are able to invade the dermis and form a tumorigenic nodule. The vertical growth phase implies that melanoma becomes biologically capable of migrating and disseminating through the lymphatic system and blood vessels producing metastatic events all over the body (Crowson et al. 2006). The prognosis in vertical growth phase depends on attributes of the tumor and of the host, but generally last phases, especially if it does the first metastasis commonly reappears and becomes incurable or difficult to treat (Markovic et al. 2009).

1.3 MELANOMA DETECTION AND CLASSIFICATION

To early detect melanoma, it is important to know the warning signals (Figure 6). It is important to control the nevus in the skin. The main warning characteristics are summarized by the ABCDE system. A is for Asymmetry. B is for Border (the edges are irregular). C is for Color (if it has multiple colors), D is for Diameter (if the spot is larger than 6mm) and E is for Evolving (if it is changing in size, shape, or color)(Friedman & Rigel 1985).

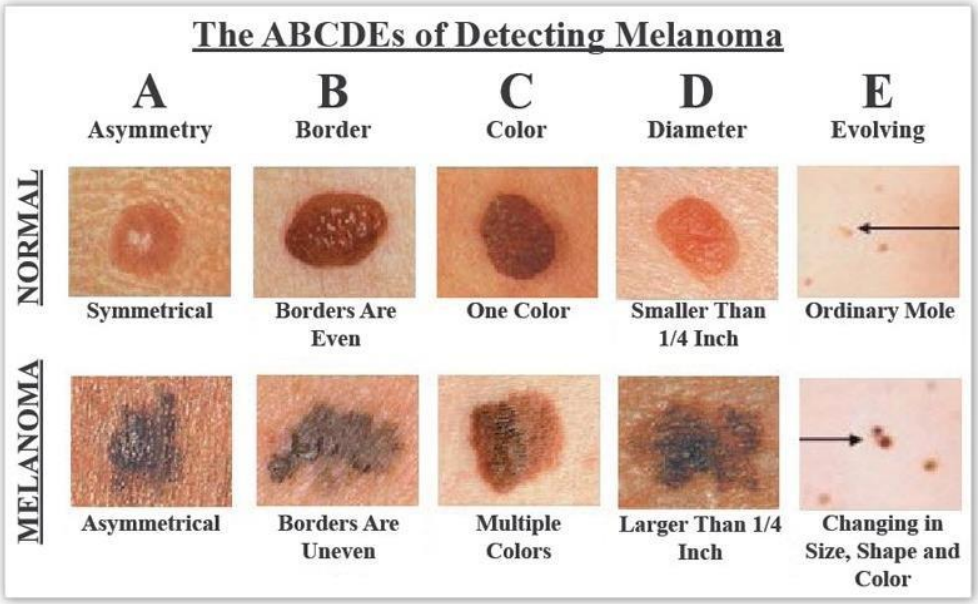

Figure 6: Benign (normal) versus malign (melanoma) pigmentations based on ABCDE method. Adapted from (https://www.cancer.org/cancer/melanoma-skin-cancer/detection-diagnosis-staging/signs-and-symptoms.html).

To classify melanoma two systems are widely used: Clark levels and Breslow index (Table 1). The Clark level system describes the depth of melanoma growth based in how many layers of the skin melanoma has grown into. Breslow index is based the thickness of the lesion (Hasney et al. 2008).

Clark		Breslow
Confined to epidermis	I	<0.75 mm
Invading papillary dermis	II	0.76–1.5 mm
Abutting papillary-reticular junction	III	1.51–4.0 mm
Invading reticular dermis	IV	>4.0 mm
Subcutaneous invasion	V	—

Table 1: Clark and Breslow systems (Hasney et al. 2008).

At present, melanoma relative survival rate after being diagnosed is 93.7% as reported by The Surveillance, Epidemiology, and End Results (SEER) program from the American Cancer Society. Most melanoma lesions (81.6%) are diagnosed when only the epidermis, the most external layer of skin, is affected. These lesions could be cured with surgery, and the 5-year survival rate is very encouraging over 99 % (localized). However, when a melanoma involves multiple layers of skin, it can spread to other parts of the body and metastasize (Shain & Bastian 2016). If the melanoma has spread to the lymphatic nodes (regional), the 5-year survival decreases to near 70%, and if the melanoma has spread through the bloodstream to distant parts of the body, the survival rate is even lower, around 30% (distant) (Siegel et al. 2020) (Figure 7). This fact highlights the importance of early detection in melanoma.

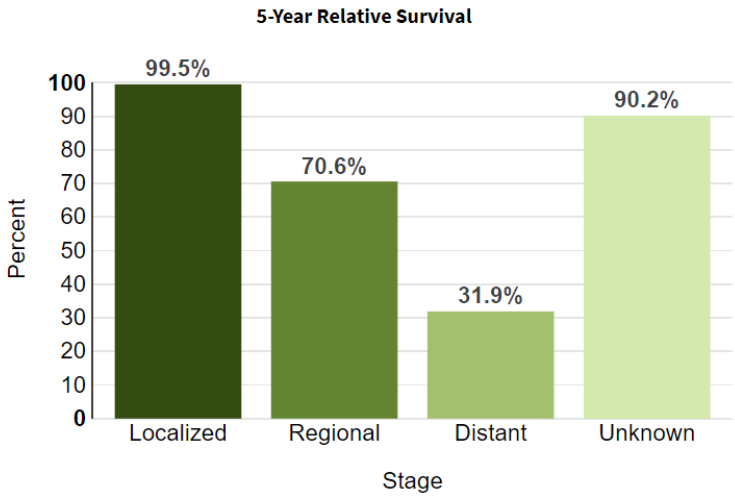

Figure 7: Five-year survival rate per melanoma stages. Data consulted at: https://seer.cancer.gov/statfacts/html/melan.html data from (Siegel et al. 2020).

Melanoma incidence changes with age and sex. Under 50 years melanoma incidence is very low, from 50-64 it increases, but increase after 65 years old is dramatical (Figure 8). Sex also affects to melanoma incidence; women developed less melanoma than man (Figure 9).

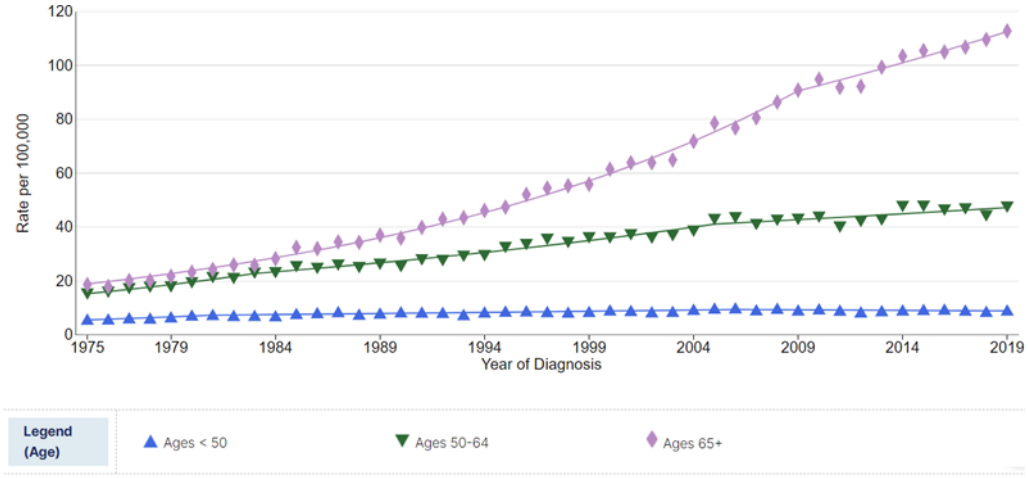

Figure 8: Long-Term Trends in SEER Age-Adjusted Incidence Rates of melanoma of the skin, 1975-2019 comparing age. Under 50 years (blue), from 50-64 (green), after 65 years old (pink). Data available at: https://seer.cancer.gov/statistics-network/explorer/application.html?site=53&data_type=1&graph_type=1&compareBy=age_range&chk_age_range_9=9&chk_age_range_141=141&chk_age_range_157=157&rate_type=1&sex=1&race=1&advopt_precision=1&advopt_show_ci=on&advopt_show_count=on&hdn_view=0&advopt_show_apc=on&advopt_display=2 data from (Siegel et al. 2020).

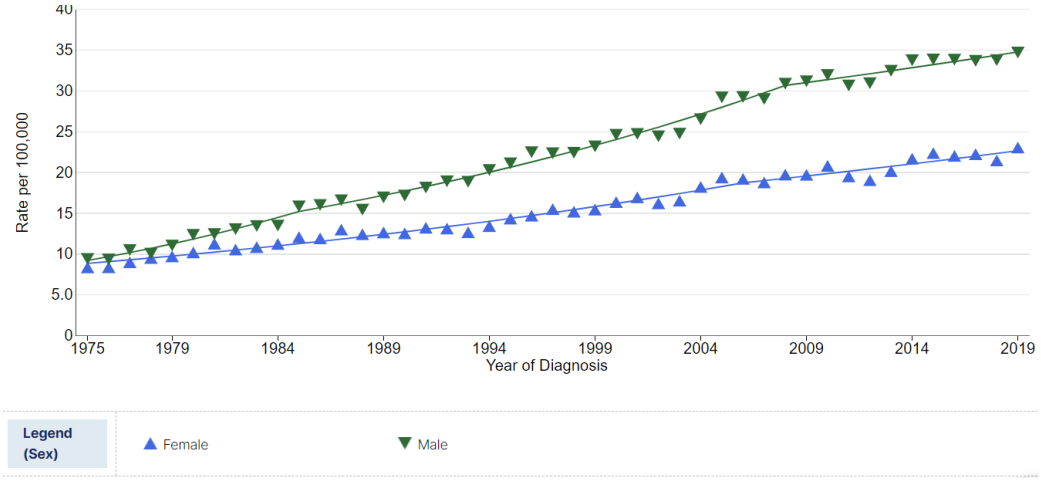

Figure 9: Melanoma of the Skin: Long-Term Trends in SEER Age-Adjusted Incidence Rates, 1975-2019 comparing sex. Women (blue) and man (green). Data available at: https://seer.cancer.gov/statistics-network/explorer/application.html?site=53&data_type=1&graph_type=1&compareBy=sex&chk_sex_3=3&chk_sex_2=2&rate_type=1&race=1&age_range=1&advopt_precision=1&advopt_show_ci=on&advopt_show_count=on&hdn_view=0&advopt_show_apc=on&advopt_display=2#graphArea data from (Siegel et al. 2020).

In Europe, Spain is one of the countries with less incidence and mortality rates. In Spain, is estimated that 7.474 new cases of melanoma would appear in 2022. The most preoccupant fact is that the incidence continues growing. In 2002 the incidence in Spain was 10.8 per 100.000 men and 10.5 per 100.000 women, while in 2022 the incidence has grown to 14.6 per 100.000 in men and 16.3 in women (https://seom.org/notas-prensa/209425-la-incidencia-del-melanoma-aumenta-en-espana-y-llegara-a-7-474-casos-nuevos-en-2022).

Melanoma could appear in different parts of the body, being the most common the areas that have had big exposure to the sun as back, legs, arms, head, neck and ears (Zito & Scharf 2022). But melanoma lesions could rarely appear also in other areas that do not receive sun exposure as in the mouth, palms of the hands, soles of the feet or genital area (Sen et al. 2021, Smith et al. 2020). If melanoma appears in the eye is called uveal melanoma and has different characteristics (Shors et al. 2002).

Currently, melanoma develops due to multifactorial conditions. It is a complex multistep process, and its understanding is crucial (Cooper 2000). This process involves not only the transformation of a cell, but also local tumor invasion,

vascularization, dissemination, tumor establishment in another site and growth of the secondary tumor (Fidler 2003). Melanoma cells should be able to adapt to different microenvironments to invade and metastasize. Crosstalk between multiple pathways points to the importance of understanding the precise role of multiple factors involved in the tumor microenvironment (Brandner & Haass 2013).

1.4 MELANOMA MOLECULAR PATHWAYS

It has been proposed that cutaneous melanoma can be divided into four subtypes according to mutation in the three most prevalent mutated genes: BRAF, NRAS, NF1 and Triple WT (wild type), without mutations in any of these genes (Cancer Genome Atlas 2015). Cutaneous melanomas often harbor BRAF mutations (≈50%) and to a lesser degree NRAS mutations (28%). BRAF is the main oncogene found in both malignant melanoma and in benign nevi. $BRAF^{V600E}$ mutations are present in most nevus, so other lesions would have to occur to develop melanoma. However, this fact points to the important role of this oncogene in melanocyte transformation at early stages.

In melanoma, the RAS-RAF-MEK-ERK (mitogen-activated protein kinase, MAPK) and the PTEN-PI3K-AKT (AKT) signaling pathways are constitutively activated through multiple mechanisms, and play several key roles in the development and progression of melanoma (Meier et al. 2005). Activation of MAPK pathway culminates in the regulation of gene transcription in the nucleus by the extracellular signal-regulated kinase ERK (Figure 10), which phosphorylates several cellular substrates enabling proliferation (Knight & Irving 2014).

NRAS and BRAF molecules belong to the MAPK signal transduction pathway, which play a key role in regulating cell growth, survival, and cell proliferation. In melanocytes, BRAF induces the activation of MEK kinase, which activates ERK, the end effector of the MAPK cascade, via phosphorylation. This results in continuous stimulation of cell proliferation and tumor growth (Palmieri et al. 2015).

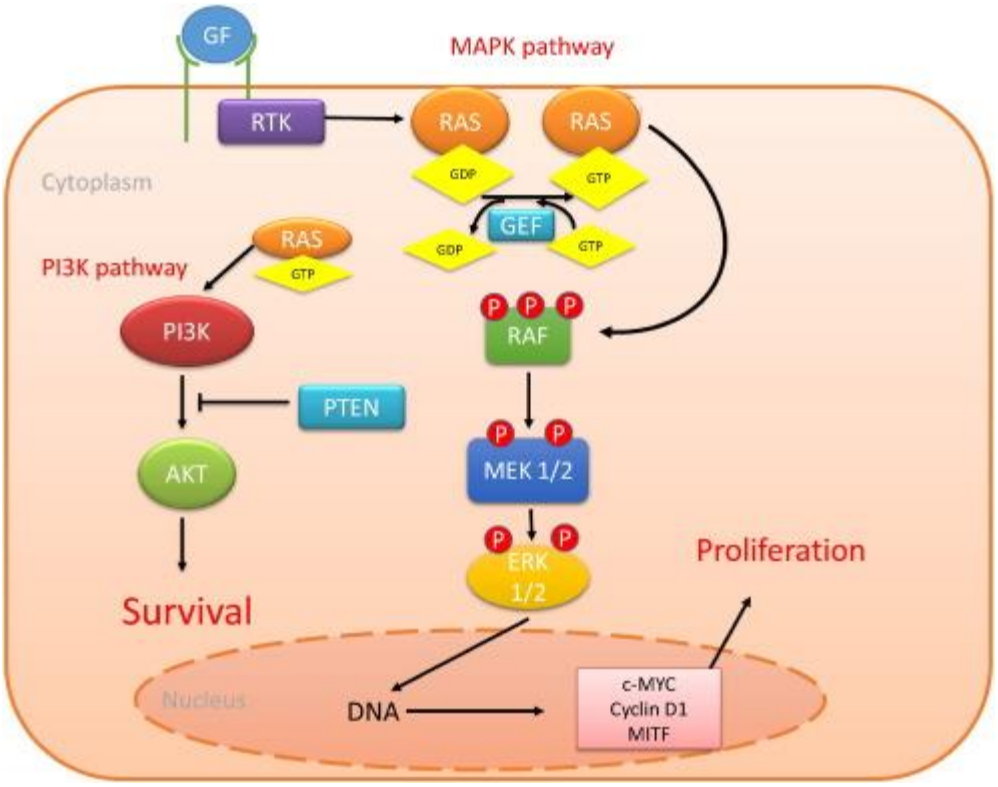

Figure 10: Schematic representation of the MAPK cascades. An extracellular signal (growth factor, GF) interacts with a tyrosine kinase receptor, which stimulates the activity of RAF via the G-protein RAS, which then activates MEK, which activates ERK. ERK phosphorylates several cytosolic and nuclear substrates (Paluncic et al. 2016).

The second major pathway of cell growth regulation is the signal transduction PTEN/PI3K/AKT cascade depending on RAS (Giehl 2005). It has been demonstrated that the activation of AKT results in the development of more metastatic melanomas in mice (Cho et al. 2015). In addition, microphthalmia-associated transcription factor (MITF) is involved in the control of proliferation and differentiation of melanocytes and is also associated with melanoma development and progression (Yajima et al. 2011). In melanoma, constitutive activation of ERK is associated with a marked degradation of MITF (Palmieri et al. 2015). The role of MITF is complex; melanoma cells expressing MITF at a high level can either differentiate or proliferate; however, low activity of MITF is related to stem cell-like or invasive potential (Hartman & Czyz 2015).

2. THE LIVER

The liver is an organ located in the upper-right part of the abdominal cavity. The liver has two large sections, called left and right lobes (Figure 11). The gallbladder sits under the liver, along with parts of the pancreas and intestines. These organs work together to digest and absorb nutrients. The gallbladder is a component of the extrahepatic biliary system where bile is stored and concentrated until needed for digestion. Bile is a fluid formed in the liver that is essential for digesting fats, excreting cholesterol, and even have antimicrobial activity (Jones et al. 2022).

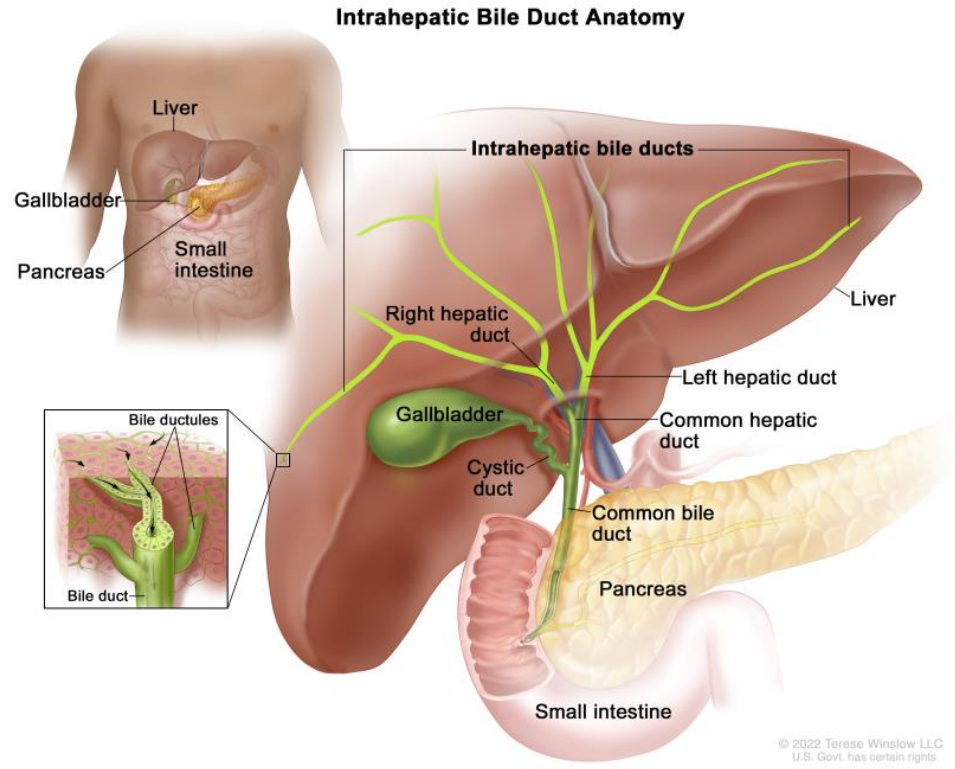

Figure 11: Anatomy of the liver. (https://www.cancer.gov/types/liver/hp/bile-duct-treatment-pdq)

Main functions of the liver are macronutrient metabolism, blood volume regulation, processing of hemoglobin, immune system support, endocrine control of growth signaling pathways, lipid and cholesterol homeostasis, and the breakdown of xenobiotic compounds, including many current drugs (Trefts et al. 2017). The liver can store glucose in the form of glycogen and assemble glucose via the gluconeogenic pathway. Other function is the oxidation of lipids but can also package excess lipid for secretion and storage in other tissues, such as adipose (Trefts et al. 2017).

2.1 NON-ALCOHOLIC FATTY LIVER DISEASE (NAFLD/NASH)

Caloric excess diets and sedentary lifestyle have led to a global epidemic of obesity and metabolic syndrome. The hepatic consequence of metabolic syndrome and obesity is nonalcoholic fatty liver disease (Anstee et al. 2019). Non-alcoholic fatty liver disease (NAFLD) is recognized as the most common liver disease worldwide with a prevalence of 25-30%. About 1.5-6.5% have non-alcoholic steatohepatitis (NASH) which occurs when inflammation is present in the liver. Metabolic comorbidities associated with NAFLD included obesity, type 2 diabetes, hyperlipidemia, hypertension, and metabolic syndrome (Younossi et al. 2016).

Over time, the incidence and prevalence of NAFLD has dramatically increased, in parallel with the global epidemic of obesity and continues growing. Research suggests that NAFLD is present in more than 75% of people who are overweight and in more than 90% of people who have severe obesity (Cotter & Rinella 2020, Machado et al. 2006). In 2016, the World Health Organization (WHO) estimated that more than 107.7 million children and 603.7 million adults were obese. In the United States, data from the National Health and Nutrition Examination Survey (NHANES) for 2017 to 2018 estimated that 42.4% of adults were obese (https://www.cdc.gov/nchs/about/factsheets/factsheet_nhanes.htm) and 18.5% of youth (Hales et al. 2017).

NAFLD is the hepatic manifestation of metabolic syndrome, ranging from simple steatosis (NAFL) to NASH and can progress to fibrosis and hepatocellular carcinoma (HCC) (Kim et al. 2021).

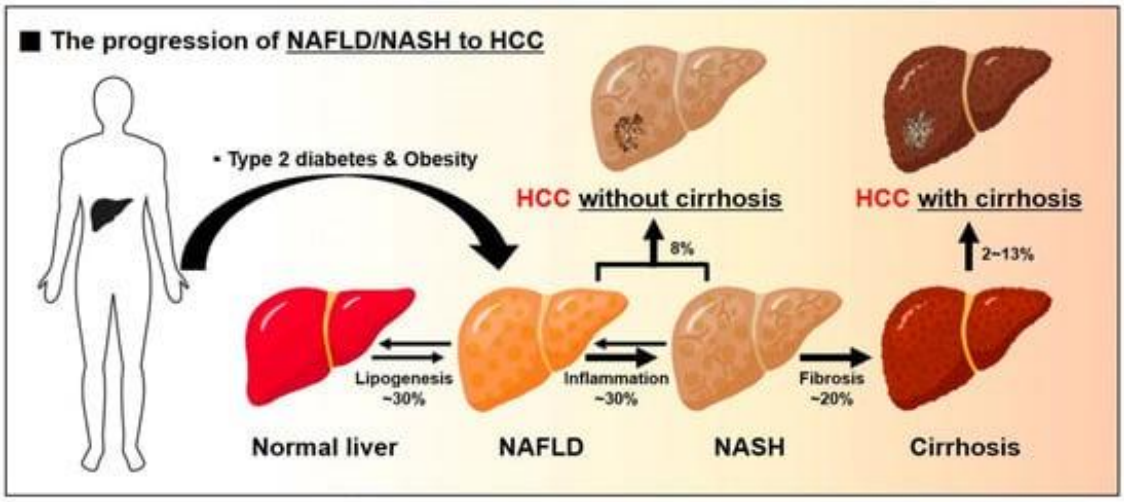

Figure 12: Progression process from a normal liver to developed NAFLD or NASH and finally could produce cirrhosis or hepatocellular carcinoma (Kim et al. 2021).

NAFLD is a group of condition of different histological features which progress with time. Abnormal lipid accumulation in hepatocytes increases oxidative stress and leads to lipotoxicity, which triggers liver inflammation, a hallmark of NAFLD progression to HCC (de Oliveira et al. 2019). NASH is considered the progressive form of NAFLD in which liver steatosis, inflammation, hepatocellular injury and different degrees of fibrosis are present (Schuster et al. 2018).

The development of NASH leads to an increase in morbidity and mortality. NASH may eventually evolve to cirrhosis and HCC; 9–20% of patients with early stage NASH progress to cirrhosis over a period of 5–10 years (Angulo 2002), and some of them develop HCC (5-year cumulative incidence of 20% in patients with late-staged liver fibrosis) (Levene & Goldin 2012, Vernon et al. 2011); HCC can also arise without cirrhosis (Piscaglia et al. 2016) (Figure 12). The pathophysiology of NASH is complex and continues under investigation. There are several mechanisms involved in the pathogenesis of NASH as: an altered gut microbiota, lipotoxicity, insulin resistance, and genetics and dietary factors (Sarwar et al. 2018).

2.2 NASH DEVELOPMENT & CLASSIFICATION

The hepatic accumulation of triglycerides seems to produce a simple hepatic steatosis. Moreover, the accumulation of highly toxic free fatty acids associated with insulin resistance induced by massive free fatty acid mobilization from adipose tissue and the increased de novo hepatic fatty acid synthesis from glucose, acts as the “first hit” that drives to NAFLD development (Bessone et al. 2019).

A “two-hit” strike theory was developed by Day and James (Day & James 1998) to provide a theoretical basis for progression from NAFLD to NASH. The “first hit” is manifested by simple hepatic steatosis. The intake of free fatty acid increases triglyceride biosynthesis, and this leads to fat accumulation in hepatocytes and a consequent increase in insulin resistance. Moreover, the export efficiency of free fatty acids, TGs, and cholesterol is severely reduced. Thus, this forms the “first hit” of NAFLD. Oxidative stress is the initiator of the “second hit” (Ma et al. 2021).

NAFLD progression seems to involve the occurrence of several simultaneous injuries, such as oxidative stress-induced mitochondrial dysfunction, release of inflammatory cytokines, endoplasmic reticulum stress, and iron overload, among many others. These factors are responsible for the triggering of a number of signaling cascades leading to inflammation, cell death, and fibrosis, the hallmarks of NASH (Yilmaz 2012). To classify NAFLD/NASH patients the histopathological abnormalities of NASH were described in the American Association for the Study of Liver Diseases (AASLD) at Clinical Single Topic Conference on NASH held in 2002 (Neuschwander-Tetri & Caldwell 2003). For the diagnosis of NASH, they identified as necessary components: steatosis, lobular inflammation, and hepatocellular ballooning (most apparent near steatotic liver cells). Fibrosis was not necessary for the diagnosis of NASH, although it is usually present (Takahashi & Fukusato 2014).

Histological evaluation remains the most common method used to assess NASH degree development. The Nonalcoholic Steatohepatitis Clinical Research Network define a scoring system definition to group NAFLD/NASH cases. The histological features used were grouped into five categories: steatosis, inflammation, hepatocellular injury, fibrosis, and miscellaneous features (Kleiner et al. 2005). Despite it is accepted that steatohepatitis is a pattern of injury composed of several features, it has been difficult to define exact diagnostic criteria that all pathologists agree on to precisely distinguish NAFLD cases with steatohepatitis from those with only steatosis and inflammation. Lobular inflammation, ballooning degeneration, and fibrosis showed significant association with the diagnosis of steatohepatitis. By the other hand, the degree or location of steatosis, Mallory’s hyaline, and megamitochondria were not significatively associated. Other works

have applied the NASH Clinical Research Network classification system to preclinical rodent models (Liang et al. 2014).

Hepatocellular ballooning is characterized as swollen hepatocytes with rarefied cytoplasm and reflects hepatocellular injury (Figure 13). Fat droplets and/or Mallory Denk Bodies, that are eosinophilic irregular-shaped aggregates in the cytoplasm of hepatocytes may be observed in ballooned hepatocytes. Hepatocellular ballooning is believed to result from alteration of the intermediate filament cytoskeleton (Brunt 2010).

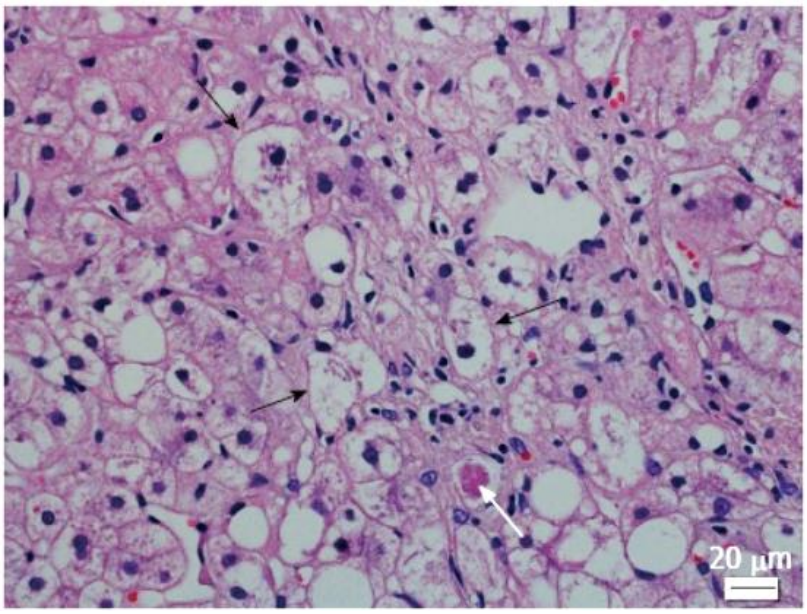

Figure 13: Ballooning and Mallory-Denk bodies in nonalcoholic steatohepatitis. Ballooned hepatocytes (black arrows) and Mallory-Denk bodies (white arrow) (hematoxylin and eosin staining) (Brunt 2010).

2.3 METABOLIC CHANGES IN NASH

The main guilty factor for the inflammatory liver damage in NASH is the lipotoxicity that is an accumulation of free fatty acids (FFAs) in lipid droplets. Hepatic metabolism of FFAs leads to the formation of toxic metabolites (e.g., diacylglycerol and ceramides). An increased lipolysis is a consequence of hyperinsulinemia and dietary fat that induce insulin resistance (IR), and increase lipogenesis (Ma et al. 2021). This can lead to lipid peroxidation, mitochondrial dysfunction, ROS generation, inflammation, and liver injury (Kasumov et al. 2015, Malhi & Gores 2008). In contrast, hepatic triglycerides (TG) accumulation in the liver is considered a nontoxic, safer form of storage for lipids in the liver (Bessone et al. 2019) (Figure 14).

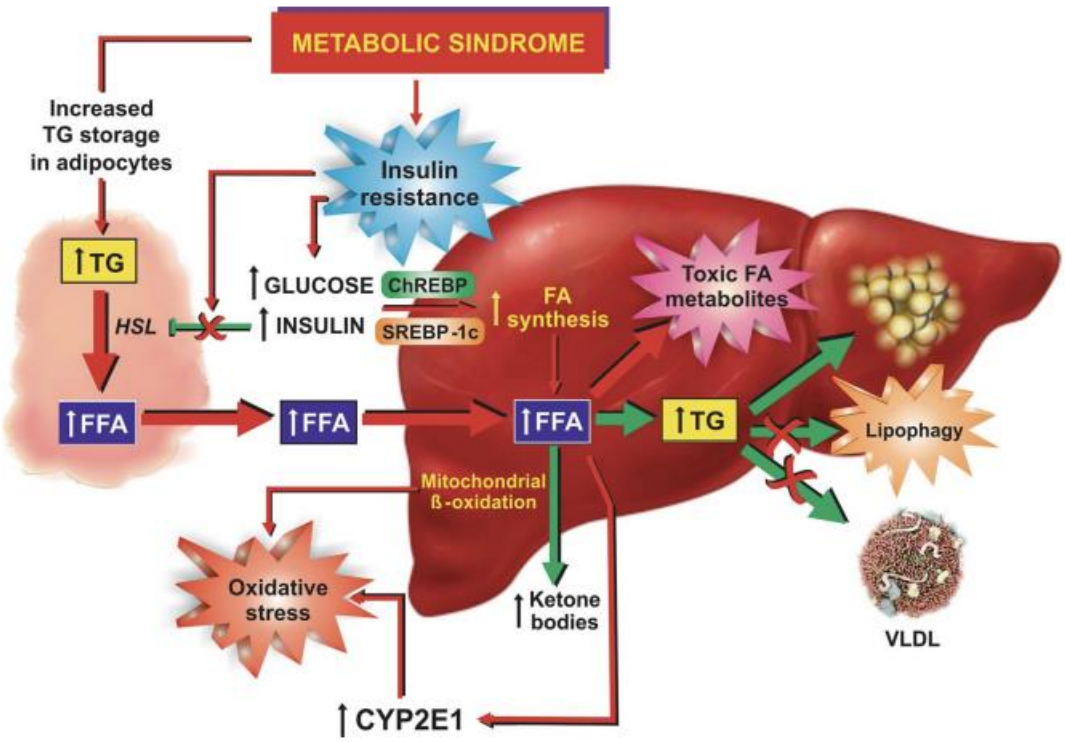

Figure 14: Metabolic basis of NAFLD pathogenesis. Insulin resistance associated with metabolic syndrome leads to unbalance between gain (red arrows) and loss (green arrows) of fat in liver (Bessone et al. 2019).

Other key factor in the development of NAFLD/NASH is insulin resistance (Pierantonelli & Svegliati-Baroni 2019), higher insulin levels also modulate hepatic lipid metabolism by increasing TG synthesis (Vatner et al. 2015). In adipose tissue, insulin resistance leads to the mobilization of FFAs from fat-overloaded adipocytes into the liver. FFAs are stored as TG in lipid droplets and exported as very low-density lipoprotein (VLDL), and oxidized by mitochondrial β-oxidation, as compensatory mechanisms to the increased FFA uptake and synthesis. Apolipoprotein B (apoB) is the main protein cofactor of VLDL, and its synthesis is also controlled by insulin, and this impairs exportation of hepatic lipids via this lipoprotein (Bessone et al. 2019, Charlton et al. 2002). Lipophagy helps to degrade TGs from lipid droplets and to deliver FFAs for these exportation routes. However, VLDL production and lipophagy are impaired in NAFLD, and enhanced mitochondrial FFA β-oxidation leads to oxidative stress. An excess of FFAs can also directly trigger oxidative stress and ROS production depending on catabolic processes, such as lipid oxidation (Pierantonelli & Svegliati-Baroni 2019).

3. INFLAMMATION

Inflammation is the response to cellular damage caused by infectious agents, toxins, or physical stress, such as radiation or previous injuries. Upon detection of a stimulus, tissue resident macrophages and epithelial cells start the inflammatory response. Then, neutrophils and monocytes, which later will be differentiated into macrophages, migrate on the way to inflammation site (Schmid-Schonbein 2006). This migration is due to the production of proinflammatory cytokines and chemokines like tumor necrosis factor alfa (TNFα), interleukins, as interleukin-1beta (IL1B) and interleukin-8 (CXCL8) by tissue resident phagocytic cells (Silva 2010). These cytokines and chemokines together with other mediators induce vasodilatation and increase blood vessels permeability causing swelling. The expression of endothelial adhesion molecules and neutrophil recruitment also increased.

3.1 CROSSTALK BETWEEN INFLAMMATION AND MELANOMA

The crosstalk between inflammation and cancer has been recognized since 1909, when Ehrlich propose the “magic bullet” theory which is now considered a precursor to chemotherapy (Ehrlich 1909). Inflammatory cells and signals contribute to cancer mechanisms from the initiation stage through tumor promotion and progression until the development of cancer (Fan et al. 2013). Tumor cell proliferation could be supported by the inflammatory tumor microenvironment, which has been shown to be crucial in the development of malignancy (Rajput & Wilber 2010).

Melanoma is one of the most immunogenic types of cancer (Ko 2017). The immunogenicity of a tumor is the capacity to induce adaptive immune responses that can prevent its growth (Passarelli et al. 2017). In addition, many studies support the concept that innate immunity plays a crucial role in the development, growth and prognosis of cutaneous malignant melanoma (Mignogna et al. 2017). A major field of study in melanoma research is the behavior and impact of innate and adaptive immune cells in the development of melanoma.

3.1.1 Macrophages in melanoma

Macrophages are phagocytic cells that acts as a first line of defense against pathogenic damage to tissues. These innate immune cells promote proinflammatory responses to pathogens and repair damaged tissues (Pathria et al. 2019). Infiltration by immune cells in the tumor is a hallmark of most forms of malignancy in cancer. In this context, tumor-associated macrophages (TAMs) are crucial regulators of the complex relation between the immune system and cancer (Ostuni et al. 2015). Important evidence for the importance of these cells is the strong association between increased macrophage density and poor survival in glioblastoma, hepatocellular, thyroid or lung cancers (Chen et al. 2005, Ryder et al. 2008, Sun et al. 2020, Zhu et al. 2008).

In general, macrophages can be classified as M1 or M2 activation phenotypes, depending on the molecules that activate them and their different metabolic programs which can influence different inflammatory responses (Mills et al. 2000). In cancer context, M1 macrophages predominantly play a role in antitumor immunity, while M2 tumor associated macrophages play a role in immunosuppression and tumor immune escape (Figure 15).

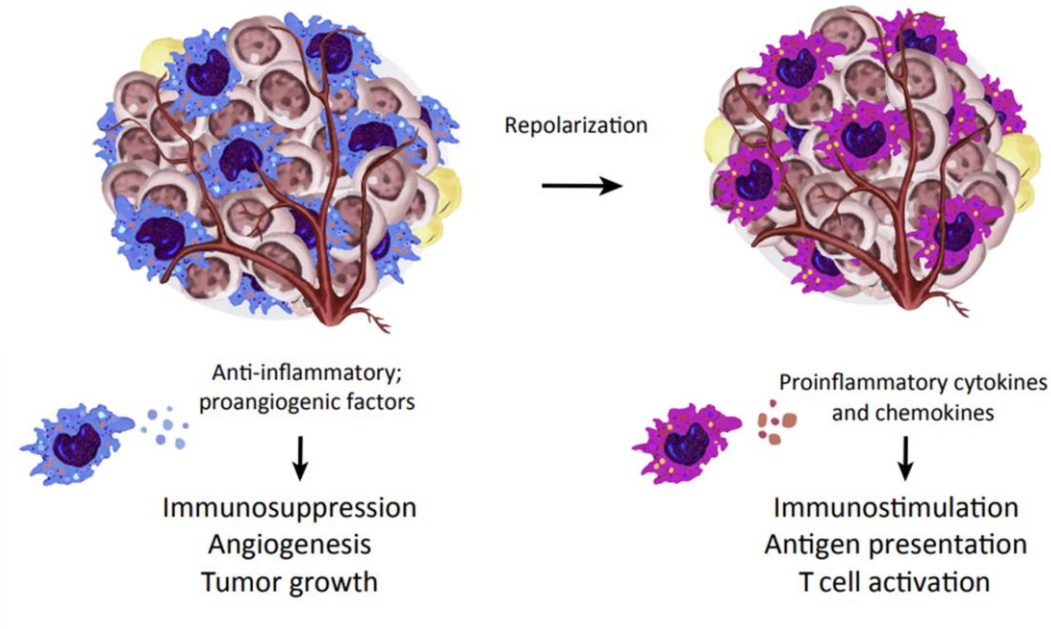

Figure 15: Macrophages are adaptable cells that can act promoting or decreasing cancer progression. Figure adapted from (Pathria et al. 2019).

Thus, TAMs express cytokines and chemokines that can suppress antitumor immunity and promote tumor progression. Prostaglandin E2 (PGE_2) has been shown to be the trophic signal required for the expansion of transformed cells at very early stages of cancer initiation. The COX-2/PGE2 pathway is critical in the earliest stages of tumor development (Feng et al. 2012). This prostaglandin can promote a macrophage M2 phenotype and can redirect dendritic cells toward a myeloid-derived suppressor cell phenotype (Heusinkveld et al. 2011, Obermajer et al. 2011). Leukocytes produce PGE_2 as trophic support for the growth of transformed cells. This reveals a key contribution of host immune cells to the optimal growth of transformed cells in these early stages of cancer initiation. Furthermore, a reduction of PGE_2 levels by inhibiting COX-2 leads to a change in macrophage behavior with increased proinflammatory activity, which results in a more active engagement and engulfment of transformed cells in a zebrafish model of early cell transformation using oncogenic *HRAS*^{G12V} (Feng et al. 2012).

Macrophages are crucial players in melanoma growth and survival. Initially assumed to be involved in anti-tumor immunity, they have been shown to promote cancer initiation, stimulate angiogenesis, and suppress antitumor immunity during malignant progression (Qian & Pollard 2010). The presence of TAMs correlates with poor prognosis in a wide range of cancers (Heusinkveld & van der Burg 2011).

The ability of melanoma exosomes to directly polarize macrophages, which would be expected to promote different pro-tumor functions, has recently been investigated. According to the polarization factors identified, such functions may include stimulating TAMs polarization, tumor growth, and metastasis, recruiting other immunosuppressive cell types, such as T regulatory cells (Tregs) and TANs, angiogenesis and promoting immune suppression (Bardi et al. 2018). Macrophages have also been shown to directly associate with growing tumor vessels and enhance tumor vascularization (Britto et al. 2018). Using zebrafish allograft models, it has been shown that chronic inflammation induced by Spint1a deficiency facilitates oncogenic transformation. These results may be of clinical relevance, as SPINT1 correlates with markers of aggressiveness, poor prognosis and tumor macrophage infiltration in human cutaneous melanoma (Gomez-Abenza et al. 2019).

3.1.2 Neutrophils in melanoma

Neutrophils are also a crucial component of the inflammatory response to tumors. New evidence indicates that tumors may manipulate Tumor Associated Neutrophils (TANs) to create different phenotypic and functional polarization states able to modify tumor behavior (Coffelt et al. 2016). Transforming growth factor-β (TGF-β) and granulocyte colony-stimulating factor (G-CSF) polarize TANs towards a pro-tumorigenic phenotype and promotes metastasis formation by regulating transcription factors, such as inhibitor of DNA binding 1 (ID-1) or interferon regulatory factor 8 (IRF8), which control the immunosuppressive functions of TANs (Casbon et al. 2015, Li et al. 2012, Papaspyridonos et al. 2015, Waight et al. 2011) .

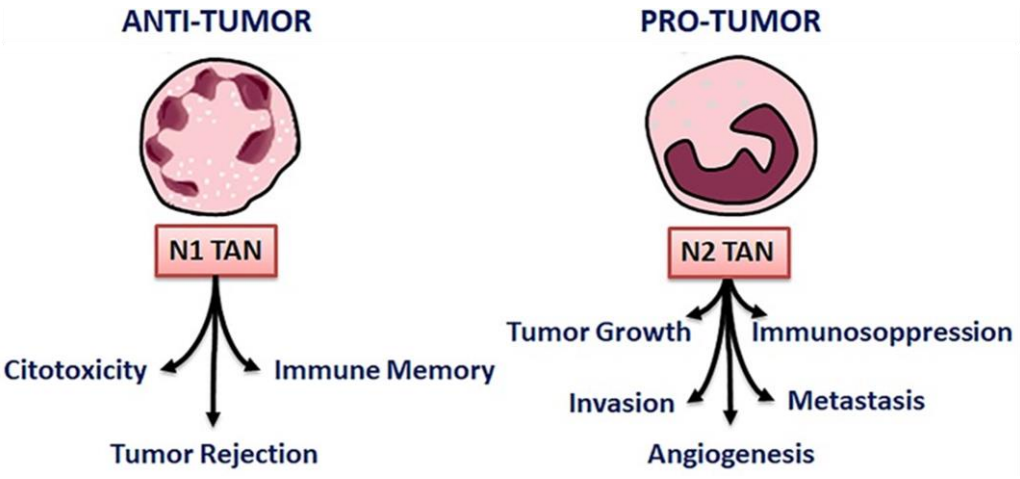

Figure 16: Neutrophils could polarize to anti-tumorigenic (N1) and pro-tumorigenic (N2). Figure adapted from (Masucci et al. 2019).

Moreover, it has been suggested that neutrophils have the ability to influence CD8+ T cells in infections (Tvinnereim et al. 2004) and cancer (Di Carlo et al. 2001, Kousis et al. 2007). Depending on specific factors derived from the tumor, the polarization of neutrophils leads to different phenotypes: N1 with "anti-tumorigenic" phenotype and N2 or "pro-tumorigenic" neutrophils (Fridlender et al. 2009) (Figure 16). N1 promote CD8+ T cell recruitment and activation by producing T-cell-attracting chemokines, such as CCL3 (C-C motif Chemokine Ligand 3), CXCL9 (CXC motif Chemokine Ligand 9), and CXCL10 (CXC motif Chemokine Ligand 10), and pro-inflammatory cytokines, such as IL-12 (Interleukin 12), TNF-α (Tumor Necrosis Factor alpha) and VEGF (Vascular Endothelial Growth Factor) (Scapini et al. 2000). N2 neutrophils do not produce high levels of pro-inflammatory agents.

Instead, they produce arginase which could act inactivating T-cell effector functions in the same way as proposed for M2 TAMs (Rodriguez et al. 2004).

In normal inflammatory situations, the inflammatory response is limited in time and immune cells can resolve the situation (Shaw & Martin 2009), but, in malignant tissues proinflammatory signals continue over time and intensify the response to satisfy tumor requirements. Neutrophils are also a crucial component of the key role played by inflammation in tumor development. In melanoma, UV-induced neutrophils have been shown to stimulate angiogenesis and enhance melanoma migration towards blood endothelial cells (Bald et al. 2014). During metastasis, neutrophils use the tumor draining lymphatic vessels to facilitate tumor cell travelling via CXCL5 (CXC motif Chemokine Ligand 5) expression (Soler-Cardona et al. 2018). Using a zebrafish model of melanoma driven by HRAS-G12V, wound induced inflammation has been found to increase tumor formation in a neutrophil-dependent manner. Mechanistically, neutrophils are rapidly recruited from a wound to pre-neoplastic cells increasing tumor cell proliferation (Antonio et al. 2015).

The relevance of chemokine in neutrophil recruitment in melanoma has also been shown in zebrafish models. For example, the proinflammatory chemokine CXCL8, which mediates neutrophil recruitment in the zebrafish inflammatory response (de Oliveira et al. 2013), has been shown to have proangiogenic activity mediated by CXCR2 (CXC motif Chemokine Receptor 2) and to enhance melanoma cell invasion (Gabellini et al. 2018).

3.2 CROSSTALK BETWEEN INFLAMMATION AND NASH

While simple steatosis in the liver is not considered malign, it can drive to NASH, which is marked by the infiltration of immune cells into the liver. The “inflamed” adipose tissue plays a key role in the release of toxic lipids, whereas alterations in the gut-liver axis have been also associated with the progression from NAFLD to NASH via dysbiosis. This alteration in the gut microbiota can trigger proinflammatory pathways finally leading to liver damage (Pierantonelli & Svegliati-Baroni 2019).

Innate immunity and hepatocyte injury and death are important hallmarks of the progression of fatty liver disease to NASH, where liver-resident macrophages infiltrating monocytes, and neutrophils play a critical role (Arrese et al. 2016).

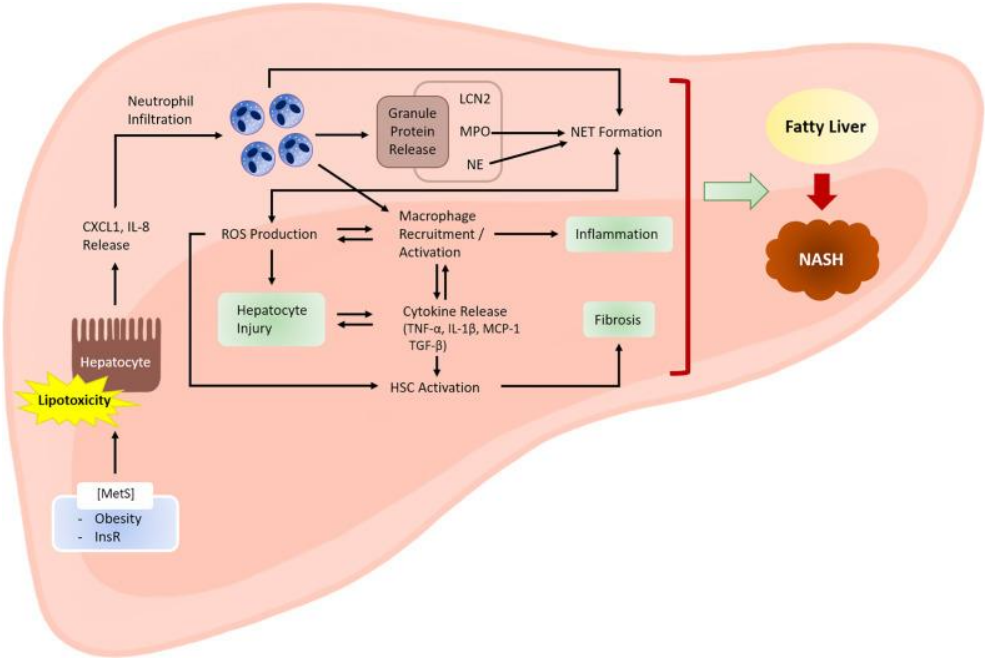

Figure 17: Role of neutrophil and macrophages in NASH development. (Hwang et al. 2021).

Under these conditions hepatocytes are exposed to lipotoxicity lipids as fatty acids, ceramides, cholesterol, and sphingolipids, leading to hepatic injury. Hepatocytes release cytokines that attract neutrophils (CXCL8, CXCL1) and these recruited neutrophils facilitates NASH development through different actions: ROS production, macrophage recruitment and hepatic injury. Macrophages cytokines could also promote fibrosis. In fact, hepatocyte injury, inflammation, and fibrosis are the three hallmarks of NASH (Hwang et al. 2021) (Figure 17).

3.2.1 Macrophages in NASH

Liver macrophage population is made up of resident macrophages also known as Kupffer cells (KCs) and circulating monocyte-derived macrophages (MoMFs). The activation of these cells during NASH progression depends on several stimuli as lipid metabolites, cytokines and other signal molecules (Li et al. 2020).

Free cholesterol, ceramides and saturated fatty acids accumulation could induce metabolic stress and oxidative stress, resulting in hepatocyte injury and death. The release of hepatocellular contents into the extracellular space

contributes to KC activation (Caligiuri et al. 2016). Several studies revealed that KCs were key regulators in the pathogenesis of NASH-driven fibrosis (Kazankov et al. 2019, Pellicoro et al. 2014, Schwabe et al. 2020). Importantly, owing to their strategic location, KCs can interact with different cells such as hepatocytes, hepatic stellate cells (HSCs) and liver sinusoidal endothelial cells (LSECs) (Li et al. 2020). In addition to KCs, macrophages located in adipose tissue are also associated with fatty liver disease through their effects on chronic inflammation, including cytokine and adipokine secretion (Kazankov et al. 2019).

Activated KCs act via producing cytokines (e.g, IL-6, TNFα, and IL-1β) (Oates et al. 2019). IL-6 contributed to insulin resistance in hepatocytes by disrupting key steps in the insulin signal transduction and affecting insulin action (Senn et al. 2002). In addition, IL-1β produced by KCs was associated with *de novo* lipogenesis and steatosis in hepatocytes (Negrin et al. 2014, Stienstra et al. 2010). Additionally, KCs were shown to remove apoptotic hepatocytes via efferocytosis, a process by which the phagocytic cell engulfs the apoptotic cells. The efferocytic clearance of dead hepatocytes prevents the release of DAMPs (Damage-associated Molecular Patterns) and subsequent inflammation (Schwabe et al. 2020).

NASH-induced hepatocyte damage stimulates KCs to release proinflammatory chemokines including CCL2, CCL5, and CXCL10 recruiting MoMFs indirectly (Lanthier 2015). Liver-resident KCs undergo cell death during NASH and recruit monocytes to the liver, where the recruited monocytes rapidly differentiate into proinflammatory MoMFs and contributes to NASH fibrogenesis.

The therapeutic inhibition of macrophage infiltration accelerates liver fibrosis regression in murine NASH (Baeck et al. 2014, Krenkel et al. 2018). Moreover, activated KCs stimulate neutrophil recruitment to expanded inflammation via chemokines (e.g., CXCL1, CXCL2, and CXCL8) and ROS production (Marra & Tacke 2014, Schuster et al. 2018).

3.2.2 Neutrophils in NASH

Neutrophil infiltration also promotes the progression of NAFLD to NASH and is considered a hallmark of this last stage (Hwang et al. 2021, Wu et al. 2020).

Cell death of lipotoxic hepatocytes releases chemokines and cytokines which recruit and activate neutrophils to initiate and amplify inflammation (Hirsova et al. 2016, Rada et al. 2020). These inflammatory cells also release factors that signal via death receptors on hepatocytes (e.g., TRAIL-R1, TRAIL-R2, TNFR1, and Fas), which may further stimulate hepatocyte death and inflammation creating a positive feedback loop (Hirsova & Gores 2015).

Hepatic neutrophil content increased in mice fed with high-fat diet (Li et al. 2020) and in the liver of NASH patients compared to fatty liver patients (Rensen et al. 2009). Moreover, the enhanced inflammation observed in NASH patients was associated with increased expression and activity of myeloperoxidase (MPO) (Rensen et al. 2009). Neutrophils produce and release ROS, proteases, and other inflammatory mediators to enhance hepatocyte injury and subsequent inflammation and fibrosis (Gao et al. 2019).

MPO was also associated with the formation of unique structures named hepatic crown-like structures in NASH (Itoh et al. 2013, Rensen et al. 2012). These structures are formed by macrophages that aggregates surrounding hepatocytes with large lipid droplets, they are associated to activated fibroblast and collagen accumulation (Itoh et al. 2013). Studies using myeloperoxidase-deficient mice have shown an attenuation of NASH development and down-regulation of pro-inflammatory cytokine production in the liver (Rensen et al. 2012).

4. CROSSTALK BETWEEN OXIDATIVE STRESS AND CANCER

Oxidative stress represents an imbalance between the normal production of free radicals such as reactive oxygen species (ROS), and the ability of the organism to detoxify the intermediates and repair the resulting damage (Gupta et al. 2014). ROS are products of cellular metabolism, most of these oxygen species are produced mainly by the NADPH oxidases family, xanthine oxidoreductase or the mitochondrial respiratory chain (Agarwal et al. 2011, Handy & Loscalzo 2012, McNally et al. 2003).

The oxidizing molecules could be not only ROS, such as superoxide anion radical, hydroxyl radical, hydroperoxyl radical, singlet oxygen and hydrogen peroxide, but also reactive nitrogen species (RNS), as nitric oxide and peroxynitrite (Jakubczyk et al. 2020). ROS and RNS, a group of highly reactive ions and molecules, are powerful signaling molecules involved in the regulation of different biological processes (Galadari et al. 2017).

In a homeostatic state, ROS are essential for cell survival and normal cell signaling, preventing cell damage. Antioxidants, like catalase, glutathione peroxidase (GPX), peroxiredoxins (PRX) and thioredoxin (TRX), help maintain ROS levels for cellular signaling (Reczek & Chandel 2015).

4.1 CROSSTALK BETWEEN ROS AND MELANOMA

It is well established that a dysregulation of intracellular ROS levels has a role in the progression and suppression of cancer (de Sa Junior et al. 2017). On the one hand, excessive ROS production could lead to oxidative stress increasing mitochondrial DNA damage and promoting the activation of oncogenes or the inactivation of anti-oncogenes, which facilitates its tumorigenic signaling pathways and tumor progression. On the other hand, cancer cells are characterized by active metabolism and high rate of proliferation and migration in comparison with non-tumor cells. For this reason, cancer cells require higher energy levels to maintain abnormal proliferate and growth rates, leading to excessive metabolism, which results in increased ROS production by mitochondria and nicotinamide adenine nucleotide phosphate (NADPH) oxidase (Galadari et al. 2017). This could derivate

into an upregulation of antioxidant systems in the cancer cell to control the excess of ROS (Xue et al. 2020) (Figure 18).

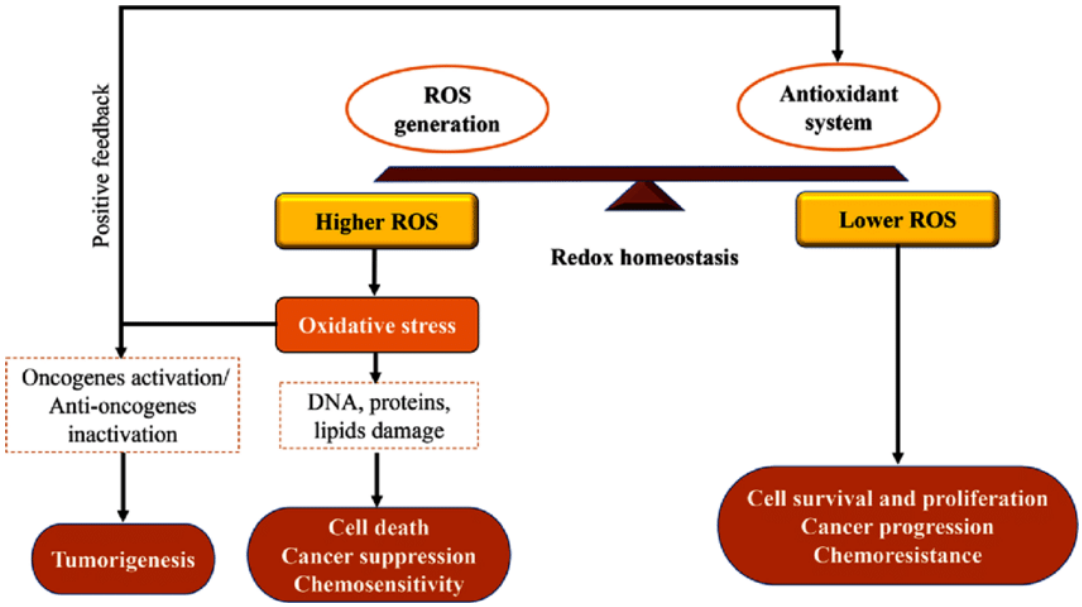

Figure 18: Regulation of redox homeostasis in cancer. Oxidative stress can promote tumor cell death, but also positively regulate the antioxidant system, inducing redox homeostasis, and promoting tumor cell survival and drug resistance (Xue et al. 2020).

Macrophages together with mast cells, eosinophils and recruited neutrophils, increase the concentration of ROS and RNS in the tumor microenvironment, attempting to participate in the natural defense against infection (Pollard 2004). However, increased concentration of ROS and RNS may have mutagenic consequences through DNA lesions or altered gene expression in proliferating cells (Figure 19). In addition, cancer cells can promote an inflammatory microenvironment that supports tumor cell proliferation (Rajput & Wilber 2010). Inflammation can also drive other processes that help tumor growth, such as angiogenesis (Marelli et al. 2017).

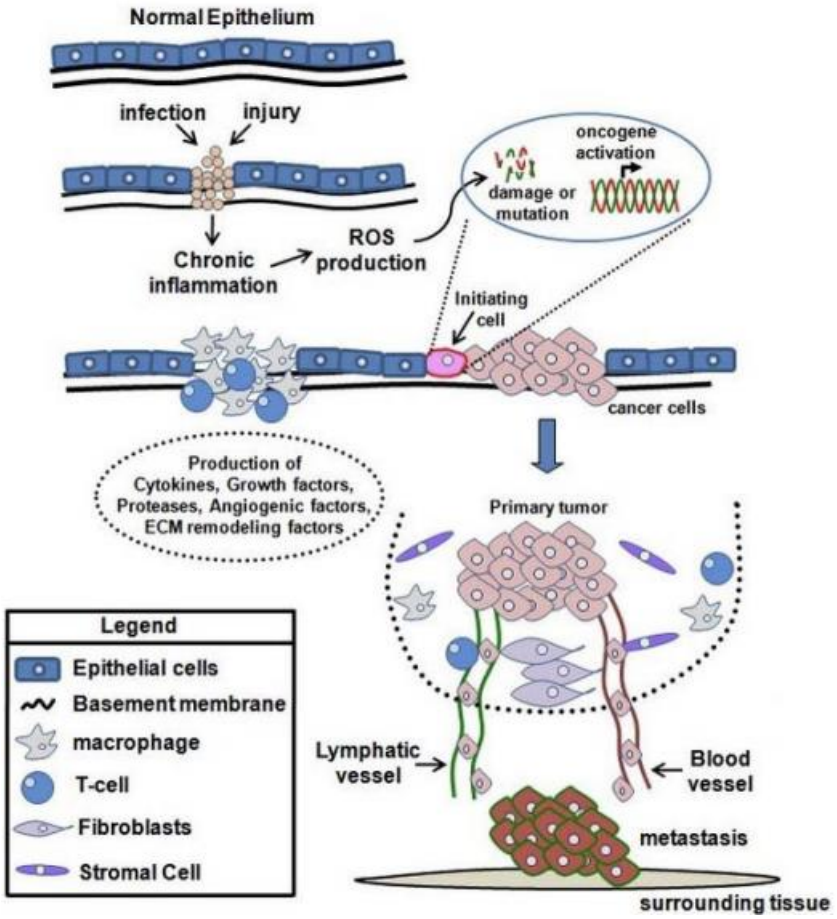

Figure 19: Potential roles of inflammatory cells during the development and progression of cancer. Chronic inflammation stimulates the production of ROS which can mediate immune recruitment, can act damaging the DNA and promote oncogen activation that initiate carcinogenesis (Rajput & Wilber 2010).

ROS may be involved in different stages of melanoma development. Melanoma cells respond to hypoxia by stabilizing the hypoxia-inducible factor-1 (HIF-1a/b), which activates several genes that regulate important biological processes, such as cell proliferation, angiogenesis, metabolism, apoptosis, and migration (Harris 2002). Furthermore, tumor cells increase the production of ATP due to their increased metabolism. These higher levels of ATP can affect ROS homeostasis and modulate the activation of cell signaling pathways, leading to enhanced cell growth (Skoyum et al. 1997). In addition, it has been shown that ROS produced by NADPH oxidase activates the master inflammatory transcription factor NF-κB and enhances melanoma cell proliferation (Brar et al. 2001). Therefore, the complexity of biochemical networks makes it difficult to distinguish between the effects of ROS produced by proliferating cells and proliferation stimulated by ROS. However, it is

clear that ROS are critically involved in the survival and proliferation of melanoma cells (Wittgen & van Kempen 2007).

In melanoma, some evidence suggests that oxidative stress plays an important role in inhibiting metastasis. Melanoma cells in the blood experienced oxidative stress that was not observed in subcutaneous tumors. A hostile environment may hinder the migration process of metastasizing melanoma cells. These cells undergo reversible metabolic changes during metastasis that allow them to adapt to survive in conditions of oxidative stress, including an increased dependence on NADPH generating enzymes in the folate pathway. Thus, oxidative stress limits distant metastasis of melanoma cells *in vivo*, raising the possibility that treatment with antioxidants may favor the progression of this cancer by promoting metastasis (Piskounova et al. 2015).

It has been shown that immune cells, such as neutrophils and macrophages, are attracted to transformed cells at surprisingly early stages. An important attractant molecule is H_2O_2 (Feng et al. 2010b), which is also an essential early damage signal responsible for driving neutrophils to wounds (de Oliveira et al. 2015, Niethammer et al. 2009, Razzell et al. 2013). H_2O_2, which is produced by both transformed cells and their healthy neighbors, can diffuse away from its site of generation and may act as a signaling factor (Figure 20). Furthermore, it is becoming clear that hydrogen peroxide plays a fundamental role in cell proliferation, migration and metabolism, as well as cell death (Sies 2017).

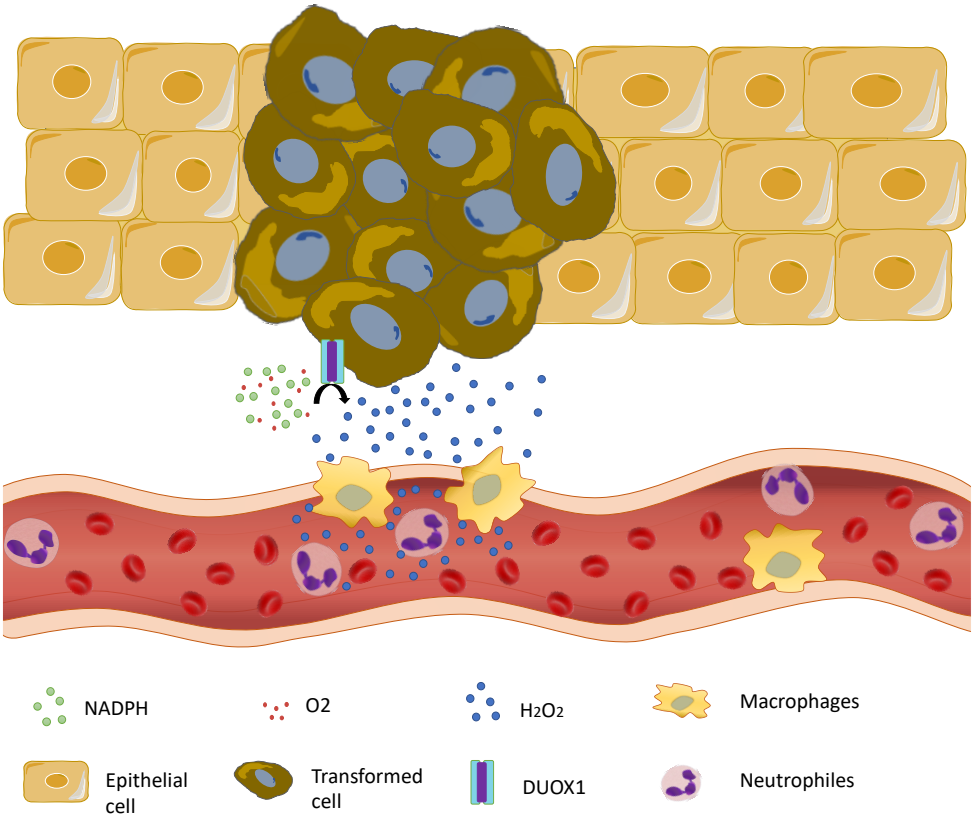

Figure 20: DUOX1-derived hydrogen peroxide from transformed cells and their neighboring cells attracts immune cells facilitating tumor growth (Pardo-Sanchez et al. 2022).

DUOX1 (Dual Oxidase 1) belong to NOX (NADPH Oxidases) family which is composed by transmembrane enzymes that carry electrons across biological membranes, reducing O_2 to $O_2^{\bullet-}$ or H_2O_2. The NOX family is formed of seven members, which are NOX1 to NOX5 and DUOX1 and 2. All NOX isoforms have six highly conserved transmembrane domains, one NADPH binding site in the C-terminal region, one FAD binding site, and two histidine-linked heme groups in the transmembrane domains III and IV. NOX5 and DUOX 1 and 2 have an intracellular calcium-binding site that is closely related to their activation (Faria & Fortunato 2020).

The enzymatic activity of the peroxidase domain of mammalian DUOX1 has never been demonstrated. Interestingly, it has been found that the peroxidase homology domain is crucial for the interaction of DUOX1 with DUOXA1, as well as for DUOX1 intrinsic activity (Carvalho & Dupuy 2017, Faria & Fortunato 2020).

DUOXA1 is the maturation factor or activator of DUOX1 (Grasberger & Refetoff 2006). The DUOXA1 protein consists of five alpha helical transmembrane regions, with extracellular loops and an intracellular tail. It associates with immature DUOX1 within the endoplasmic reticulum to promote its proper folding, glycosylation and transport to the plasma membrane to generate a mature, fully functional enzyme (Luxen et al. 2009) (Figure 21).

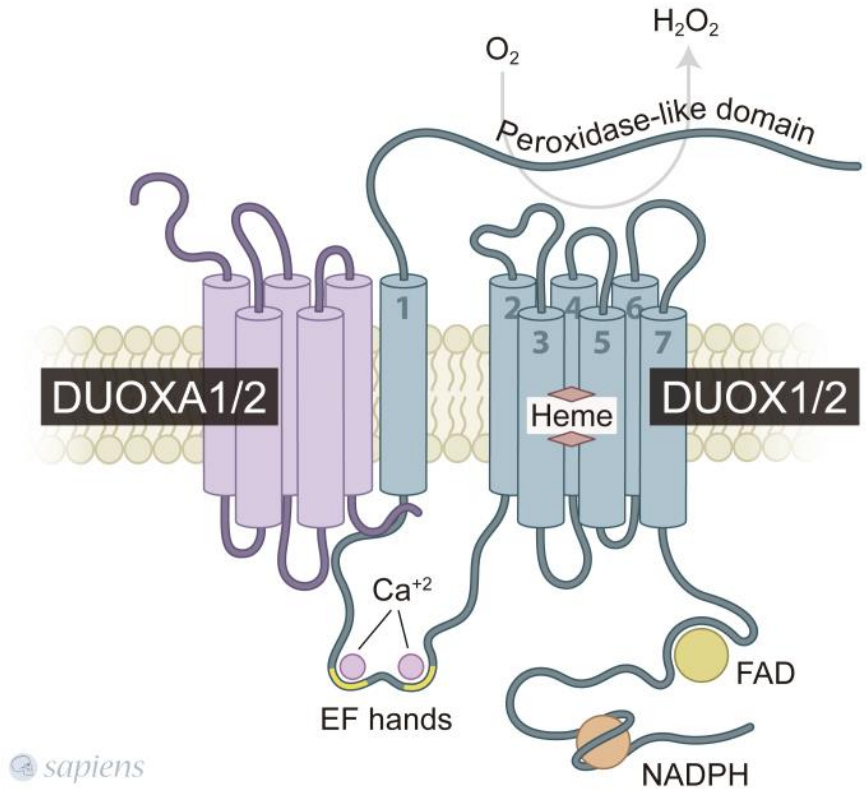

Figure 21: DUOX1 and DUOXA1 structures (Faria & Fortunato 2020).

Although DUOX1 was first described as a source of H_2O_2 in the thyroid, new data suggests that is one of the main sources of H_2O_2 in several epithelial cell types (Allaoui et al. 2009). Recently, the expression of DUOX1 has been reported in epidermal keratinocytes (Hirakawa et al. 2011). It has been demonstrated that the lack of DUOX1, and consequently its production of H_2O_2, affects the differentiation, adhesion, and junction mechanisms in normal human keratinocytes. Thus, DUOX1 alterations in the epidermis could contribute to skin pathologies such as atopic dermatitis, psoriasis and skin cancer (Choi et al. 2014).

When hydrogen peroxide synthesis is blocked, pharmacologically or by knockdown of Duox1, the number of neutrophils and macrophages attracted to transformed cell clones is reduced, resulting in a decrease in the number of transformed cells (Feng et al. 2010b). These results suggest that innate immune cells play a supporting role in early transformation. In addition, proinflammatory macrophages without DUOX1 expression show an improved antitumor response by increasing the production of some proinflammatory cytokines, such as TNFα, IFNγ and CXCL9, among other (Meziani et al. 2020).

Another important observation made *in vivo* for the first time using the transparency of zebrafish is that oncogenic *RAS* induces ROS that eventually leads to a DNA damage response and aberrant cell proliferation (Ogrunc et al. 2014) (Figure 22). Mechanistically, RAS-induced ROS are produced by NOX4. ROS scavengers and Nox4 inhibition rescues cell death and larval malformations promoted by the overexpression of oncogenic *RAS* (Ogrunc et al. 2014). These results may be of clinical relevance since NOX4 is increased in human pancreatic tumors, and specific inhibition of NOX4 with small molecule inhibitors act synergistically with chemotherapeutic agents in mouse models of this type of cancer (Ogrunc et al. 2014).

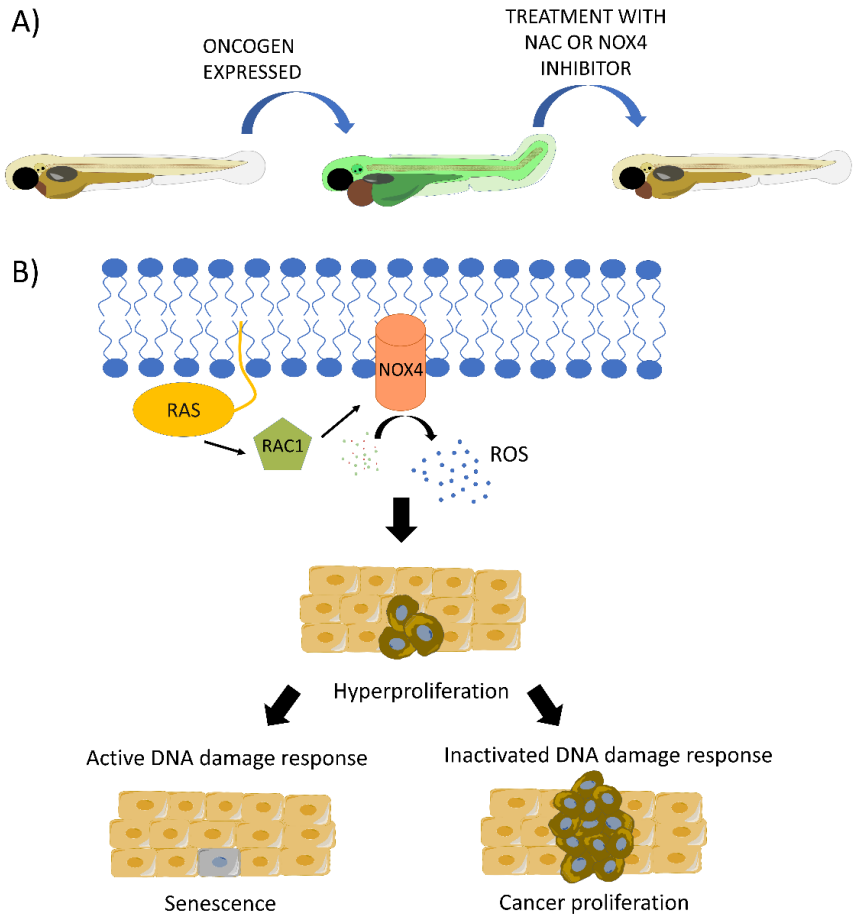

Figure 22: ROS produced by NOX4 induces tumor hyperproliferation. A) ROS scavengers and NOX4 inhibition rescue cell from death and larval malformations originated by the overexpression of oncogenic RAS; B) RAS-induced ROS are produced by NOX4 and induce tumor hyperproliferation by dependent and independent DNA damage response mechanisms (Pardo-Sanchez et al. 2022).

4.2 CROSSTALK BETWEEN ROS AND NASH

Oxidative stress represents the basis mechanism for the "second hit" in the NASH development theory (Day & James 1998, Masarone et al. 2018). Moreover, it can induces the progression of NAFLD to NASH by stimulating KCs, hepatic stellate cells, and hepatocytes (Ma et al. 2021).

Redox reactions of ROS species with DNA, proteins, and lipids within cells could promote oxidative injury. The ROS excess elimination is essential to alleviate lipid accumulation in damaged hepatocytes. In addition, oxidative stress mediates hepatocyte apoptosis and cell death (Ma et al. 2021). Furthermore, the excess of

fatty acids in the hepatic cells, their energy depletion and consequent mitochondrial dysfunction lead to an increase in oxidative stress levels and, finally, cellular damage (Couillard et al. 2005) that helps NAFLD progress from steatosis to steatohepatitis (NASH), fibrosis and cirrhosis or HCC.

Neutrophil-derived myeloperoxidase (MPO) catalyzes the generation of ROS crucial to defense against microorganism and involved in the tissue damage (Aratani 2018). To induce hepatocellular damage, ROS can inhibit mitochondrial respiratory chain enzymes and inactivate glyceraldehyde-3-phosphate dehydrogenase and membrane sodium channels (Giorgio et al. 2013). ROS could also act increasing lipid peroxidation, cytokines production and lipid accumulation, promoting inflammation and fibrosis through several protein kinases and nuclear transcription factor activation pathways (Ma et al. 2021).

Some molecules have been studied as treatment of NAFLD, for example: flavanols which act as scavengers of hydrogen peroxide (Wang et al. 2021); curcumin a natural polyphenol with antioxidant and anti-inflammatory properties (Inzaugarat et al. 2017); vitamin E (Iida et al. 2009), coenzyme Q10 (Chen et al. 2019) or metformin (Arroyave-Ospina et al. 2021, de Oliveira et al. 2019).

Despite several clinical works have studied the correlation between oxidative stress and metabolic syndrome, oxidative stress and NAFLD relation still need to be investigated. A study by Palmieri et al demonstrated that patients with metabolic syndrome and steatosis shows decreased antioxidant protection and increased lipid peroxidation (Palmieri et al. 2006).

Xanthine dehydrogenase gene (*XDH*) encodes the oxidative stress generating enzyme xanthine oxidoreductase (XOR). This enzyme has two interconvertible forms with different activities: although it generally carries dehydrogenase activity (XDH), it could be also converted into an oxidase (XO) under various pathophysiologic conditions (Sekine et al. 2021). Its XDH activity reduces NAD^+ to NADH but, during inflammatory conditions, reversible oxidation of critical cysteine residues (535 and 992) or limited proteolysis convert XDH to XO which reduces O_2 to superoxide and H_2O_2 (Cantu-Medellin & Kelley 2013b). Both activities are able to participate in ROS production, as XDH has also been noted to generate oxidants (Lee

et al. 2014). Xanthine oxidase has also other activity reducing nitrites to nitric oxide (Figure 23) (Cantu-Medellin & Kelley 2013b).

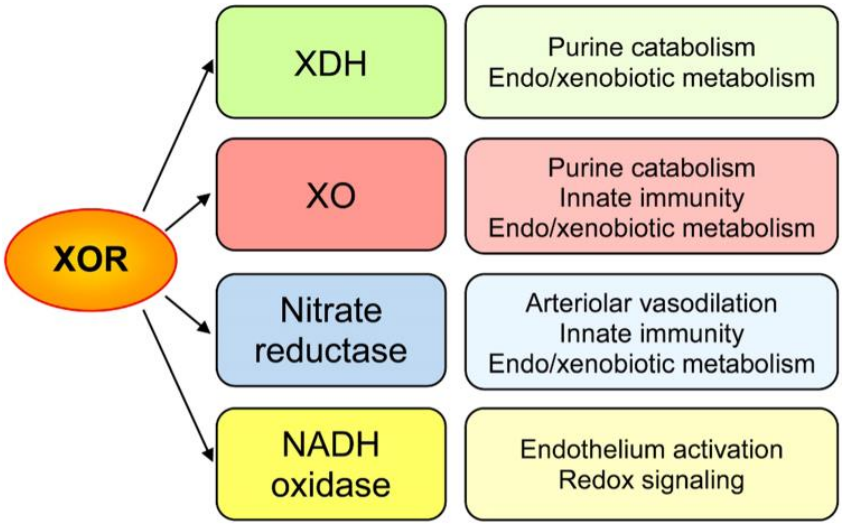

Figure 23: XOR enzymatic activities and their main functions (Battelli et al. 2019)

XDH is a complex molybdoflavin enzyme that catalyzes terminal steps of purine degradation catalyzing the oxidation of hypoxanthine to xanthine to uric acid, producing hydrogen peroxide during the reaction (Figure 24) (Kelley et al. 2006, Pratomo et al. 2021).

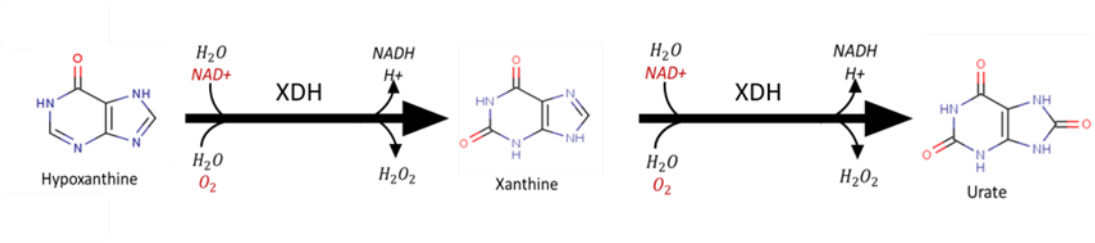

Figure 24: XDH acts in the transformation of hypoxanthine to urate.

Xanthine dehydrogenase, which is expressed in various tissues such as the liver and intestine (Figure 25), is also associated with the increase of proinflammatory cytokines, such as IL-1 β, tumor necrosis factor (TNF)-α, and interferon (IFN)-γ (Cantu-Medellin & Kelley 2013a, Kelley et al. 2006).

Figure 25: XDH is a ROS-producing enzyme mainly expressed in hepatocytes (https://www.proteinatlas.org/ENSG00000158125-XDH/tissue).

In all cells, the expression of *XDH* gene generates XDH with the housekeeping role of purine catabolism. However, liver cells utilize XDH, XO and nitrate reductase activities of XOR as well for the metabolism of other endogenous and exogenous substrates, including some drugs. Xanthine is preferably accumulated and excreted over hypoxanthine. This is due to extensive hypoxanthine recycling by the salvage pathway for which xanthine is not a substrate in humans (Mateos et al. 1987).

XDH also participates in the production of uric acid, which is a DAMP released in stress conditions and is associated with nonspecific inflammation response or neutrophils recruitment to the inflammation site (Hughes & O'Neill 2018). In patients the lack of XDH/XO activity is known as xanthinuria and leads to undetectable levels of uric acid, hypouricemia, and increased serum and urinary xanthine concentrations (Mraz et al. 2015, Sekine et al. 2021). Hyperuricemia is considered one of the complications of metabolic syndrome (Nakagawa et al. 2005) and it has been related to decreased renal uric acid excretion (Agarwal et al. 2011, Lopez-Suarez et al. 2006). Moreover, the serum level of XOR is correlated to obesity-associated metabolic disorders (Battelli et al. 2019) and to NAFLD (Toledo-Ibelles et al. 2021).

Xanthine dehydrogenase has been proposed as a prognostic biomarker related to tumor immunology in hepatocellular carcinoma. Decreased *XDH* mRNA expression was detected in human cancers originating from the liver, bladder, breast, colon, bile duct, kidney, and hematolymphoid system. In HCC, a low XDH

mRNA level predicted poor overall survival. Loss of XDH expression seems to be an immune evasion mechanism for hepatocellular carcinoma (Lin et al. 2021).

5. ZEBRAFISH AS A RESEARCH MODEL

Zebrafish (*Danio rerio*) is a teleost freshwater fish belonging to the *Cyprinidae* family. Its originally from India and Nepal, it inhabits rivers and streams (Sundin et al. 2019). The zebrafish is an established model organism for studying developmental biology and molecular genetics. It is used in diverse topics such as: the immune system (Traver et al. 2003), hematopoiesis ((Jagannathan-Bogdan & Zon 2013, Rodriguez-Ruiz et al. 2020)), neurogenesis and regeneration (Kizil et al. 2012, Schmidt et al. 2013), aging and vertebrate behavior (Cayuela et al. 2018, Norton & Bally-Cuif 2010), and cancer research (Fazio et al. 2020, Mione & Trede 2010).

Currently, it is a powerful model organism in biomedical research and its popularity has increased in recent years mainly due to its advantages over other models (Trede et al. 2004) (Figure 26). Among them are:

- Its small size and ease of maintenance.
- Its high fecundity that allows many replicates (around 200 eggs/couple/week).
- Its rapid development, with organs fully formed 48 hours postfertilization (hpf).
- Its short generation time for a vertebrate, typically 3 to 4 months, making it suitable for selection experiments.
- Its transparency in the embryo and larval stages, together with, the increasing availability of transgenic lines, enabling *in vivo* tracking of different cell types.
- Its easy tractability for genetic and embryological manipulation allowing large drug screenings at lower cost compared to other animal models (Amatruda et al. 2002).
- Its completed sequenced genome and its remarkable homology with human: zebrafish shares 71.4 % of genetic similarity with humans, and 82 % of human disease-related genes can be linked to at least one zebrafish orthologue (Howe et al. 2013).
- The increasing availability of powerful genetic tools, that enable in a relatively easy way the generation of transgenic and mutant zebrafish.

Facilitating the characterization of gene function via overexpression, transient depletion, or genome editing by applying variated gene editing technologies, including the latest CRISPR/Cas-based method (Ablain et al. 2018, Varshney et al. 2015).

- Specially in melanoma studies, the translucency of zebrafish larvae and the existence of transparent Casper mutants (roy$^{a9/a9}$; nacre$^{w2/w2}$), in which pigment cell production is inhibited (White et al. 2008), is a key advantage that allows *in vivo* imaging of the process at the very early stages of oncogenic transformation and studying their interaction with immune cells.

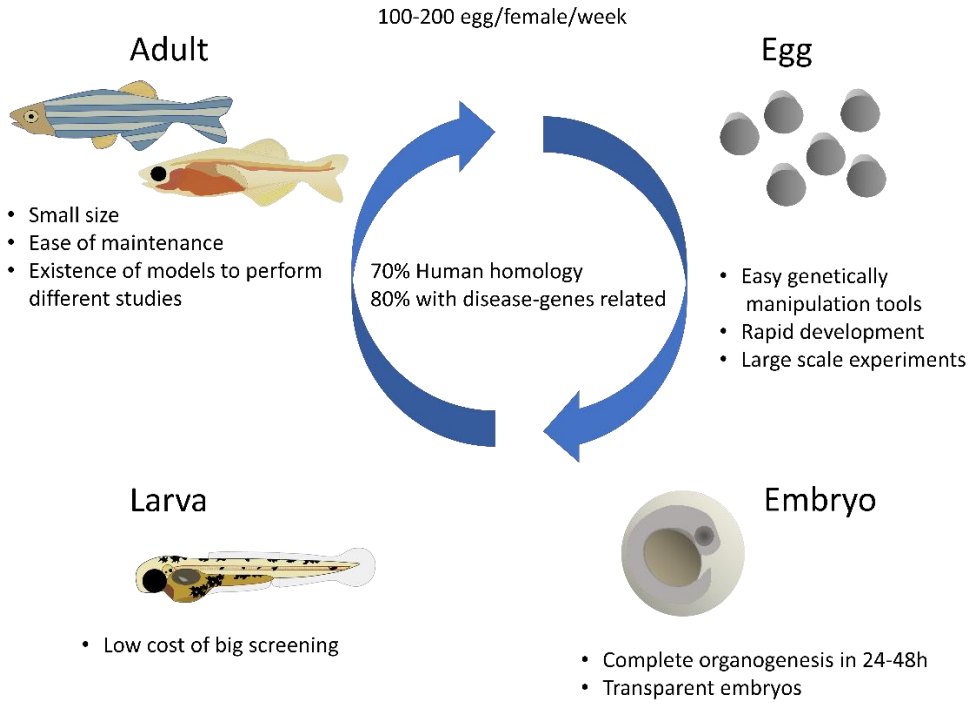

Figure 26: Zebrafish model advantages.

5.1 ZEBRAFISH IN CANCER

To better understand the mechanisms underlying tumor initiation, growth and progression zebrafish can be used as an excellent tool. Zebrafish embryos are produced in large numbers and are accessible for rapid screening and experimental manipulation, this together with the availability of fluorescent reporter lines and transparent models (Casper) facilitates the study of tumor initiation, cell migration *in vivo* and lately tumor growth.

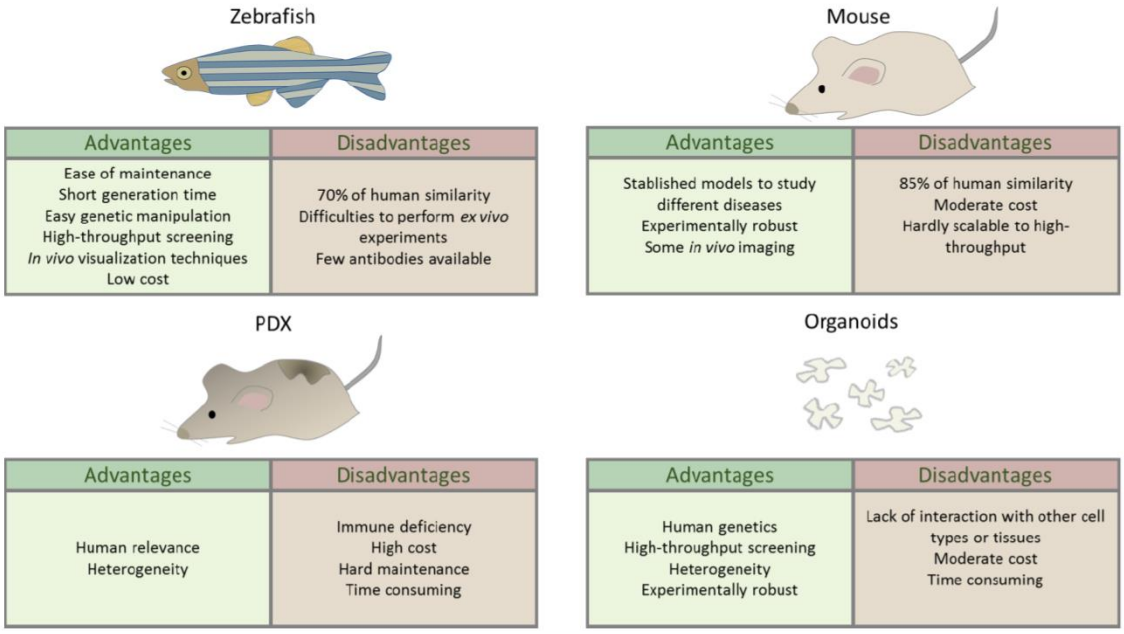

Figure 27: Advantages and disadvantages of zebrafish model compared with mouse, patient-derived xenograft (PDX), and human organoid models (Pardo-Sanchez et al. 2022).

Most of the analyses of the metastatic process have been performed using *in vitro* cell cultures (Kunapuli et al. 2003, Mohapatra et al. 2019) or in mice models (Hooijkaas et al. 2012, Zaidi et al. 2008). Cell cultures neglect the complexity of the process, and it is not possible to observe the dissemination of these cells or the interaction with the tumor microenvironment. To address these issues, *in vivo* models are mandatory. But in mice, it is difficult to study the first steps of tumor development; small lesions are impossible to observe *in vivo* due to the depth of the tissues that mice have and usually have to be sacrificed. Therefore, the metastatic process is usually assessed at the endpoint and not during the development (Figure 27). Furthermore, the number of individuals used in each experiment is limited and the statistical power cannot be as high as it should be (Teng et al. 2013).

Recently, zebrafish has emerged as a complementary model to overcome these disadvantages (Barriuso et al. 2015, Mione & Trede 2010), offering alternative options to study the processes involved in the development of cancer (Figure 28).

In cancer studies, the transparency of zebrafish larvae is a key advantage that allows *in vivo* imaging of the process at the very early stages of oncogenic transformation and studying their interaction with immune cells. For example, interactions between TAMs and tumor cells have been observed thanks to these

unique imaging properties that zebrafish offer *in vivo*. Thus, it was shown that macrophages are recruited to the tumor site and are able to transfer cytoplasm to melanoma cells, thereby increasing tumor cell motility and promoting tumor cell dissemination (Roh-Johnson et al. 2017). Finally, another main advantage is its amenability for *in vivo* chemical screening.

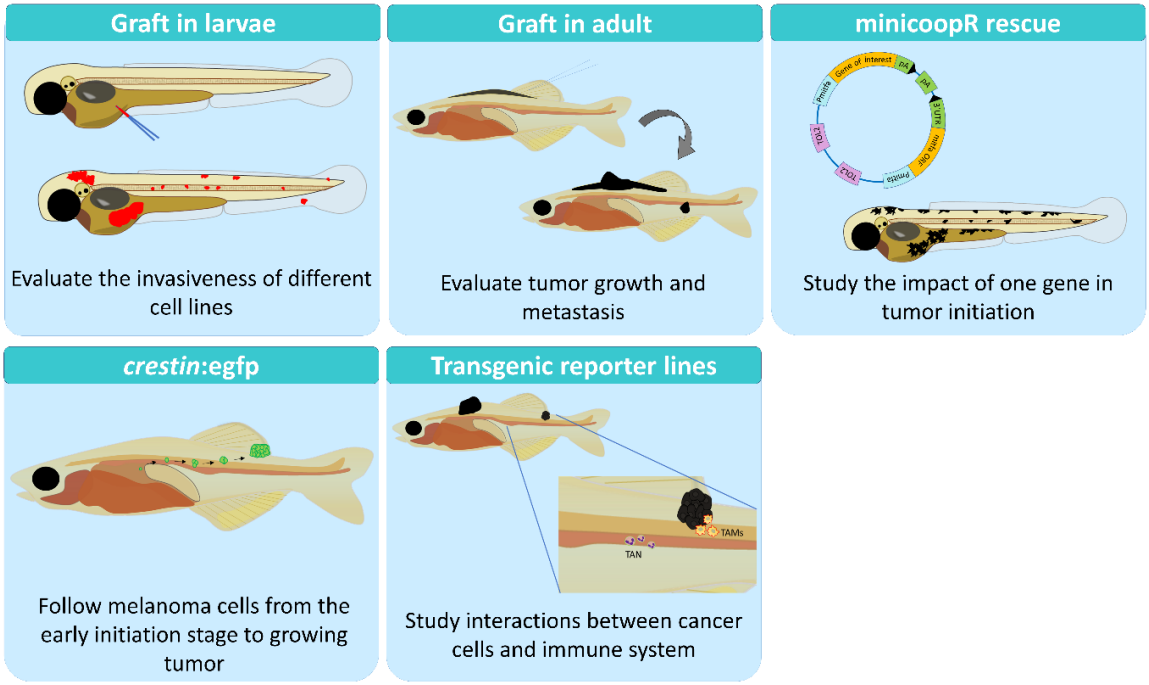

Figure 28: Zebrafish tools to study cancer (Pardo-Sanchez et al. 2022).

5.1.1 Genetics models

To address the study of melanoma, zebrafish models expressing different human oncogenes were developed. A model expressing transgenic human $BRAF^{V600E}$ combined with the tumor protein P53 (TP53) mutation was first established (Patton et al. 2005). Later, to study the role of NRAS using zebrafish, transgenic human-$NRAS^{Q61K}$ mutants were also described (Dovey et al. 2009). Recently, the relevance of the zebrafish model in melanoma research was highlighted by the identification of loss of SPRED1 in mucosal melanoma (Ablain et al. 2018) and the role of anatomical position in determining oncogenic specificity (Weiss et al. 2022).

5.1.2 Xenograft in larvae

Microinjection of human and mouse cancer cells into zebrafish embryos is a widely used technique to study migration and invasion processes. It is usually performed at 48 hpf, when the adaptive immune response has not yet been

established (Konantz et al. 2012, Lam et al. 2004), so this method does not require immunosuppression. First, the cells must be labelled with a fluorescent probe, such as cM-Dil, to allow the monitorization of the cancer cells (Corkery et al. 2011). After injection of the cells into the yolk sac, the ability of the cancer cells to proliferate or invade different tissues through the larvae can be followed and measured (Haldi et al. 2006). Considering the possibility of using transgenic zebrafish lines with fluorescently labelled immune cells, this model allows the study of essential interactions between tumor cells and the host immune microenvironment *in vivo* (Amatruda & Patton 2008).

5.1.3 Allograft in adults

The study of cancer in adult zebrafish allows *in vivo* analysis of tumor engraftment and migration after transplantation. This technique consists of injecting disaggregated cancer cells from a donor fish into the dorsal subcutaneous cavity of a recipient fish to visualize their proliferation and dissemination *in* vivo (Li et al. 2011). One of the pitfalls of this technique is the immune rejection of transplanted cells in adults, which makes the immunosuppression of zebrafish by irradiation necessary (Langenau et al. 2004).

Another drawback for transplanting cells into adults is that the natural pigmentation of the fish does not allow following most of the cellular processes. To solve this, unpigmented zebrafish models, named “Casper”, were developed to study mechanisms such as angiogenesis, migration, invasion, or tumor growth in adult zebrafish. The Casper zebrafish model is a combination of two mutations: the first one, *nacre* which has a mutation in *mitfa*, which regulates neural crest derived pigment (Lister et al. 1999), and results in a loss of melanoblast and mature melanocytes; while the second mutation is *roy,* that affects the *mpv17* gene and results in a severe disruption of melanocyte numbers and patterning and loss of iridophores (White et al. 2008). Using melanin or GFP as markers, melanoma cells are easier to visualize and track. Furthermore, combining this model with transgenic lines that label immune cells, such as neutrophils (Renshaw et al. 2006) or macrophages (Ellett et al. 2011, Walton et al. 2015) or vasculature (Lawson & Weinstein 2002), helps to gain a more detailed understanding of how the transformed cells interact with the immune system and their niche. It is possible to

track not only innate immune cells, but also some adaptative immune cells, such as T cells with the *lck* promoter (Langenau et al. 2004), or specific $CD4^+$ T cells (Dee et al. 2016). Unfortunately, there are no available lines with labelled NK cells to track them *in vivo* and study their relevance in tumor immunosurveillance.

One of the most important applications of this model is the possibility to test drugs *in vivo* and in an easier and cheaper system than mouse models. For example, it has been used to test long term administration of drugs in adult Casper zebrafish intraperitoneally transplanted with a zebrafish melanoma cell line (ZMEL1), and a tumor reduction could be observed after the oral administration of the drug (Dang et al. 2016).

5.1.4 Xenograft in adults

Transplantation of human tumor cells into zebrafish is easy in larval stages where the immune system is not fully developed, but in adults it requires laborious work and transient methods of immune suppression that limit engraftment and survival of the tumor, or it does not reproduce the characteristics of these malignancies (Khan et al. 2019). Xenograft models in adult zebrafish have previously been used to study pancreatic cancer progression (Guo et al. 2015) and tumor cell intravasation in T-Lymphoblastic Lymphoma (Feng et al. 2010a). More recently, immunodeficient zebrafish were generated to visualize human cancer and therapy responses (Yan et al. 2019). This fish model has mutations in *prkdc* and *il1rga* genes that result in a lack of adaptive immunity and NK cells. Notably, this model is grown at 37 °C allowing engraftment of a wide array of human cancers injected in the peritoneal cavity, including patient-derived xenografts, and the study of their dynamics and therapy responses.

5.1.5 Early transformation

A powerful method has been developed to follow the melanoma initiation cells at very early stages. This is possible due to the knowledge about the expression of *crestin* in the neural crest during embryogenesis; it is no longer expressed after 72 hpf and is only re-expressed in melanoma tumors when melanoma precursor cells re-initiate an embryonic neural crest signature (White et al. 2011). Therefore, the

crestin-GFP model allows to follow cancer development when a tumor starts at very early stages *in vivo* (Kaufman et al. 2016).

5.1.6 The MiniCoopR system

A useful tool for melanoma research has recently been developed to study the effect of a gene on tumor initiation. The MiniCoopR method consists of a plasmid that allows the gene of interest (GOI) to be placed under the *mitfa* promoter and also contains a *mitfa* minigene, which combined with the use of Casper zebrafish, allows one to easily follow which cells transform because they recover melanin expression (Iyengar et al. 2012) (Figure 29). For example, this method has identified the histone methyltransferase SETDB1 as a gene capable of accelerating melanoma formation (Ceol et al. 2011).

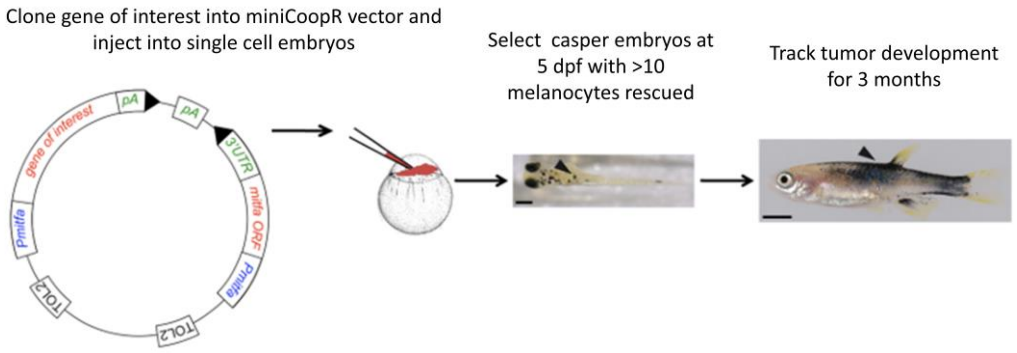

Figure 29: Use of the MiniCoopR vector. Scheme of the MiniCoopR plasmid. After the injection, embryo with rescued melanocytes containing the MiniCoopR vector and the gene of interest were selected. Adapted from (Iyengar et al. 2012).

The second most common oncogene driving malignant melanoma is NRAS. Recently, a zebrafish model has been generated to study NRAS mutant melanoma using the *MiniCoopR* vector (*mcr:NRAS*) (McConnell et al. 2019). In this model, tumor development occurs without mutations in TP53, and the development of melanoma is faster than in previous lines, such as the BRAF and NRAS stable mutant lines (Dovey et al. 2009, Patton et al. 2005).

In summary, the unique advantages of zebrafish for *in vivo* imaging together with the ease of genetic manipulation and the high throughput drug screening make this model a key tool to study cancer, more specifically melanoma (van Rooijen et al. 2017). Zebrafish facilitate the study of melanoma initiation, using Casper zebrafish

or the recent zebrafish model *crestin:eGFP,* including the monitoring of the development, tumor growth and metastasis in adult stages. It also makes it easier than other models to study the invasiveness potential and drug resistance of patient tumor cells using xenografts in larvae (Avatar models) and it makes easier the generation of genetic mutants to study the impact of a GOI on melanoma development. In addition, the recent development of the MinicoopR system makes it possible to study the impact of a GOI on tumor biology from early initiation to tumor development.

5.2 ZEBRAFISH AS A NAFLD/NASH MODEL

Zebrafish is a powerful model organism for liver disease research, including NAFLD and HCC. Similarities between zebrafish and mammals in hepatocellular composition, function as well as genetics it is a crucial advantage to provide insight into the pathogenesis of many major liver diseases. Zebrafish rapid development is one of the main advantages of the model, indeed all of their digestive organs are mature in larvae by 5 dpf. Importantly, all hepatic functions evaluated so far are found in larvae at this age (Goessling & Sadler 2015).

There are some features that characterize NAFLD which are similar in humans and zebrafish, such as hepatocyte enlargement and ballooning, triglyceride accumulation and increases in reactive oxygen species (ROS) (Goessling & Sadler 2015). In addition, it was shown that zebrafish larvae fed with high fat and high fat cholesterol diets developed steatosis for 7 and 10 days. The incidence and degree of steatosis were more severe adding cholesterol to the HF diet, it promotes higher hepatic lipid accumulation (Dai et al. 2015).

OBJECTIVES

The specific objectives for this work are the following:

1. Study the role of DUOX1 in early progression, aggressiveness and metastasis of skin cutaneous melanoma.
2. Identification of specific DUOX1 chemical inhibitors.
3. Generation of Xdh-deficient zebrafish to study the role of this enzyme in non-alcoholic fatty liver disease.

MATERIALS & METHODS

Human skin cutaneous melanoma dataset analysis

Normalized gene expression, patient survival data and GO-associated functions were downloaded on January 2023 from the skin cutaneous melanoma (SKCM) repository of The Cancer Genome Atlas (TCGA, Firehose Legacy, https://datacatalog.mskcc.org/dataset/10490) from cBioPortal database (https://www.cbioportal.org/). This cohort includes 480 patient samples. No cleaning filter was applied and all patient data available for each study were used: 469 samples for expression analysis, 317 samples for survival analysis by stage and 468 GO-associated functions. Clark levels at diagnosis were used for patient stratification: I, II and III stages were categorized as early-stage melanoma, while IV and V as late-stage melanoma. Gene expression plots and regression curves for correlation studies were obtained using GraphPad Prism 5.03 (GraphPad Software).

Experimental models

Wild-type zebrafish (*Danio rerio* H. Cypriniformes, Cyprinidae) were obtained from the Zebrafish International Resource Center (ZIRC, Oregon, USA) and mated, staged, raised and processed as described in the zebrafish handbook (Westerfield & Streisinger 1994). Zebrafish fertilized eggs were obtained from natural spawning of wild type and transgenic fish held at our facilities following standard husbandry practices. Animals were maintained in a 12 h light/dark cycle at 28 °C. Nine-twelve month-old transparent roy $^{a9/a9}$; nacre$^{w2/w2}$ (Casper) in which pigment cell production is inhibited (White et al. 2008) were used for transplantation.

The experiments performed comply with the Guidelines of the European Union Council (Directive, 2010/63/EU) and the Spanish RD 53/2013. Experiments and procedures were performed as approved by the Consejería de Agua, Agricultura, Ganadería y Pesca de la CARM (authorization number # A13180602). To carry out the allotransplant experiments in adult zebrafish, the fish were tracked to ensure the healthy state of the animals. To determine humane endpoint, we used a scoring list of independent variables which were: the loss of equilibrium during swimming, a loss of body weight, abdominal distension, fish behaviour (gasping for air or loss of mobility) and tumor size. We euthanized the fish when the

accumulative total score exceeds a threshold or if one of the variables obtain the higher score of severity.

Tumor generation using MiniCoopR vector

MiniCoopR technology was used to study melanoma initiation in early steps (Ceol et al. 2011, Iyengar et al. 2012) (Figure 30). A key reagent in this assay is the MiniCoopR vector, which couples a wild-type copy of the *mitfa* (melanocyte inducing transcription factor a) to a recombination cassette into which candidate melanoma genes can be recombined. The MiniCoopR vector has also a *mitfa* rescuing minigene which contains the promoter, open reading frame and 3'-untranslated region of the wild-type *mitfa* gene. The MiniCoopR method allows to place the gene of interest (GOI) under the *mitfa* promoter, specific for melanocytes, this technology allow us to make constructs using full-length open reading frames of candidate melanoma modifiers. Because they are physically coupled to the *mitfa* rescuing minigene, candidate genes are expressed in rescued melanocytes producing melanin.

We used three MiniCoopR vectors (mcr:GOI): mcr:NRAS-Q61R, mcr:DN-Duox1 and mcr:EGFP. MiniCoopR mitfa:NRAS-Q61R (Addgene plasmid #118847; http://n2t.net/addgene:118847; RRID:Addgene_118847) and MiniCoopR mitfa:EGFP (Addgene plasmid #118850; http://n2t.net/addgene:118850; RRID:Addgene_118850) were a gift from Leonard Zon and were previously described (Ablain et al. 2018). The MiniCoopR mitfa:DN-Duox1 was generated by MultiSite Gateway assemblies using LR Clonase II Plus (Life Technologies) according to standard protocols, and using Tol2kit vectors described previously (Kwan et al. 2007).

We used MiniCoopR mitfa:NRAS-Q61R (mcr:NRAS) to express this oncogen and transform the melanocytes coupled with one of the other MiniCoopR vector mcr:DN-Duox1 or mcr:EGFP. The Dominant Negative (DN) consists in engineer mutations in the protein of interest that abolish its function and simultaneously inhibit the function of the wild-type protein (Sheppard 1994). The DN-Duox1 is a truncated form of the zebrafish wild-type Duox1 which lacks the entire flavin domain (residues 1–1232) and robustly inhibits endogenous Duox1 (de Oliveira et al. 2014). We used MiniCoopR mitfa:EGFP as a control. Rescued melanocytes (visually expressing melanin) would simultaneously express the NRAS oncogen and

DN-Duox1 or EGFP, depending on the experimental condition. The effect of Duox1 inhibition on melanoma initiation and melanoma cell behaviour was measured using melanoma-free survival curves and transplantation assays.

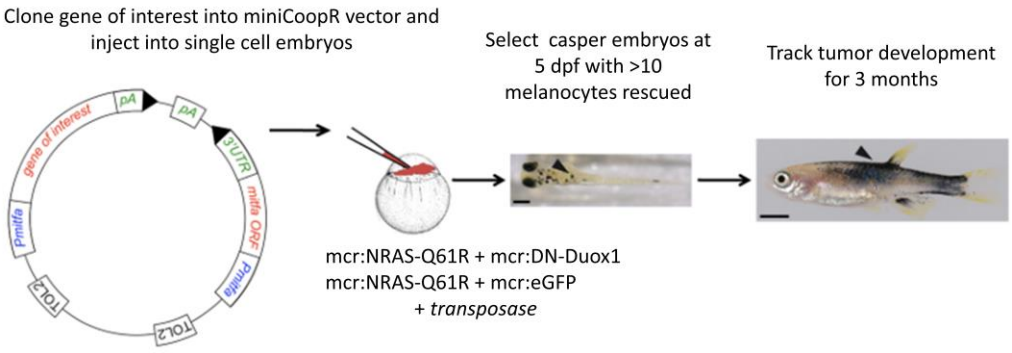

Figure 30: MiniCoopR technology. MinicoopR vector containing the gene of interest under a *mitfa* promoter and a *mitfa* minigene. mcr:NRAS-Q61R + mcr:DN-Duox1 or mcr:NRAS + mcr:EGFP vectors were microinjected in single cell zebrafish embryos with tol2 transposase to integrate them into the genome. At 5 dpf, embryos with more than 10 melanocytes rescued were selected and the fish were tracked monthly for three months. Adapted from Iyengar et al. 2012.

Twenty-five pg of each MiniCoopR plasmid and 25 pg of tol2 transposase mRNA were microinjected into one-cell Casper eggs. Larvae were screened at 5 dpf to select those with melanocyte rescue. These fish were tracked and score monthly for three months (Figure 30). The fish were categorized in five groups depending on the repigmentation state and the development of tumors, as followed: 1) Normal, fish without any repigmentation visible; 2) Low repigmentation, fish with some melanocytes rescued dispersed through all the body; 3) Nevus, fish with a local growth of these rescued melanocytes; 4) Black, fish with a wide repigmentation but not nodular tumors visible; 5) Nodular tumor, fish with some clear vertical growth forming nodular tumors in the fish.

Tumor sampling

Tumors from donor fish euthanized with buffered-tricaine were excised using a scalpel, placed in 1ml of dissection medium (DMEM/F12 (Life Technologies), 100 U/ml penicillin, 100 µg/ml streptomycin, 0.075 mg/ml Liberase (Roche)) and allow the Liberase to act at least 15 minutes at room temperature. Then the dissection medium and the tumor mass were placed in a petri dish and manually

disaggregated using a clean razor blade. After this step, the cells were recovered and washed with the washing medium (DMEM/F12 with penicillin/streptomycin, and 15% heat-inactivated fetal bovine serum (FBS, Life Technologies). The cell suspension was filtered twice through a 40 µm filter (BD), counted, centrifuged at 800 g for 5 min at 4 °C and resuspended in PBS containing 5% FBS to have a final dilution of 100,000 cells/µL.

Allotrasplant in adult zebrafish

Adult zebrafish used as transplant receptors were immunosuppressed to prevent rejection of the donor material. They were anesthetized, using a dual anesthetic protocol to minimize over-exposure to tricaine (Dang et al. 2016). Briefly, fish were treated with tricaine and then transferred to tricaine/isoflurane solution. Afterwards, fish were treated with 30 Gy of split dose sub-lethal X-irradiation (YXLON SMART 200E, 200 kV, 4.5mA) 2 days before the transplantation.

Around 20 anesthetized fish per tumor were injected with 300,000 cells into the dorsal subcutaneous cavity using a 26S-guaged syringe (Hamilton). The syringe was washed in 70% ethanol and rinsed with PBS between uses. Following transplantation, fish were placed into a recovery tank of fresh fish water and then return to the system.

Finally, transplanted fish were tracked weekly during a month, anesthetized and photographed using a mounted camera (Nikon D3100 with a Nikon AF-S Micro Lens) to follow the growth of the tumor cells in the injection area. Then the pigmented tumor size was measured using Adobe Photoshop 2022 as the number of pigmented pixels. Tumor scoring was blind, and experiments were independently repeated at least 3 times. For DN-Duox1 condition, five different tumors were transplanted, while for the GFP condition three different tumors were used.

Generation of DUOX1 and DUOXA1 stable cell lines

HEK293T cultured in DMEM supplemented with 10% FBS, 1% glutamine and 1% penicillin/streptomycin were transfected with lipofectamine 2000 following the manufacturer's instructions. The transient transfection was done with the empty vector pcDNA3.1-N-DYK, and the vector containing the construction with human DUOX1-HA and DUOXA1-V5 obtained from Dr. Thomas L. Leto (Morand et al. 2009). Stable cell lines were selected with 160ug/ul hygromycin resistance. The cells were cultured for 2-4 weeks to allow them to form clones. When a clone appeared was transferred to different wells to expand and continue growing alone. We obtained thirty-five positive clones in this step that grow in the selective medium and were checked by western blotting.

Western Blotting

The clones selected with hygromycin were washed twice with PBS and solubilized in lysis buffer (50 mM Tris-HCl, pH 7,5, 1% IGEPAL, 150 mM NaCl and a 1:20 dilution of the protease inhibitor cocktail P8340 from Sigma-Aldrich). Samples were centrifuged (13.000 g, 10 min at 4ºC) and quantified using the Pierce BCA Protein Assay Kit. They were resolved on 10-8% SDS-PAGE at 120V and transferred 1h at 300 mA to nitrocellulose membranes. Membranes were blocked 1h at RT and incubated overnight at 4°C with anti-HA (1:3000, A00169, GenScript) or a-V5 (1:1000, 461157, Thermofisher). For detection, corresponding horseradish peroxidase conjugated secondary antibodies (1:5000, Amersham) were used. After repeated washes, the signal was detected with the enhanced chemiluminescence Kit Western Bright Sirius (Advansta, K-12043-D10) and ChemiDoc XRS Biorad.

Pharmacological screening

The selected clones were washed with 1X PBS, centrifuged 200 x g for 5 minutes, and counted to plate 25,000 cells/well in 96-wells plates. Cells were then stimulated with 2mM luminol, 40U/mL HRP and 10 μM calcium ionophore A23187 (Sigma-Aldrich) and the luminescence was quickly measured (Figure 31). We acquired kinetics points every 45 seconds during 90 min at 428nm in a Fluostar Omega (BMG Labtech). 500uM Apocynin (CAS 498-02-2, Calbiochem) was used as a negative control.

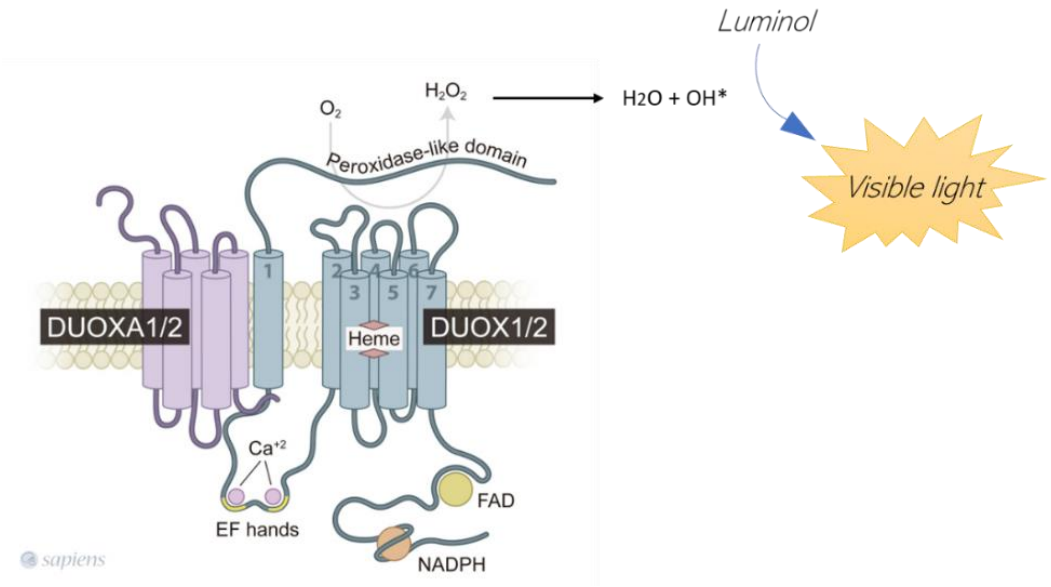

Figure 31: Scheme of peroxide production measurement by luminol. DUOX1 produces hydrogen peroxide, that is broken by HRP, and the reactive oxygen species produced oxidized the luminol that releases energy in the form of light. Adapted from (Faria & Fortunato 2020).

When methods conditions were stablished, we used SCREEN-WELL® FDA approved drug library V2 (ENZO) and test 256 compounds in DUOX1-DUOXA1 overexpressing cell lines.

xdh mutant generation by CRISPR

The crispr RNA (crRNA) obtained from Integrated DNA Technologies (IDT) with the following guide sequence was used: *xdh* crRNA: 5′-GGGTCTGACAGGAACCAAAC-3′. It was resuspended in duplex buffer at 100 µM, and 1 µl was incubated with 1 µl of 100 µM trans-activating CRISPR RNA (tracrRNA) at 95°C for 5 minutes and then 5 minutes at room temperature (RT) to form the complex. Then, the mix was diluted with 1.40 µl of duplex buffer. One µl of this complex was mixed with 0.20 µl of recombinant Cas-9 (10 mg/ml, IDT), 0.25 µl of phenol red, and 2.55 µl of duplex buffer. The mix was injected into one-cell zebrafish eggs.

The F0 generation was crossed with wild type zebrafish to obtain the F1, heterozygotic for the mutation (+/-) and these fish were incrossed to obtain homozygotic mutants (-/-). F1 and F2 generations were genotyped using a PCR to

amplify the fragment affected by the mutation, it was done with the following primers:

Crispr_Xdh-A/B F 5´- GGAATCTGACATTGAGTATTTCCTT-3´

Crispr_Xdh-A/B R 5´- ACATGGTTGCATGAAGAGCC-3´

The purified PCR fragment was sent to do Sanger sequencing to the CAID (Centro de Apoyo a la Investigación y Desarrollo) UMU Service using the primer Crispr_Xdh-A/B R.

Metabolic measure of hypoxanthine, xanthine and uric acid

Twenty 5 days post fertilization (dpf) larvae of each condition (wild type and *xdh* mutant) were transferred to a 1.5ml tube, the medium was removed, and the samples were frozen in dry ice. Methanol (80 %) was added to the samples and supplemented with 1 mM N-Acetyl-Glutamine as an internal standard. Next, they were homogenized using the Omni Tissue Homogenizer. Samples were shaking for 30 minutes at 37°C. Then, they were centrifuged 5-10 minutes at 4°C at 13,000 x g and transferred to fresh tubes. Samples were dried in Vacufuge plus at room temperature for 4-5 hours.

The samples were analyzed by high-performance liquid chromatography-mass spectrometry (HPLC-MS). Samples were injected in an Agilent 6550 Q-TOF Mass Spectrometer (Agilent Technologies, Santa Clara, CA, USA) using an Agilent Jet Stream Dual electrospray (AJS-Dual ESI) interface. The mass spectrometer was operated in the positive mode. Standards were analyzed in the range 10,000-10 nM. The peak area data of standards were used for the calculation of the calibration curve, from which the concentration of both compounds in samples was obtained. Hypoxanthine, xanthine and uric acid concentrations were measured.

NASH feeding and sampling

The diets were prepared using Golden Pearl diet 5-50 nm Active Spheres (Brine Shrimp Direct) as previously described (Michael et al. 2021). Two different diets were used to feed the fish, normal diet as control (ND) and 10% High Cholesterol Diet (HCD), supplemented with 10% of cholesterol.

At 7 days post fertilization (dpf), 80 larvae of each condition were transferred to the feeding tanks where they were acclimatized for 1 day. At 8 dpf, they were fed until 15 dpf with ND and HCD. The amount of food given was calculated to feed 0.1 mg of food per larvae per day, and larvae were fed twice each day. Each tank was provided with 6-8 mg of ND or HCD daily. Tanks were regularly clean and larval density checked. To sample the larvae for each technique, a vacuum system was used to aspirate 90-95% of the water and then larvae were transferred from the tanks to petri dishes.

Oil Red O Staining (ORO)

To address diet induced hepatic steatosis, twenty larvae per condition (fed with ND or with HCD) were transferred to a 2 mL round bottom tube and place on ice about 10 minutes. Most of the media was removed, and larvae was rinsed twice with 1X PBS. To fix the larvae, they were incubated overnight in 2 mL of 4 % of paraformaldehyde (PFA) solution at 4°C. Next morning, larvae were washed three times with 2 mL of 1X PBS and transferred with a glass pipette from the tube to a 12 well plate with mesh well inserts filled with 5mL of 1X PBS. Then, the inserts with the larvae were transferred to another well with 5 mL of 60% isopropanol and incubated for 30 minutes. Afterwards, the mesh insert with the larvae were transferred to fresh-prepared 0.3% ORO in 60% isopropanol solution and incubated 3h at with gentle rocking protected from light. After the staining, larvae were washed twice for 30 minutes each with 60% isopropanol and thrice for 5 min in 1X PBS-0.1% Tween, and then stored in 80% glycerol at 4°C until imaging. finally, larvae were imaged using a Porcelain Spot Plate with 80% of glycerol and positioning the liver optimally with an eyelash tool. Images were taken under a stereomicroscope with a color camera. Hepatic steatosis was scored as: no ORO staining = none; light red ORO staining = mild; red-dark red ORO staining = severe.

Histology

Twelve to fifteen 15 dpf larvae per condition (fed with ND or with HCD) were rinsed with clean fish water and fixed in 10 % formalin solution at 4°C overnight. Three larvae per cassette were mounted in a drop of 2 % low melting point agarose and orientated with an eyelash to be in the same stack. When the drop was dry, the

agarose with the immobilized larvae was cut and put into the histology cassettes. Three larvae per cassette were mounted and at least three cassettes per group were used. The experiment was repeated three times. The samples were processed, cut and stained with hematoxylin and eosin by the Albert Einstein College of Medicine Histotechnology and Comparative Pathology Facility. All the images were coded to be analyzed by two independent histopathologist and classified attending to NASH histological features.

ROS detection

Ten 15 dpf larvae per condition (fed with ND or with HCD) were incubated with 10 µM dihydroethidium (DHE) for 1 h at 28.5 °C in the dark, rinsed in E3 medium and anesthetized with 1X tricaine (200 µg/mL) dissolved in E3 medium. To image them we use a special device described in (Huemer et al. 2017). Briefly, the zWEDGI device has a microfluidic system which allow to immobilize larvae to image them in the right position at advanced ages when the swimming bladder is well developed. Images were captured with an epifluorescence LEICA MZ16FA stereomicroscope set up with green and red fluorescent filters. All images were acquired with the integrated camera on the stereomicroscope and were analyzed to determine the amount of ROS present in the zebrafish livers. ImageJ software was employed to obtain the mean intensity fluorescence of the zebrafish larvae liver drawing a region of interest (ROI).

Proteomics

S-trap protein digestion

Twenty 15 dpf larvae per condition (fed with ND or with HCD) were anesthetizing in 1xTricaine prepared in cold PBS, livers were collected quickly into a prechilled tube, supernatant was discarded, and tubes were immediately frozen into liquid nitrogen. Twenty zebrafish livers were extracted for each condition. Samples were then homogenized in 5 % SDS, 50mM TEAB, 17% DTT and incubated 30 minutes at 60 °C. Samples were then alkylated with 20 mM iodoacetamide in the dark for 30 minutes. Afterward, phosphoric acid was added to the sample at a final concentration of 1.2 %. Samples were diluted in six volumes of binding buffer (90% methanol and 10 mM ammonium bicarbonate, pH 8.0). After gentle mixing, the

protein solution was loaded to an S-trap filter (Protifi) and spun at 500 g for 30 sec. The sample was washed twice with binding buffer. Finally, 1 µg of sequencing grade trypsin (Promega), diluted in 50 mM ammonium bicarbonate, was added into the S-trap filter and samples were digested at 37°C for 18 h. Peptides were eluted in three steps: (i) 40 µl of 50 mM ammonium bicarbonate, (ii) 40 µl of 0.1% TFA and (iii) 40 µl of 60% acetonitrile and 0.1% TFA. The peptide solution was pooled, spun at 1,000 x g for 30 sec, and dried in a vacuum centrifuge.

Sample desalting

Prior to mass spectrometry analysis, samples were desalted using a 96-well plate filter (Orochem) packed with 1 mg of Oasis HLB C-18 resin (Waters). Briefly, the samples were resuspended in 100 µl of 0.1% TFA and loaded onto the HLB resin, which was previously equilibrated using 100 µl of the same buffer. After washing with 100 µl of 0.1% TFA, the samples were eluted with a buffer containing 70 µl of 60% acetonitrile and 0.1% TFA and then dried in a vacuum centrifuge.

LC-MS/MS Acquisition and Analysis

Samples were resuspended in 10 µl of 0.1% TFA and loaded onto a Dionex RSLC Ultimate 300 (Thermo Scientific), coupled online with an Orbitrap Fusion Lumos (Thermo Scientific). Chromatographic separation was performed with a two-column system, consisting of a C-18 trap cartridge (300 µm ID, 5 mm length) and a picofrit analytical column (75 µm ID, 25 cm length) packed in-house with reversed-phase Repro-Sil Pur C18-AQ 3 µm resin. To analyze the proteome, peptides were separated using a 180 min gradient from 4-30% buffer B (buffer A: 0.1% formic acid, buffer B: 80% acetonitrile + 0.1% formic acid) at a flow rate of 300 nl/min. The mass spectrometer was set to acquire spectra in a data-dependent acquisition (DDA) mode. Briefly, the full MS scan was set to 300-1200 m/z in the orbitrap with a resolution of 120,000 (at 200 m/z) and an AGC target of 5x10e5. MS/MS was performed in the ion trap using the top speed mode (2 secs), an AGC target of 1x10e4 and an HCD collision energy of 35. Proteomic was performed by the Albert Einstein College of Medicine Proteomics Facility.

Proteome raw files were searched using Proteome Discoverer software (v2.4, Thermo Scientific) using SEQUEST search engine and the SwissProt human database

(updated February 2020). The search for total proteome included variable modification of N-terminal acetylation, and fixed modification of carbamidomethyl cysteine. Trypsin was specified as the digestive enzyme with up to 2 missed cleavages allowed. Mass tolerance was set to 10 pm for precursor ions and 0.2 Da for product ions. Peptide and protein false discovery rate was set to 1 %. Following the search, data was processed as described previously (Aguilan et al. 2020). Briefly, proteins were log2 transformed, normalized by the average value of each sample and missing values were imputed using a normal distribution 2 standard deviations lower than the mean. Statistical regulation was assessed using heteroscedastic T-test (if p-value < 0.05). Data distribution was assumed to be normal, but this was not formally tested. For proteomics analysis we used Excel to manage and order the data, as well as, to represent Principal Component Analysis (PCA). R studio was used to perform the Volcano plots analysis. Some databases were used as GOrilla (http://cbl-gorilla.cs.technion.ac.il/) to visualize the upregulation and downregulation of pathways between comparisons. STRING (https://string-db.org/) was used to create protein-protein interaction networks and Cytoscape to represent these data.

Statistical analysis

Data are shown as mean ± SEM and they were analyzed by analysis of variance (ANOVA) and a Tukey multiple range test to determine differences among groups. The survival curves were analyzed using the log-rank (Mantel-Cox) test. The sample size for each treatment is indicated in the graph and/or in the figure legend. Statistical significance was defined as *p < 0.05 **p<0.01, *** p<0.001 ****p<0.0001. The differences between two samples were analyzed by the Student *t*-test. The contingency graphs were analyzed by the Chi-square (and Fisher's exact) test and correlation studies with Pearson's correlation coefficient.

CHAPTER 1

RESULTS

1. *DUOX1* expression is associated with melanoma patient prognosis

The survival rate of patients with high, medium and low expression of *DUOX1* in melanoma patients of The Cancer Genome Atlas (TCGA) cohort was analyzed. The patient's data were included in four different quartiles, being the first quartile, low expression, second and third quartile medium expression and the fourth quartile high expression. Surprisingly, high *DUOX1* transcript levels in early-stage melanoma were associated with poor patient survival, while low *DUOX1* levels showed similar prognosis than patient with medium levels (Figure 32A). However, no statistically significant differences in patient survival were observed associated to *DUOX1* levels in late-stage melanoma (Figure 32A). As expected, the survival of late stage-melanoma was significantly lower than in early-stage melanoma (Figure 32B). Furthermore, *DUOX1* mRNA expression was lower in metastatic than in primary melanoma (Figure 32C) and enrichment analysis of pathways of genes that negatively correlated with DUOX1 expression revealed alterations in pathways involving immune system, complement activation and allograft rejection, among others (Figure 32D).

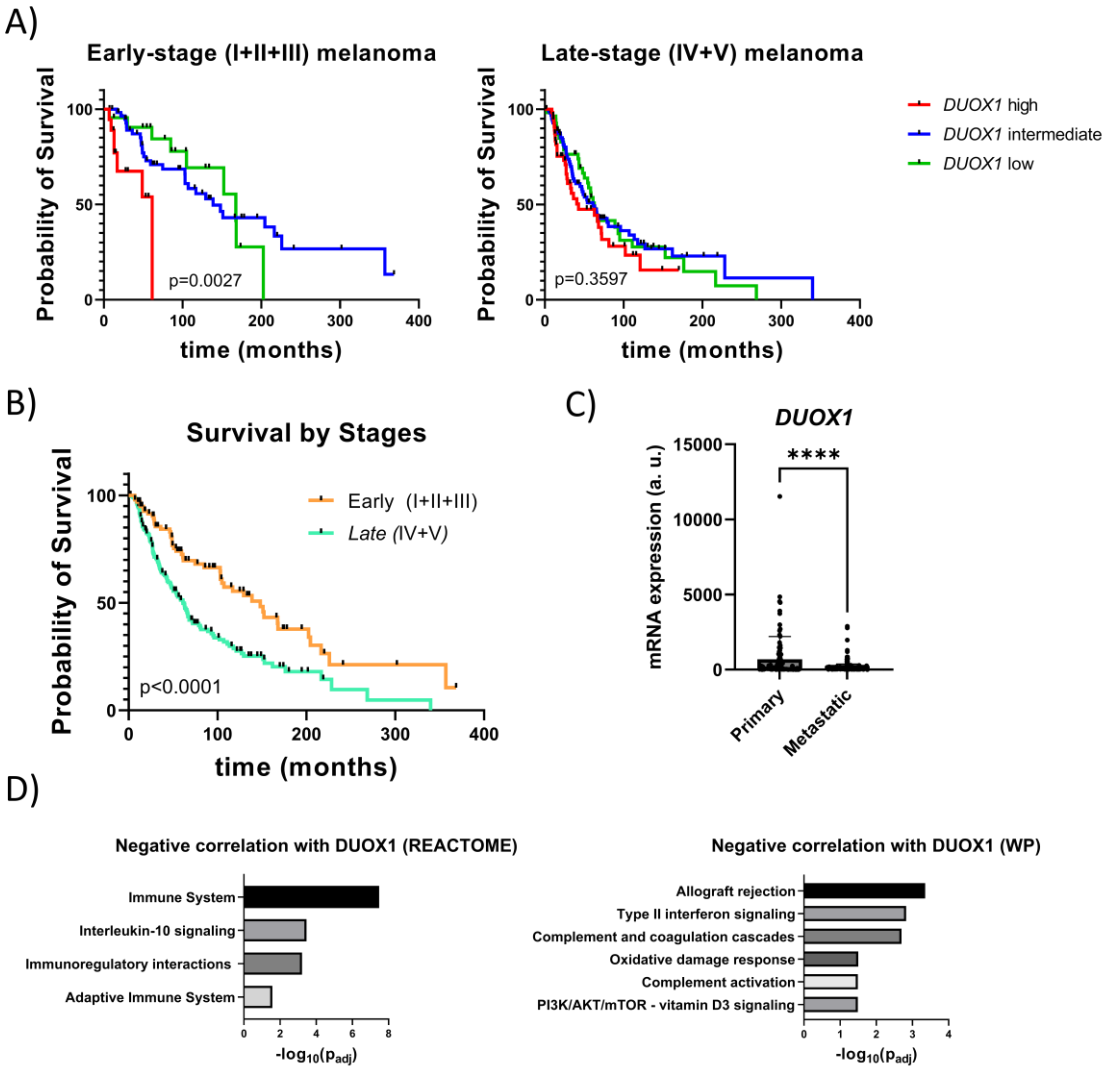

Figure 32: *DUOX1* expression correlates with melanoma patient survival and decreases in metastatic melanoma. A) Kaplan-Meier survival analysis of TCGA cohort of early (I+II+III Clark levels at diagnosis) and late (IV and V Clark levels at diagnosis) stage melanoma patients according to their *DUOX1* transcript levels: first quartile (Low), second and third (Medium) and fourth (High) Statistical significance was calculated with Mantel-Cox test. B) Kaplan-Meier survival analysis of TCGA cohort of melanoma patients according to Clark level classification at diagnosis: early (I+II+III) and late (IV+V). Statistical significance was calculated with Mantel-Cox test C) *DUOX1* transcript levels in primary and metastatic melanoma from TCGA melanoma cohort. Each dot represents a patient, and the mean is also shown. ****p<0.0001 according to unpaired Student *t* test. D) Enrichment analysis of Reactome and WP (Refseq non redundant proteins)-associated functions in TCGA melanoma patients according to *DUOX1* expression levels. Only the pathways with the highest statistical significance are shown. a.u., arbitrary units.

2. Melanocyte Duox1 inhibition does not affect melanocyte transformation and early melanoma progression.

To study the role played by DUOX1-derived reactive oxygen species in melanoma early transformation we used the MiniCoopR technology. MiniCoopR vector is a plasmid that express the GOI under the *mitf*a promoter, this promoter is specific for melanocytes and the GOI will be expressed only in cells that express *mitfa*. This plasmid contains also a *mitfa* minigene to easily follow the transformed cells producing melanin in Casper fish (Iyengar et al. 2012).

MiniCoopR mitfa:DN-Duox1 (mcr:DN-Duox1) and MiniCoopR mitfa:NRAS-Q61R (mcr:NRAS-Q61R) constructs were microinjected in one-cell Casper eggs to co-express oncogenic NRAS and inhibit Duox1 in melanocytes. As a control, MiniCoopR mitfa:EGFP (mcr:EGFP) was injected instead of mcr:DN-Duox1. Fish were screened at 5 dpf to select those ones with more than 10 melanocytes rescued and then the fish were tracked for three months to see the development of tumors (Figure 33A). Melanomas were categorized in five groups depending on the repigmentation or appearance of tumors: I normal, II low repigmentation, III nevus, IV black, V nodular tumor (Figure 33B). The first group included fish with no melanocyte rescue, the second group included fish with some isolated melanocytes, the third group is made up of fish with a bigger zone of melanocytes that grow together forming a nevus, the fourth group included fish with more than 50% of the body showing melanocyte rescue but no presence of tumor that growth over the skin, and the fifth group included fish with presence of nodular tumor generally in the dorsal, anal or caudal fins or in the back of the fish. Although the difference between nodular and black groups was established when vertical growth could be appreciated, the fourth group might contain some fish with nodular tumors.

While at 30dpf the fish injected with mcr:NRAS-Q61R/mcr:DN-Duox1 showed a higher percentage of nodular tumors, this effect was no longer observed at later time points and did not show statistically significant differences (Figure 33 C & D).

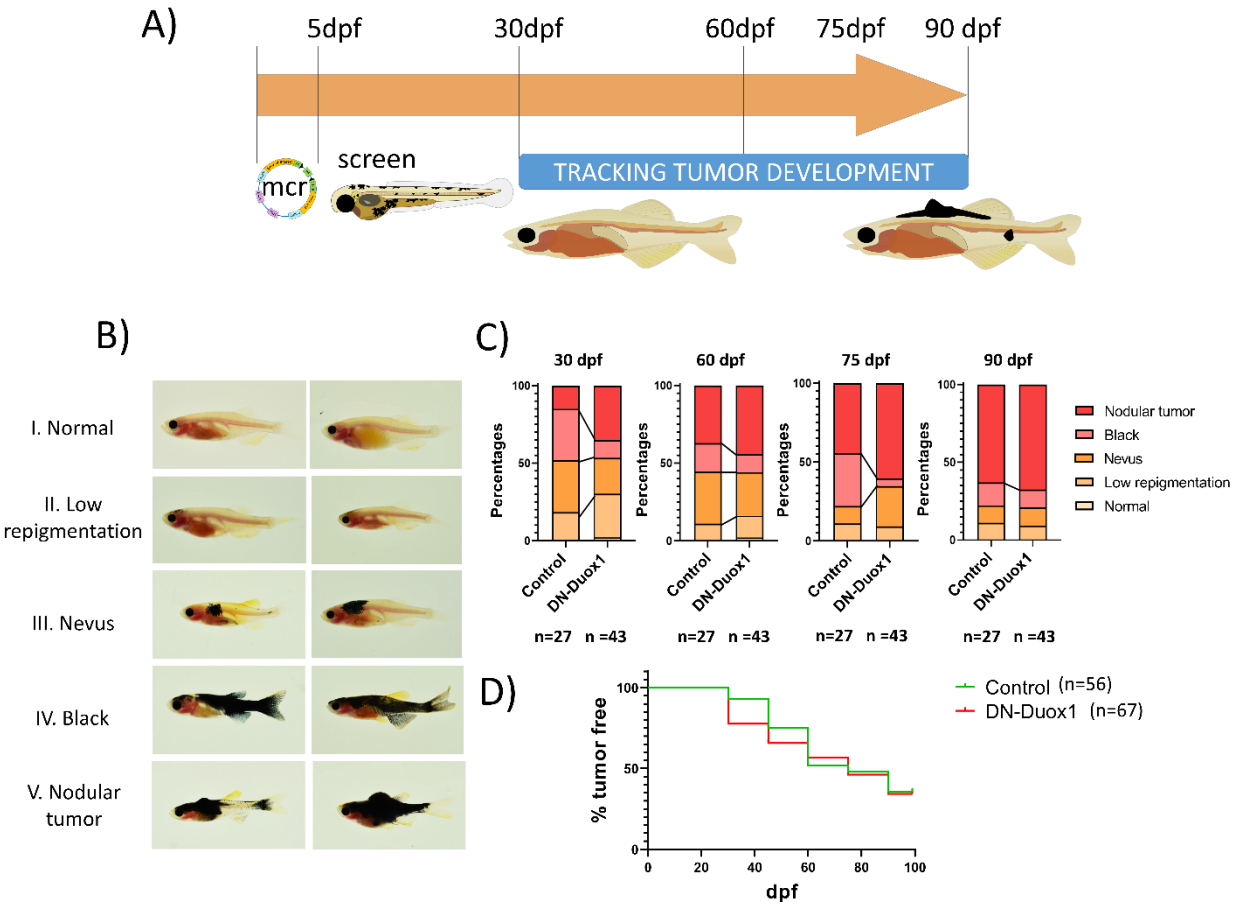

Figure 33: Melanocyte Duox1 inhibition does not affect melanocyte transformation and early melanoma progression. A) Schematic representation of the procedure to co-express oncogenic NRAS-Q61R and DN-Duox1 in melanocytes. Zebrafish one-cell Casper eggs were injected with mcr:NRAS-Q61R + mcr:DN-Duox1 (DN-Duox1) or with mcr:NRAS-Q61R + mcr:EGFP (Control). Larvae were screened at 5 dpf for the presence of melanocytes and images were acquired monthly for 3 months to track melanoma development. B) Representative images of the 5 different categories established to classify tumor progression. C) Percentages of fish in the different categories at 30, 60, 75 and 90 dpf. D) Tumor free curve. Representation of the percentage of fish without nodular tumors. ns, non-significant.

3. Duox1 inhibition cell-autonomously reduces aggressiveness and growth of transplanted melanomas

To investigate the role of Duox1 in melanoma aggressiveness and invasiveness, 300,000 cells from melanoma nodular tumor developed with the MiniCoopR system were transplanted in the dorsal sinus of one-year old adult Casper recipients previously irradiated with 30 Gy. The development of melanomas was tracked for one month weekly. Both sides of the fish were imaged to visualize tumor cell growth and dissemination *in vivo* over time (Figure 34A).

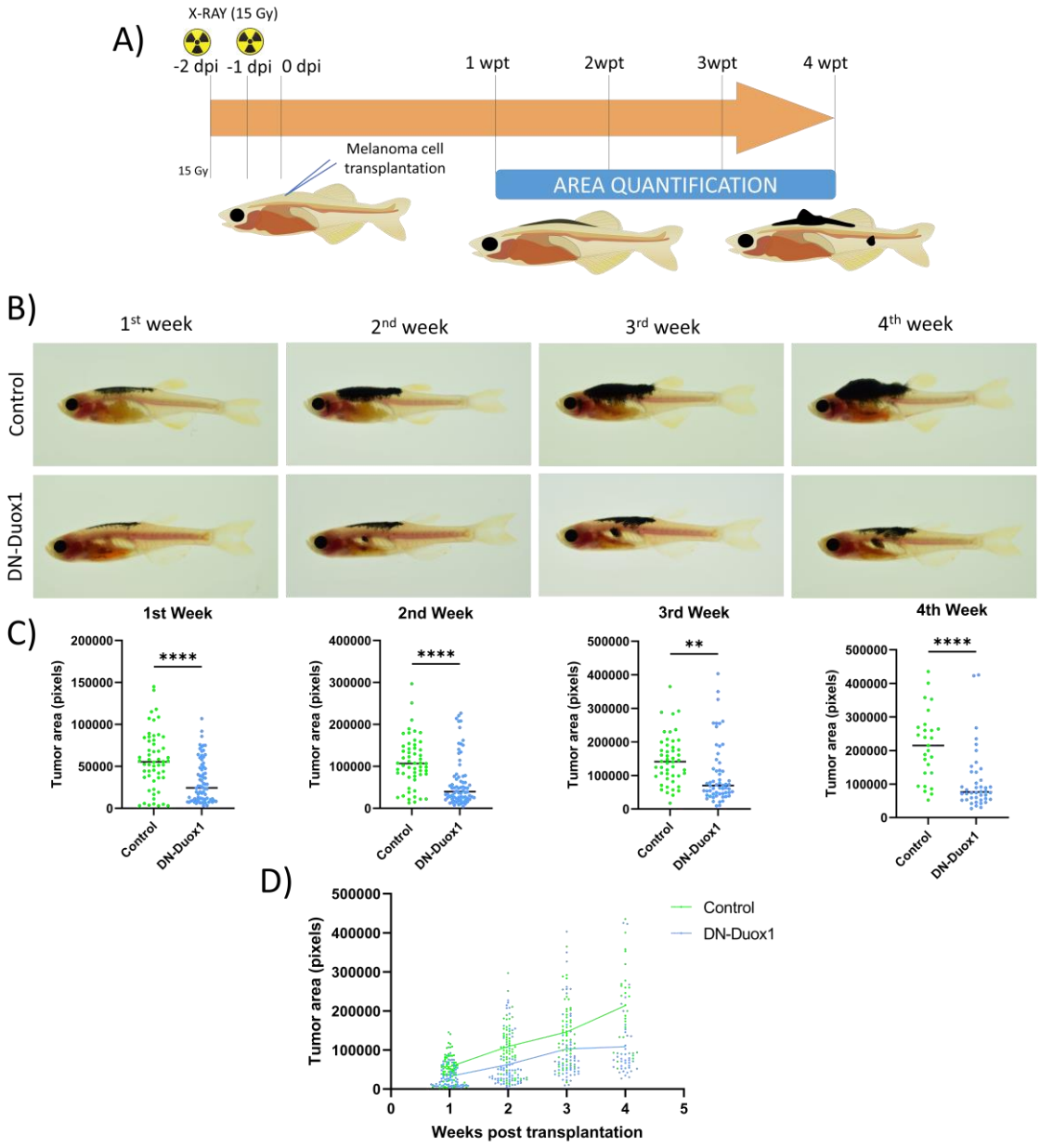

Figure 34: Duox1 inhibition cell-autonomously reduces aggressiveness and growth of transplanted melanomas. A) Scheme showing adult transplantation procedure. One-year-old Casper zebrafish were irradiated 2 days post transplantation to avoid tumor rejection. Three hundred thousand cells from the nodular tumors of either mcr:NRAS-Q61R/mcr:DN-Duox1 (DN-Duox1) or mcr:NRAS-Q61R/mcr:EGFP (Control) fish were subcutaneously injected in pre-irradiated recipients and images were taken weekly during the following 4 weeks post transplantation (wpt) and analyzed as indicated in the Materials and Methods section. B) Representative images of transplanted melanoma growth rate of mcr:NRAS-Q61R/mcr:DN-Duox1 and mcr:NRAS-Q61R/mcr:EGFP in pre-irradiated adult Casper zebrafish. C) Average tumor size for each week post transplantation. Each dot represents a recipient-transplanted fish and the mean is also shown. **p<0.01, ****p<0.0001 according to unpaired Student *t* test. D) Growth rate of transplanted mcr:NRAS-Q61R/mcr:DN-Duox1 (DN-Duox1) and mcr:NRAS-Q61R/mcr:EGFP melanomas (Control). DN-Duox1 (N=5 tumors and 111 recipient fish) and for EGFP (N=3 and 72 recipient fish).

Tumor engrafment was visible at 7 days post-trasplantation in both conditions (Figure 34B) and 41.7% of control and 46.0% of DN-Duox1 remained alive at the end of the experiments. The recipient fish trasplanted with Duox1-deficient-melanomas showed significant smallest tumors than their control counterparts since the first week after transplantation to the end of the experiment (Figure 34C). In addition, recipients trasplanted with Duox1-deficient-melanomas showed a significant lower growth rate than fish transplanted with control melanomas (Figure 34D). The sex of the recipient fish did not affect the growth of either control or Duox1-deficient melanomas (data not shown). Strikingly, fish transplanted with Duox-1 deficient melanomas showed more incidence of cells migrating to distant parts of the injecction area (metastasis) than the ones injected with control melanomas (Figure 35).

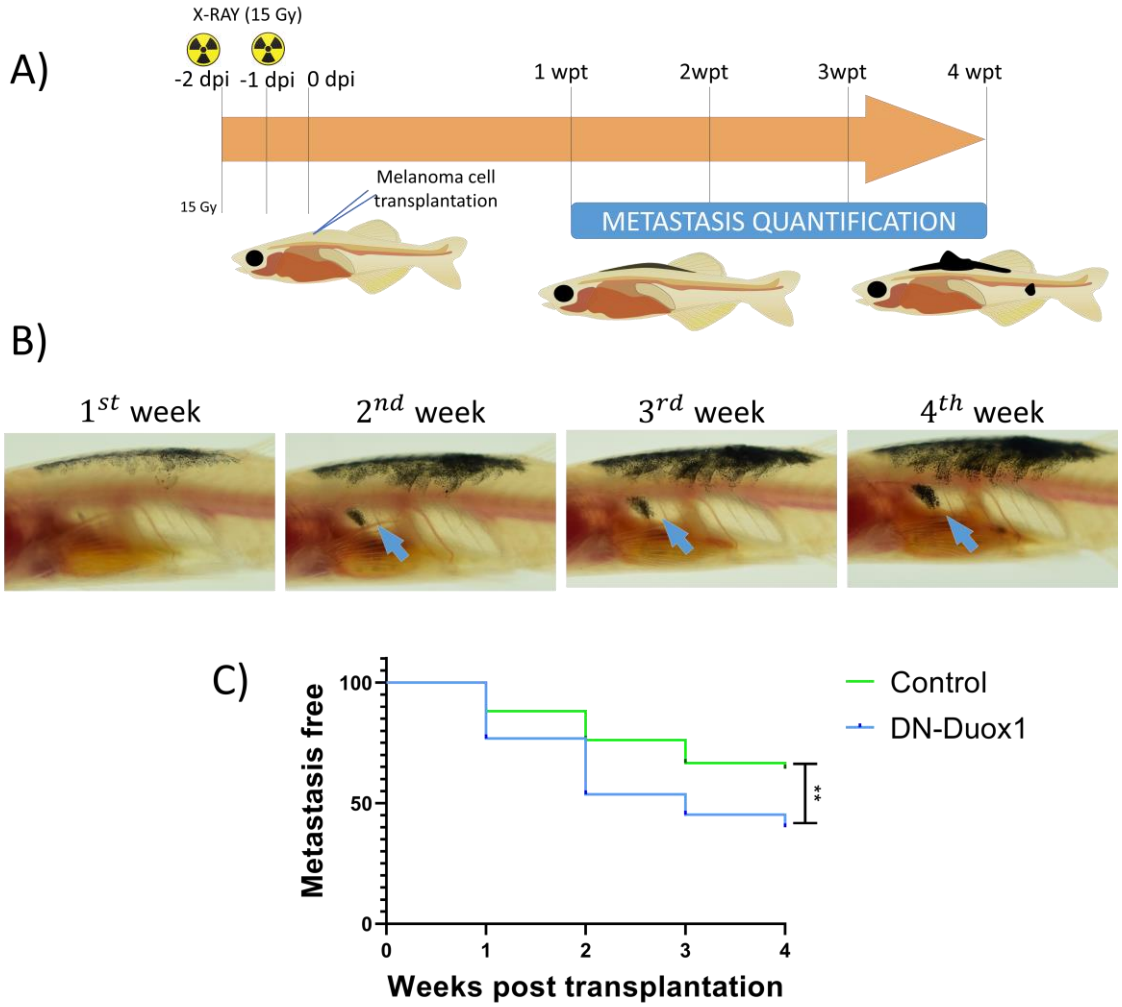

Figure 35: Duox1-deficient oncogenic melanocytes show more invasiveness than the controls. A) Scheme diagram of adult allotransplantation assays. B) Representative images of a metastasis done in 4 weeks post transplantation (wpt). Arrows indicate the metastasis C) Metastasis-free curve of adult zebrafish injected with mcr:NRAS-Q61R/mcr:DN-Duox1 (DN-Duox1) and with mcr:NRAS-Q61R/mcr:EGFP (Control). **p<0.01 according to a Log rank Mantel-Cox test.

4. DUOX1 specific pharmacological screening

In order to find specific inhibitors for DUOX1, HEK293-T cells stably expressing human DUOX1-HA and DUOXA1-V5 were stablished. Thirty-five clones were obtained using a selection with hygromycin. DUOX1 and DUOXA1 co-expression was checked by western blot and three positive clones were obtained, named 7, 20 and 30 (Figure 36). We chose clone number 25 as a negative control due to its good growth rate and lack of expression of both proteins.

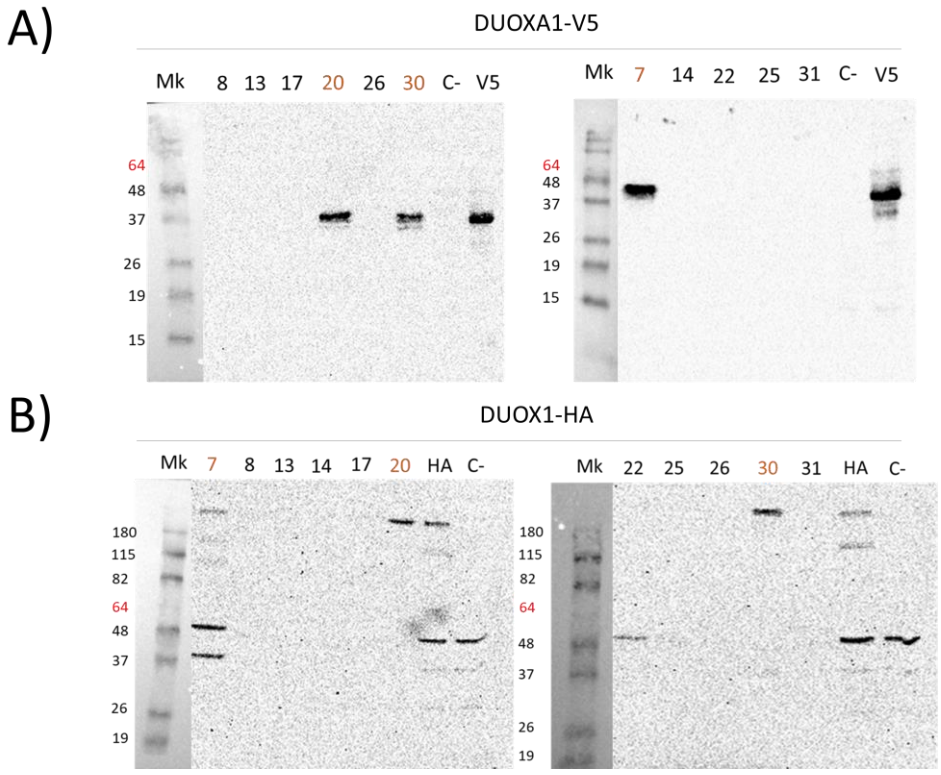

Figure 36: Screening for DUOX1 and DUOXA1 positive clones. Expression of DUOX1 and DUOXA1 in clones by Western Blot with anti-V5 (A) and anti-HA (B), epitopes fused to the proteins of interest. Molecular weight markers (Mk). Empty vector was used as a negative control (C-) and transitory transfection with the DUOXA1-V5 or DUOX1-HA vectors were used as positive control (V5 and HA respectively).

Once the expression was confirmed, we test the functionality of these proteins measuring peroxide production, the main activity of DUOX1. Using these cell lines, we stablished a method to detect peroxide production by DUOX1 based in HRP activity and luminol (Zhu et al. 2016). The peroxidase uses the peroxide produced by DUOX1 forming water and oxygen radicals that oxidate luminol which

emit light or energy in the process producing luminescence measures. For DUOX1 activation we used a calcium ionophore because the enzyme is calcium dependent.

After trying different cell densities to perform the assay in 96-well plates maintaining the cells in optimal conditions, we checked several ionophore concentrations to activate DUOX1 and different concentration of apocynin, used as inhibitor. We observed that 500 µM apocynin reduced hydrogen peroxide levels to the expression of the DUOX1/DUOXA1 negative clone. Once the conditions were well stablished, we tried 259 compounds from the SCREEN-WELL® FDA approved drug library V2 (ENZO) identifying inhibitors as compounds that inhibited peroxide production. Surprisingly, we identified some compounds increasing DUOX1 activity.

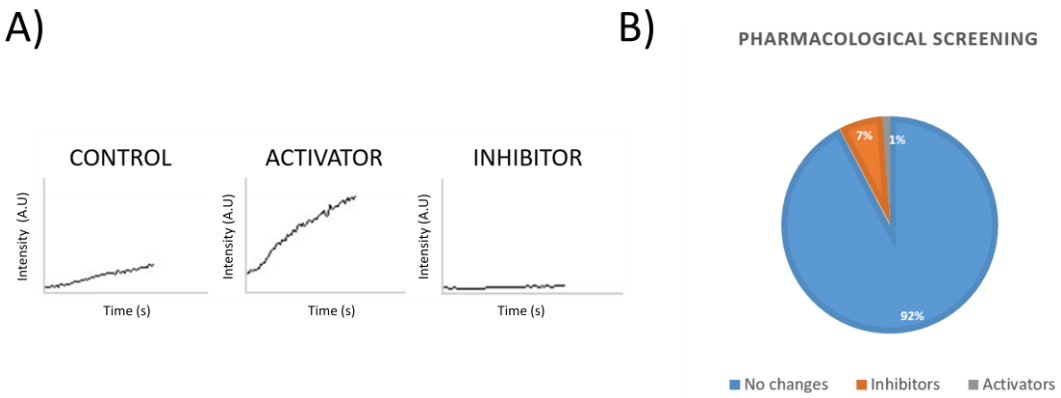

Figure 37: Pharmacological screening of FDA-approved drug library. A) Examples of the detection of control, activators and inhibitors. An activator compound produces an increase of luminescence and an inhibitor a decrease compared to the control. B) Percentage of activators and inhibitors identified in the pharmacological screening.

Among the 256 compounds checked, we identified activators that increase the luminescence intensity and inhibitors that decreased the normal luminescence production (Figure 37A). We found 17 potential inhibitors (7 % of total compounds tried in this assay) and 3 potential activators of DUOX1 (1 % of total compounds) (Figure 37B).

As it is shown in Table 2, we found drugs used to treat several cancers, such as leukemias, Kaposi´s sarcoma, glaucoma, breast cancer or lymphomas; drugs used to combat infections, antipsychotic, etc. We discard some drugs, including Daunorubicin HCl, Doxorubicin HCl, Lomeflaxacin HCl and Raloxifene HCl because

they could be displaying an unspecific inhibitor effect due to the HCl molecule that could be reacting directly with the OH* radical promoting its reduction. The rest, need to be tested to check their selectivity against DUOX1.

INHIBITORS	Treatment for	Mechanism of action
Artesunate	Severe malaria	Generate free radicals which inhibit protein and nucleic acid synthesis
Astemizole	Allergy	Antagonist of histamine receptor
Butaclamol	Antipsychotic	Dopaminergic antagonist
Clozapine	Antipsychotic	Serotonin and dopaminergic antagonist
Daunorubicin HCl	Leukemia	Interference with DNA replication
Dipyridamole	Postoperative thromboembolic event	Blocks uptake and metabolism of adenosine by erythrocytes and vascular endothelial cells
Doxorubicin HCl	Various cancers and Kaposi's Sarcoma	Intercalation, DNA strand breakage and inhibits topoisomerase II activity
Gemfibrozil	Hyperlipidemia	Activates PPARα which alters lipid metabolism
Idarubicin	Acute myeloid leukemia (AML)	Intercalation, DNA strand breakage and inhibits topoisomerase II activity
Lomefloxacin HCl	Infections	Interference with the activity of the bacterial enzymes DNA gyrase and topoisomerase IV
Physostigmine sulfate	Glaucoma	Inhibits acetylcholinesterase
Raloxifene HCl	Osteoporosis and invasive breast cancer	Estrogen agonist and antagonist via differential effects on the tissue-specific receptors
Telmisartan	Hypertension, diabetic nephropathy, and heart failure	Interferes the binding of angiotensin II with its receptor
Terfenadine	Antihistamine	Compete with histamine for binding H1 receptors
Tylosin tartrate	Infections	Inhibit protein synthesis by binding the 50S ribosome
Vinblastine sulfate	Breast and testicular cancer, neuroblastoma, Hodgkin's and non-Hodgkins lymphoma, and Kaposi's sarcoma.	Interaction with tubulin, which inhibits mitosis at metaphase
Xamoterol hemifumarate	Heart failure	β1-adrenoceptor partial agonist
ACTIVATORS	**Treatment for**	**Mechanism of action**
Ceftazidime	Infections	Direct inhibition of specific Proteien Binding Penicillin
Idebenone	Visual impairment	Increases ATP production, reduces free radicals, inhibits lipid peroxidation, and protects from oxidative damage
Isoniazid	Tuberculosis infections	Inhibits the synthesis of mycoloic acids

Table 2: DUOX1 activators and inhibitors identified. The diseases for which they are approved in the clinic and its mechanisms of action are shown. Information was obtained from https://go.drugbank.com/drugs/.

DISCUSSION

Melanoma is the fifth most common cancer worldwide, and the most aggressive skin cancer because of its high ability to metastasize. Emerging evidence suggested that oxidative stress is involved in the development of several chronic diseases and in the transformation and progression of many common cancers, including melanoma. In particular, it has been shown a complex crosstalk between oxidative stress and inflammatory and immune responses (Cannavo et al. 2019). The inflammatory response induces the recruitment of innate and adaptive immune cells within the tumor which, in turn, can induce oxidative stress that is involved in many steps of melanoma development, such as DNA damage and mutation of melanoma-associated genes, cell metabolism, response to hypoxia, tumor immunity and metastasis (Wittgen & van Kempen 2007).

The crosstalk between melanoma cancer cells and immune cells is unclear and remains under investigation. The interaction of melanoma cells with other resident cells in the tumor microenvironment can influence tumoral proliferation, differentiation, and progression. Tumor cells could be eliminated by the immune system, immunosurveillance, or could use mechanisms to proliferate, immune escape (Passarelli et al. 2017). Even could be using cells as macrophages to survive and travel to other organs metastasizing (Qiu et al. 2021).

It is well established that ROS play a crucial role in the early development, progression, and suppression of many types of cancer. In this study, we have focused on DUOX1, an important NADPH oxidase highly expressed in the skin (Candel et al. 2014). We found that while high *DUOX1* transcript levels in early-stage melanoma are associated with poor patient survival, low *DUOX1* levels show similar prognosis than patient with medium levels. However, no statistically significant differences in patient survival were observed associated to *DUOX1* levels in late-stage melanoma, suggesting the relevance of DUOX1 in early melanoma progression. In addition, it is important to highlight that altered signaling pathways involved in immune system, complement activation and allograft rejection were observed in melanoma expressing low levels of *DUOX1*, suggesting the importance of oxidative stress balance in melanoma progression and the dramatic impact of the dysregulation of DUOX1-derived ROS in melanoma patient prognosis. This complex role of DUOX1 in melanoma may be explained considering the dual role of ROS in cancer (Galadari et

al. 2017). Thus, it has been shown that on the one hand elevated ROS production could cause DNA damage and prompt to oncogene activation or anti-oncogene inactivation, which facilitates tumor progression. In these conditions, cancer cells require higher energy levels to maintain the abnormal growth rates and excessive metabolism, resulting in higher ROS production (Galadari et al. 2017). On the other hand, cancer cells could attract immune cells and promote an inflammatory microenvironment that supports tumor cell proliferation (Pollard 2004, Rajput & Wilber 2010). This could explain why antioxidants suppress cancer initiation in some contexts (Gao et al. 2007, Glasauer & Chandel 2014) while increasing cancer initiation in other contexts (Harris et al. 2015, Sayin et al. 2014). Several articles have shown that increasing dietary antioxidants does not reduce cancer incidence (Alpha-Tocopherol 1994, Deghan Manshadi et al. 2014, Ebbing et al. 2009, Goodman et al. 2004, Moyer & Force 2014). Others shown the good properties of some dietary flavonoids (Merlin et al. 2021) and polyphenols (Khan et al. 2020) as antioxidants by supressing cancer via p53 signalling pathway. Despite the comercial popularity of a huge amount of antioxidant molecules and its benefits, the role of antioxidants in therapy for many diseases needs to be determined and requires more investigation to shed ligh on this complex topic (Athreya & Xavier 2017, Harris & DeNicola 2020, Yasueda et al. 2016).

The impact of ROS in melanoma seems to be even more complex, since melanoma cells in the blood experienced oxidative stress that was not observed in subcutaneous tumors and, thus, oxidative stress limits distant metastasis of melanoma cells in vivo (Piskounova et al. 2015). These results are consistent with poor survival of melanoma patients with high expression of *DUOX1* and with the downregulation of *DUOX1* in metastatic melanomas. Furthermore, they suggest that DUOX1 plays a dual role in melanoma, as it was confirmed with our zebrafish model with inhibition of Duox1 in melanoma cells. Although we did not find any significant effect of this enzyme in melanocyte transformation and early melanoma progression, allotransplantation experiments in pre-irradiated, i.e immunocompromised, zebrafish recipients revealed that Duox1-deficient melanoma cells showed decreased growth but, paradoxically, generated more metastasis than control melanomas. Therefore, Duox1-derived ROS may facilitate primary melanoma growth but limit distant metastasis in zebrafish, as it has been

shown with xenotransplanted human melanoma cell lines in immunocompromised mice (Piskounova et al. 2015). These results, together with the enrichement of immune system pathways observed in human melanoma expressing low levels of *DUOX1*, highlight the relevance of the crosstalk between DUOX1-derived ROS and antitumor immunity. Future experiments overexpressing Duox1 in melanoma cells and using immunocompromised Casper individuals injected with the MinicoopR would be very informative to clarify these issues.

The relevance of DUOX1 in melanoma (this study) and in skin chronic inflammatory diseases (Candel et al. 2014), point to DUOX1 as a pharmacological target. Therefore, we developed a melanoma cell line that overexpress both DUOX1 and its maturation factor DUOXA1, to perform pharmacological screening in order to find specific activators or inhibitors of this enzyme. Although several promising hist were found, more experiments will be needed to confirm their specificicity over DUOX1 and discard those that also inhibit other NADPH oxidases.

CHAPTER 2

RESULTS

1. Generation of a Xdh-deficient zebrafish line

To investigate *in vivo* the role played by Xdh in NAFLD/NASH disease, we generated a mutant with a deficiency in this enzyme. The *xdh* mutant was generated using the Crispr-Cas9 technology as it was explained in Materials and Methods. We designed a guide against the third exon, and the target region was amplified and sequenced to check that the predicted sequence and the actual sequence were identical. Then we injected the guide with recombinant Cas9 and checked the efficiency by PCR amplification, Sanger sequencing and bioinformatic analysis of the target sequence. The F1 was genotyped by PCR as described in Materials & Methods to find *xdh* heterozygotes with a mutation that generates a premature stop codon, which were then incrossed to obtain the F2 and obtain *xdh* mutant (-/-). Finally, the different mutant alleles were identified by Sanger sequencing.

After genotyping we found females and males homozygotes for a 11 bp deletion (AGTTTGGTTCC). The deletion was generated at 150 bp from the starting methionine, in the third exon of the gene (Figure 38). Xdh is a protein of 1351 amino acids which is encoded by 36 exons. The truncated protein generated would have 50 amino acids from the original Xdh and 2 additional ones that were not present in the original protein. The mutation is c.151-162del(p.G50Mfs*2) (Figure 39).

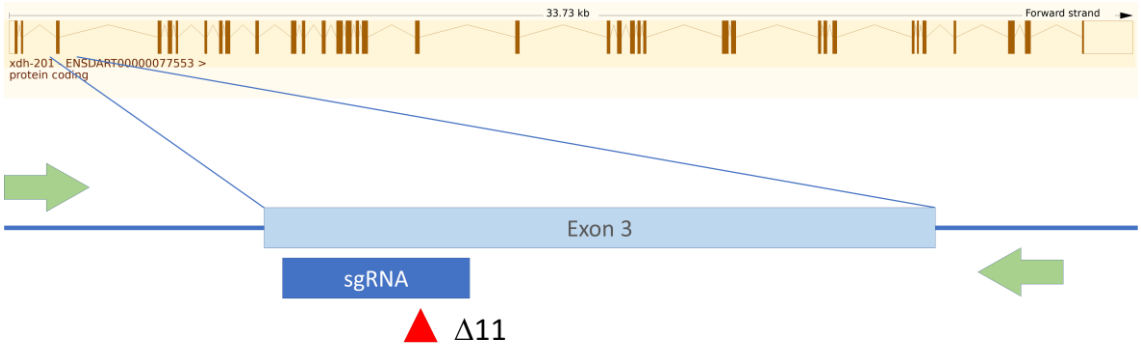

Figure 38: Schematic representation of the sequence of the *xdh* mutant allele. The guide used is shown in blue, the generated mutation is shown in red, and the third exon of *xdh* is shown in light blue. The primers used to sequence the mutation are shown in green. The figure was done using the information from Ensembl (https://www.ensembl.org/Danio_rerio/Transcript/Summary?db=core;g=ENSDARG00000055240;r=17:33340675-33374538;t=ENSDART00000077553).

Figure 39: Schematic representation of Xdh protein domains. G50Mfs*2 is the mutation generated in the *xdh* mutant. The figure was done using the information available in Ensembl (https://www.ebi.ac.uk/interpro/result/InterProScan/iprscan5-R20230129-093421-0764-14068842-p1m/).

After confirming that the mutation is predicted to generate an early truncated Xdh protein, we checked if the mutants had a non-functional enzyme. Xdh main activity is to catalyze the hydroxylation of hypoxanthine to xanthine, and this product to uric acid which is the final product excreted (Figure 40A). Therefore, we measured hypoxanthine, xanthine, and uric acid metabolites by HPLC-MS in 5 dpf Xdh mutant larvae.

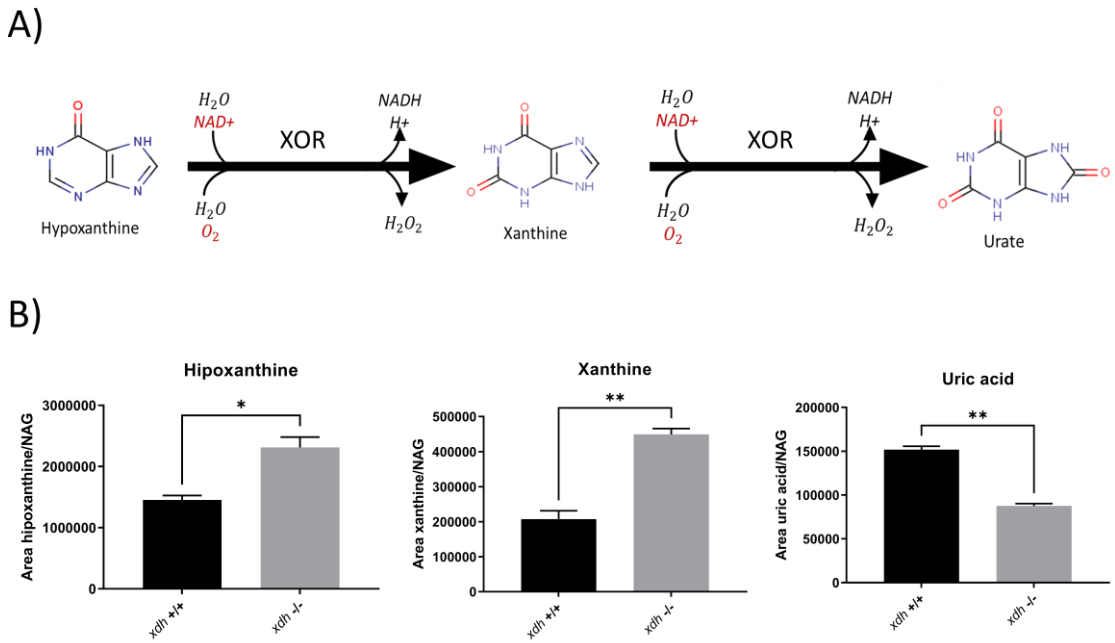

Figure 40: Determination of Xdh-dependent metabolites in Xdh-deficient larvae. A) Schematic representation of Xdh metabolic pathway. B) Hypoxanthine, xanthine and uric acid determination in 25 complete larvae of 5 dpf per group from 3 different experiments. The mean ± S.E.M. for each group is also shown. *p≤0.05, **p≤0.01 according to a t-test.

The results showed accumulation of hypoxanthine and xanthine, while reduced amount of uric acid, in Xdh-deficient larvae compared with their wild type siblings (Figure 40B).

2. Xdh deficiency alleviates HCD-induced liver lipid accumulation

It was reported using a murine model of nonalcoholic fatty liver disease/steatohepatitis (NAFLD/NASH) and human samples that plasma XDH activity increased in NASH condition (Kawachi et al. 2021). Taking these data into account, we decided to evaluate the impact of Xdh in NASH progression by feeding the fish during 7 days with a High Cholesterol Diet (HCD), containing 10% of cholesterol, and a Normal Diet (ND) as control. The fish started to be fed at 8 dpf and at 15 dpf the larvae were collected and analyzed as it is described in the Materials and Methods section (Figure 41). Zebrafish larvae developed NASH with similar histological changes than humans, and leukocyte infiltration and liver injury was observed (de Oliveira et al. 2019).

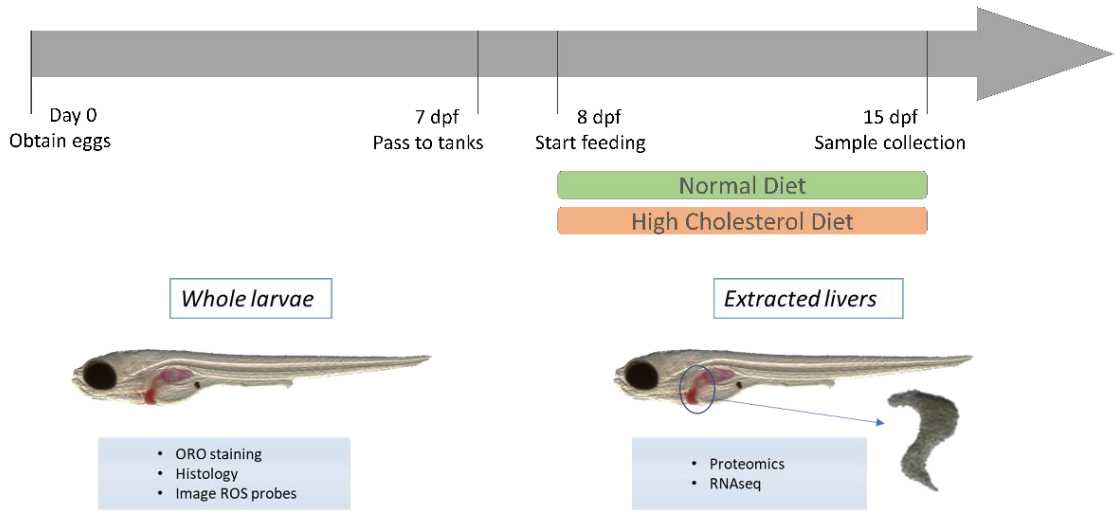

Figure 41: HCD-induced steatosis zebrafish model.

Firstly, using Oil Red O (ORO), a lipid stain, steatosis state was evaluated, and larvae were classified in three phenotypes attending to the severity of lipid accumulation: I. Normal, larvae without lipid accumulation; II. Mild phenotype, larvae with some lipid staining in the liver, and III. Severe phenotype with lipid accumulation in the whole liver (Figure 42A). It was found that a HCD led to liver lipid accumulation in wild type and Xdh-deficient larva. Notably, mutant larvae showed a milder phenotype than their wild type and heterozygote counterparts (Figure 42B).

.

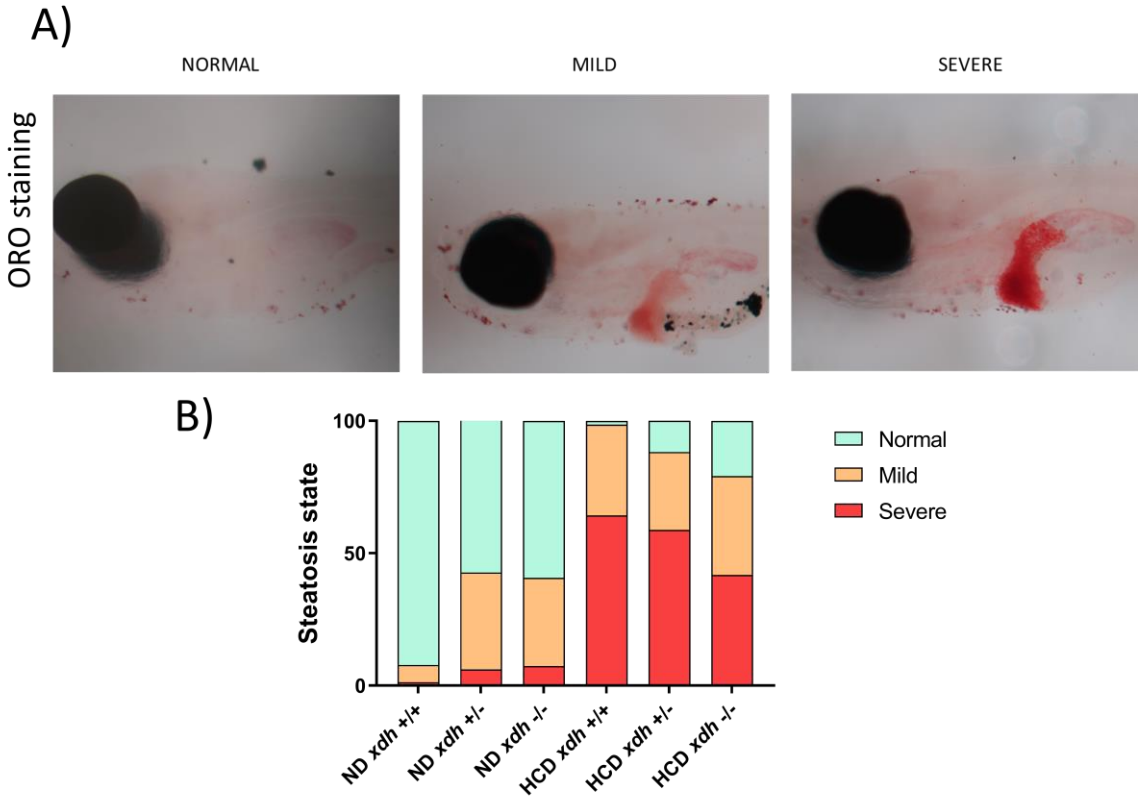

Figure 42: Xdh deficiency alleviates HCD-induced liver lipid accumulation. A) Representative images of ORO-stained larvae with a normal, mild and severe phenotypes. B) Classification of steatosis state attending to the larvae phenotypes in the different conditions. Hepatic steatosis was scored as: no ORO staining = normal; light red ORO staining = mild; red-dark red ORO staining = severe. Twenty larvae of 15 dpf were used per group. The experiment was independently repeated 5 times.

3. Xdh deficiency alleviates hepatocellular injury

It is well established that HCD feeding promotes accumulation of lipid droplets in the liver and hepatocellular injury (Neuschwander-Tetri & Caldwell 2003). Hematoxylin & eosin staining of zebrafish liver sections revealed normal hepatic features in all ND groups. However, wild type larvae fed with HCD accumulated lipid droplets and showed swelling and rounding up of hepatocytes, a phenomena called ballooning, a NASH key feature (Figure 43 A & B). Strikingly, Xdh-deficient larvae fed with HCD showed a markedly reduced ballooning.

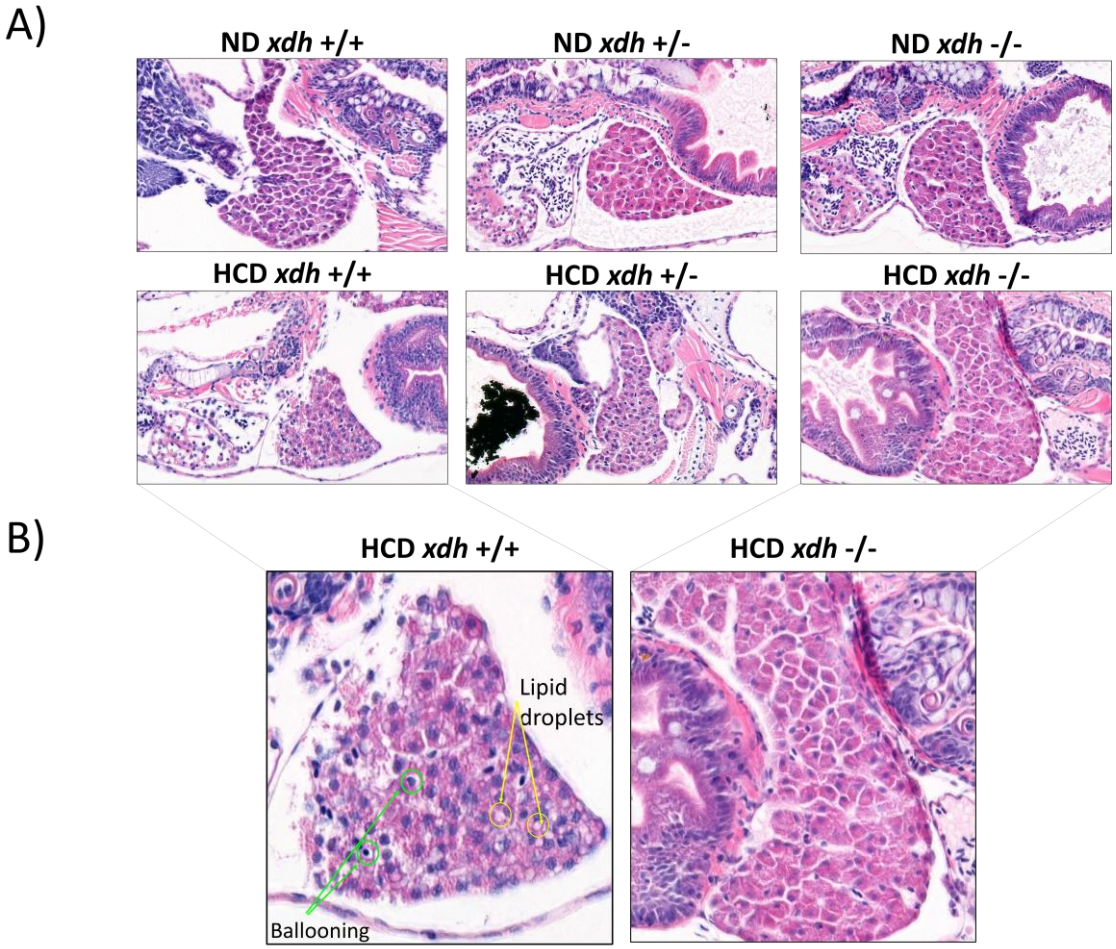

Figure 43: Xdh deficiency alleviates hepatocellular injury. A) Representative images of hematoxylin & eosin-stained liver sections of 15 dpf larvae fed with either HCD or ND. B) Zoomed images to show ballooning and lipid droplet accumulation in HCD-fed wild type and Xdh-deficient larvae. Experiments were repeated 3 times and 20 larvae per group were used.

4. Xdh deficiency alleviates HCD-induced liver oxidative stress

During the hydroxylation of hypoxanthine and xanthine, Xdh produces H_2O_2, an important ROS that can contributes to NASH progression. So, we decided to study ROS production in the liver of larvae fed with a HCD and the relevance of Xdh in this process.

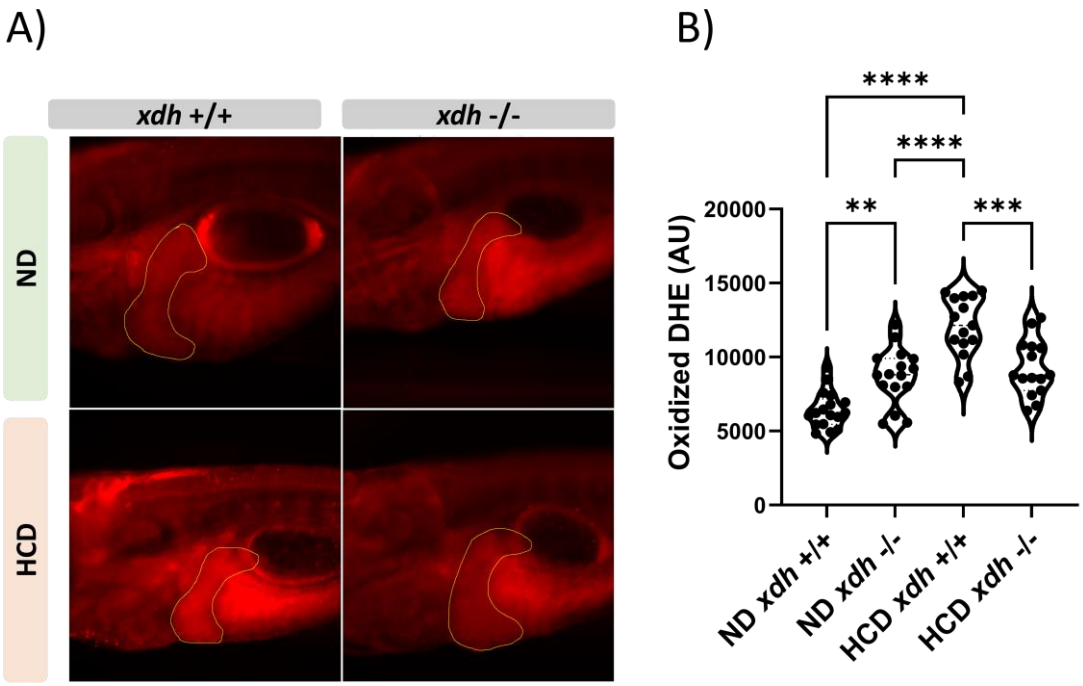

Figure 44: Xdh deficiency alleviates HCD-induced liver oxidative stress. A) Representative images of ROS released in the liver (with a yellow line), assayed with Dihydroethidium (DHE) staining. B) Quantification of ROS levels in the liver in 10 larvae of 15 dpf per group pooled from 3 different experiments. Each dot represents a larva and the mean ± SEM is also shown. **p≤0.01, ***p≤0.001 ****p<0.0001 according to ANOVA test.

It was found that HCD increased ROS levels in the liver of wild type larvae, but this induction was robustly attenuated in Xdh-deficient larvae. Surprisingly, Xdh-deficient larvae fed with ND showed higher liver ROS production than their wild type siblings (Figure 44 A & B).

5. The proteomic changes induced by HCD in the liver of zebrafish larvae resembles the ones promoted by Western diets in human

In order to have a more global picture of the impact of HCD in the liver of zebrafish larvae, we performed a proteomic assay. We dissected the livers from 20 larvae per group and analyzed them by MS. We compared wild type fish fed with HCD and ND to see the differences promoted by the diet. Principal Component Analysis (PCA) shows that the samples were very well clustered (Figure 45A). Moreover, one hundred seventy differentially expressed proteins (DEP) were found (Figure 45B).

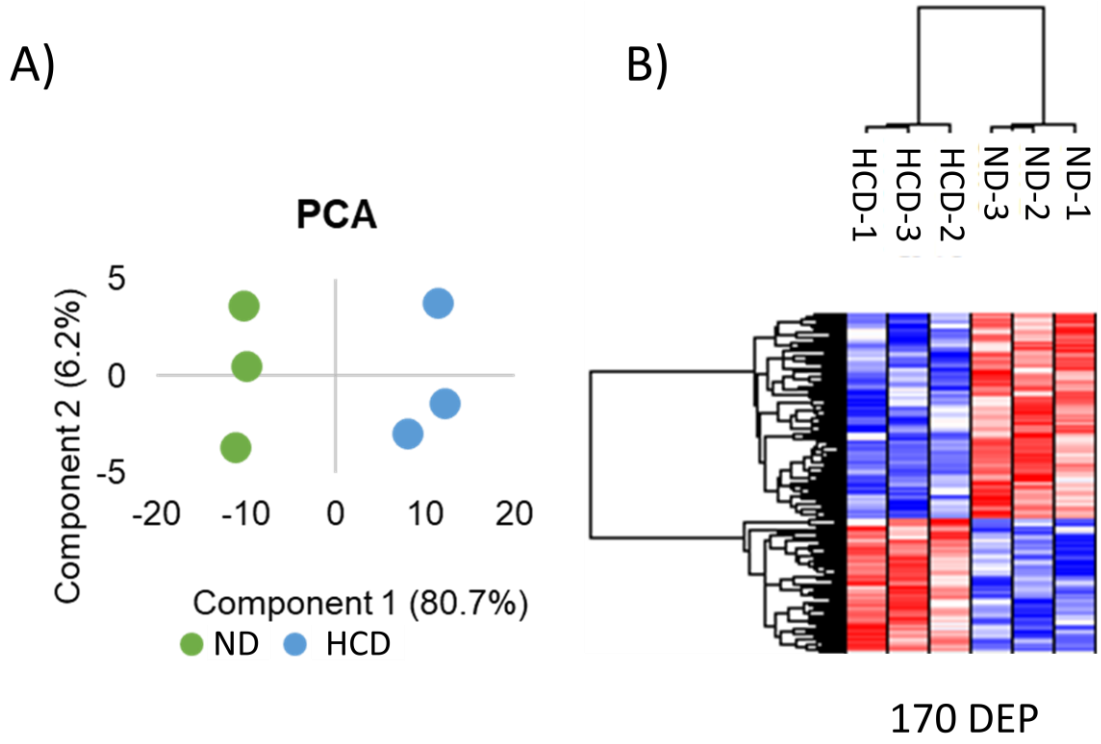

Figure 45: Proteomic analysis of liver from ND- and HCD-fed larvae. A) Principal component analysis and B) Heatmap comparing wild type ND and wild type HCD groups.

We found that HCD led to dysregulation of metabolic pathways and upregulation of several targets previously associated with human NASH (Figure 46).

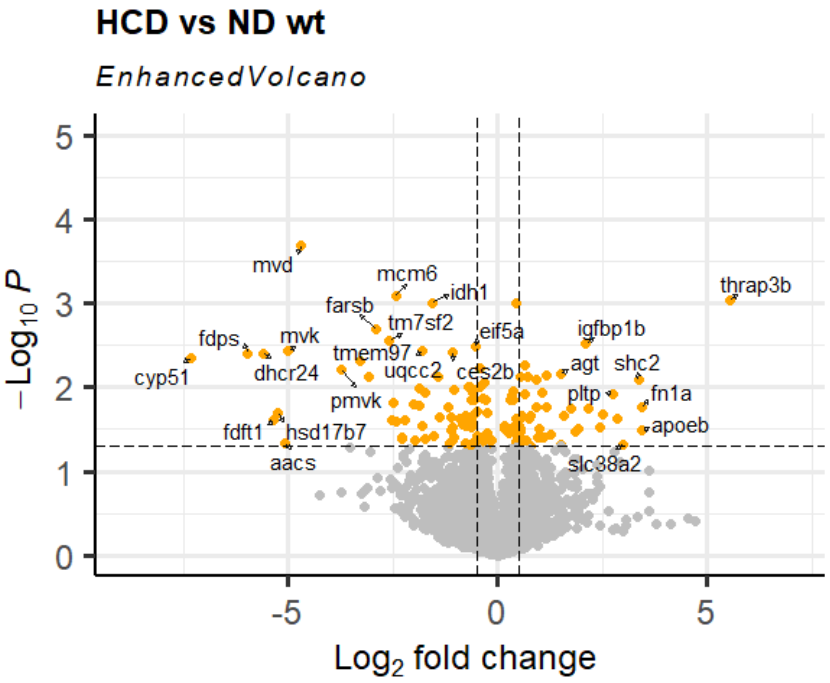

Figure 46:Proteins upregulated and downregulated in livers from larvae fed with HCD compared to larvae fed with ND. Volcano plot showing the DEP represented using R studio.

Comparing HCD with ND in wild type larvae, several proteins previously associated with human NAFLD/NASH, were overexpressed in the fish fed with HCD, such as Apoeb, Igfsp1, Pltp, Fn1a and Fn1b, Ferritin, Aifm2 and Soat2, and other down expressed, such as Mvd, Mvk or Pmvk (Figure 46).

The proteomic analysis of livers from wild type larvae fed with HCD showed downregulation of some enzymes related with lipid metabolic pathways, such as fatty acid oxidation, cholesterol and lipids biosynthesis, retinol, butanoate metabolism, BCAA (Branched-Chain Amino Acids) degradation (valine, leucine e isoleucine) and β-oxidation of VLCFA (Very Long Chain Fatty Acids) (Figure 47A).

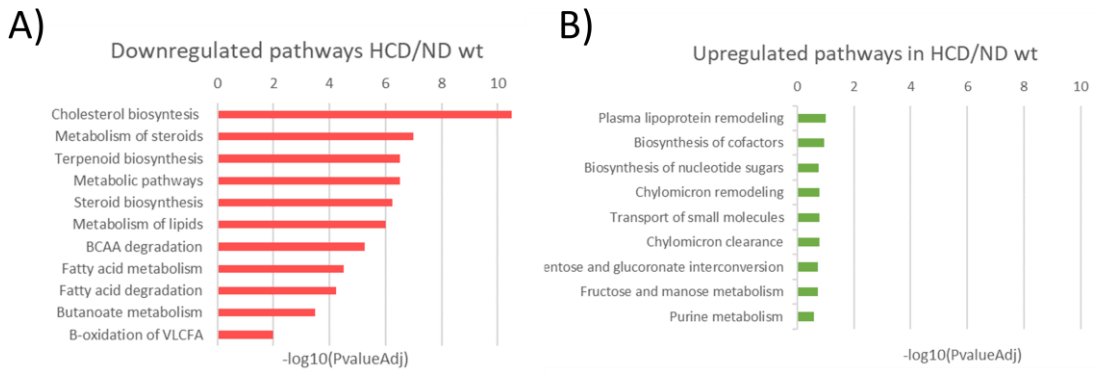

Figure 47: Metabolic pathways modulated by HCD in wild type larval liver. A) Top of most important downregulated pathways (red) and B) Top of most important upregulated pathways (green).

There were also some enzymes upregulated by HCD involved in pathways related to chylomicron clearance and remodeling, lipoprotein transport and biosynthesis of cofactors, sugars, purines, aminoacids, nucleotides, etc. (Figure 47B). Then we used STRING database to represent protein-protein interaction between the most up (Figure 48) and down-regulated proteins (Figure 49).

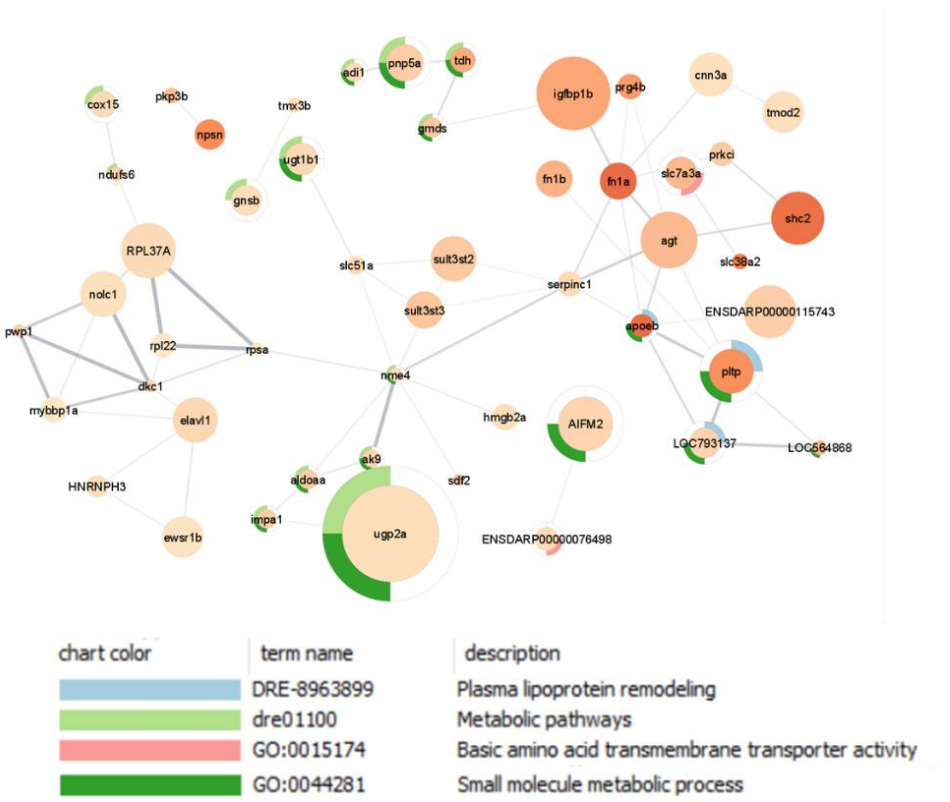

Figure 48: Biological Processes upregulated in HCD conditions. Bubble size represents the abundance of the protein in the sample and bubble darkness represents fold change. Graph done using Cytoscape.

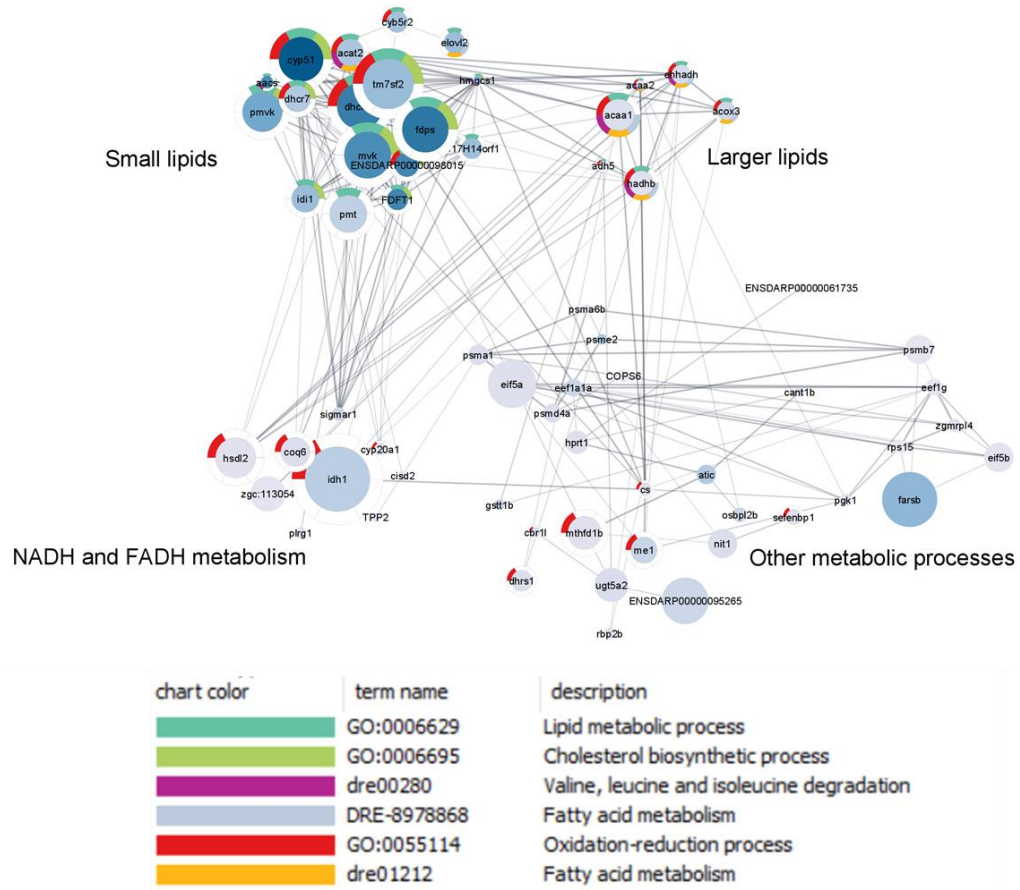

chart color	term name	description
	GO:0006629	Lipid metabolic process
	GO:0006695	Cholesterol biosynthetic process
	dre00280	Valine, leucine and isoleucine degradation
	DRE-8978868	Fatty acid metabolism
	GO:0055114	Oxidation-reduction process
	dre01212	Fatty acid metabolism

Figure 49: Biological Processes downregulated in HCD conditions. Bubble size represents the abundance of the protein in the sample and bubble darkness represents fold change. Graph done using Cytoscape.

6. Xdh deficiency reverses the proteomic changes induced by HCD in the liver

To understand the mechanism involved in the alleviation of NASH by Xdh, we compared Xdh-deficient fish fed with HCD with wild type fish fed with the same diet. PCA showed that the replicates of each experimental group were very similar (Figure 50A). Moreover, two hundred seventy DEP were found (Figure 50B & 51).

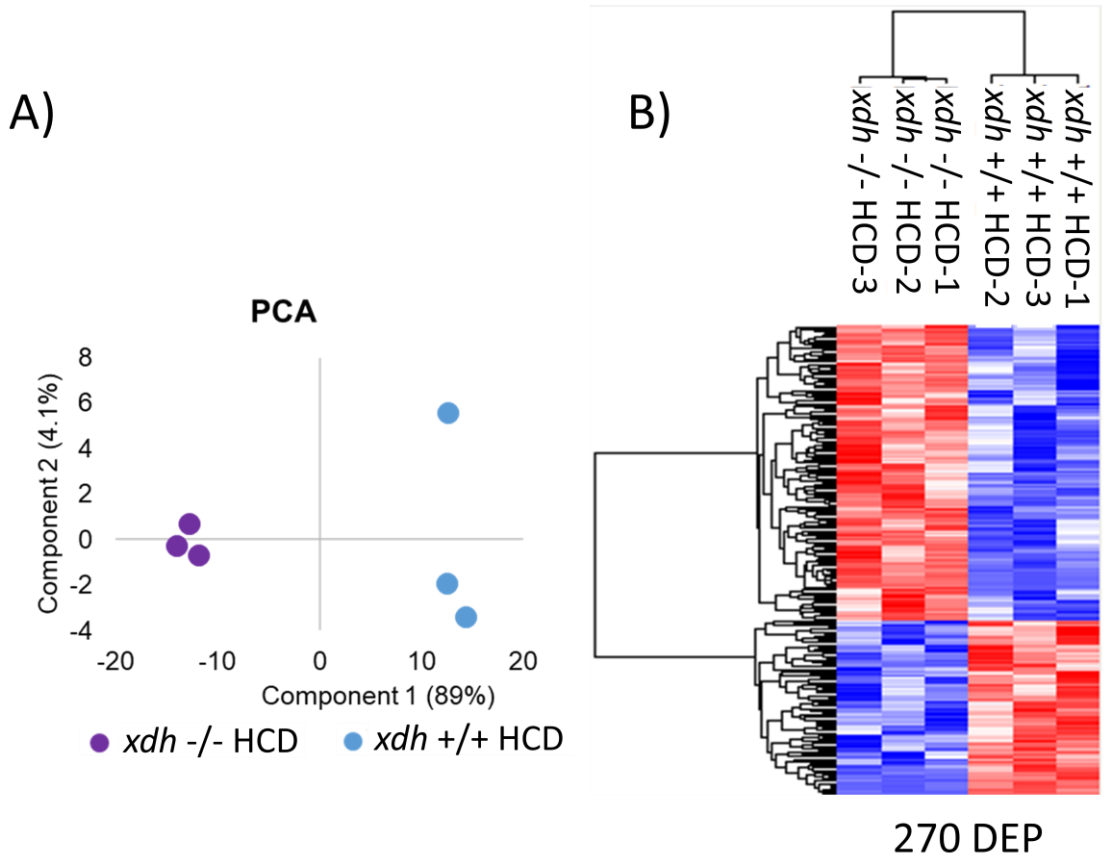

Figure 50: Impact of Xdh deficiency in the liver proteome of larvae fed with HCD. A) Principal component analysis and B) Heatmap comparing wild type and Xdh-deficient larvae fed with HCD.

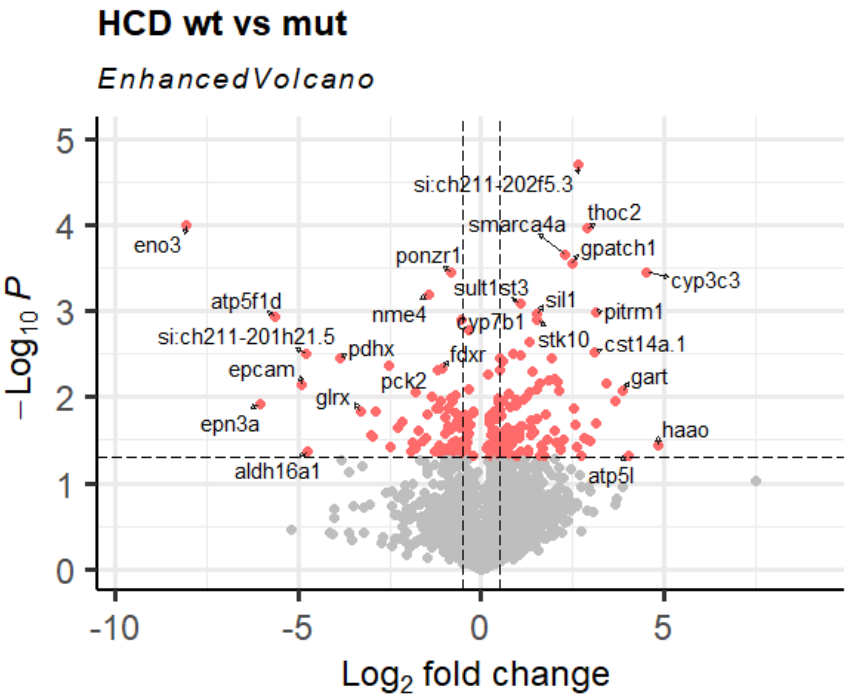

Figure 51: DEPs in Xdh-deficient larvae compared to wild type larvae both fed with HCD. Volcano plot showing the DEPs represented using R studio.

Xdh deficiency led to downregulated lipid metabolic pathways, such as fatty acid degradation, retinol metabolism or glycerolipid metabolism (Figure 52A), and to upregulated oxidative phosphorylation and inflammatory pathways, such as inflammasome, neutrophil degranulation and innate immune system, although the latter with much less statistical significance (Figure 52B).

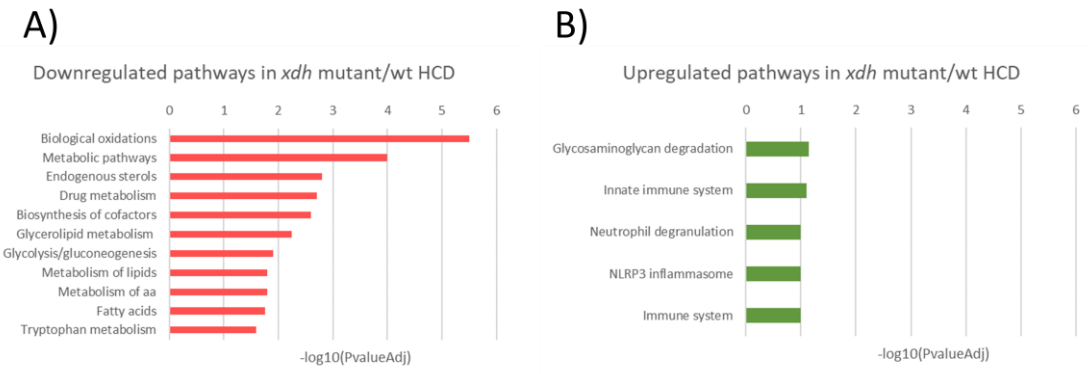

Figure 52: Pathways modulated by Xdh deficiency in larvae fed with HCD. A) Top of most important downregulated pathways (red) and B) Top of most important upregulated pathways (green).

We also used STRING database to represent protein-protein genetic interaction between the most up- (Figure 53) and down-regulated proteins (Figure 54) in Xdh-deficient larvae compared with their wild type siblings.

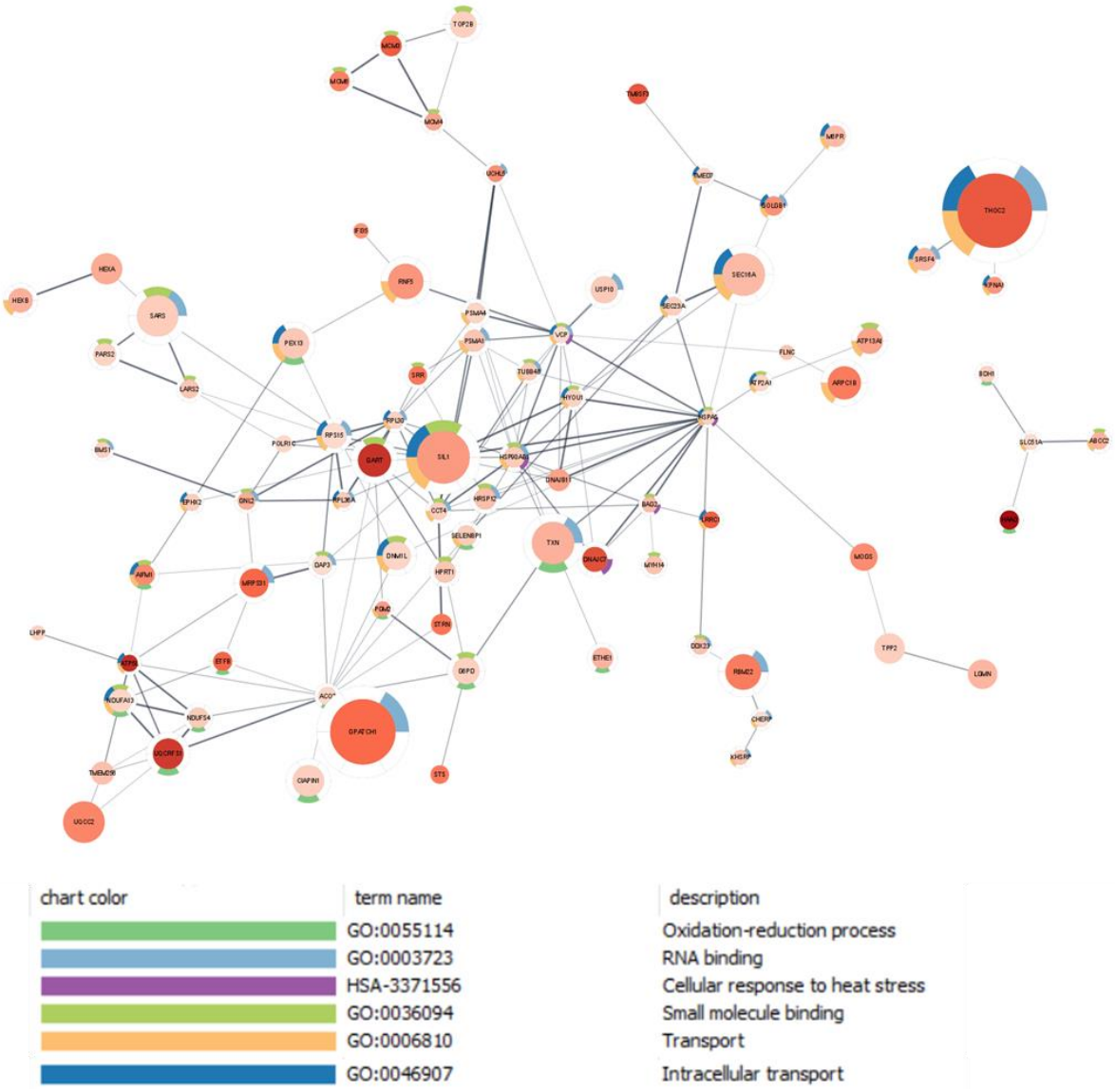

Figure 53: Biological Processes upregulated in Xdh-deficient larvae compared with wild type fed with HCD. Bubble size represents the abundance of the protein in the sample and bubble darkness represents fold change. Graph done using Cytoscape.

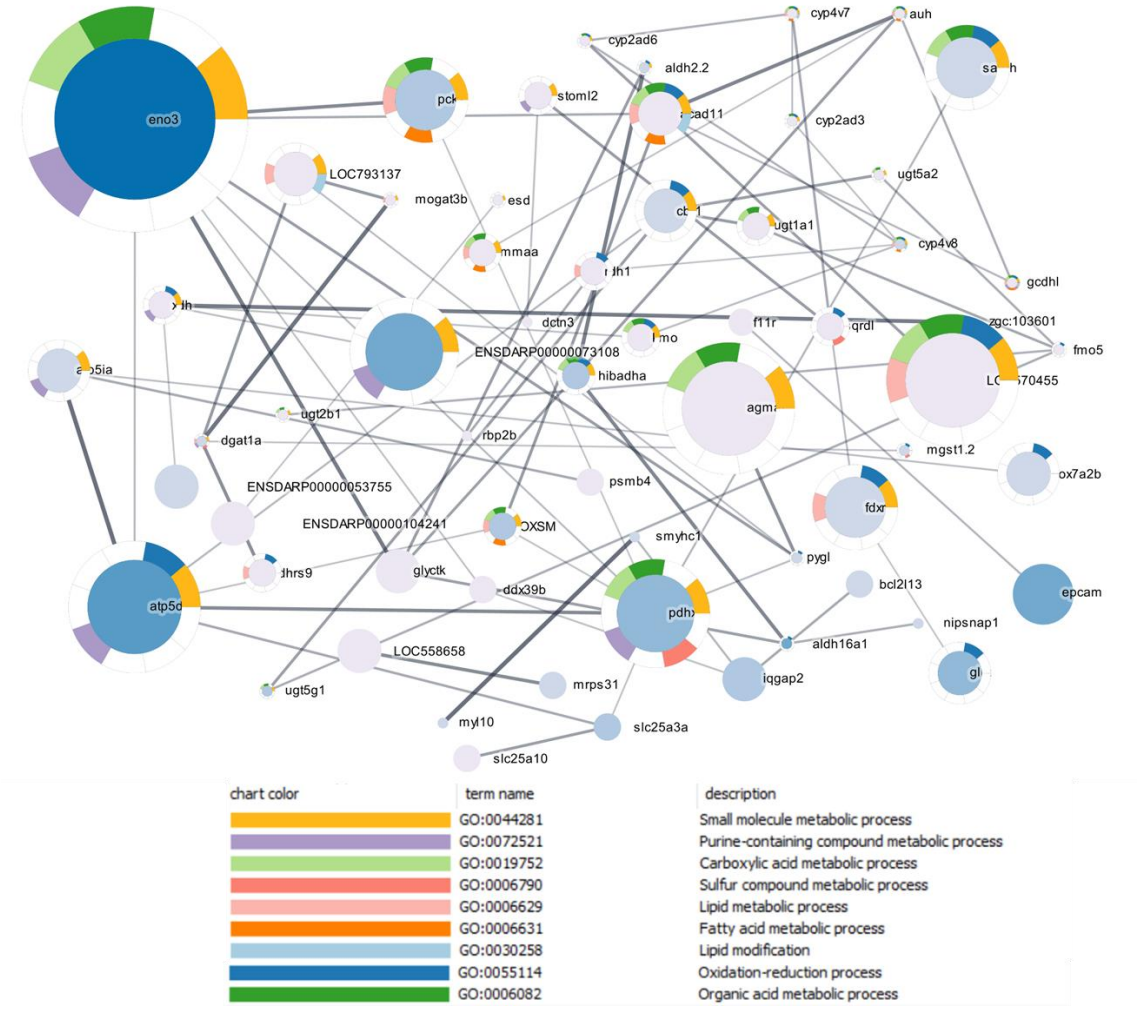

Figure 54: Biological Processes downregulated in Xdh-deficient larvae compared with wild type fed with HCD. Bubble size represents the abundance of the protein in the sample and bubble darkness represents fold change. Graph done using Cytoscape.

DISCUSSION

Non-alcoholic fatty liver disease (NAFLD) is the hepatic manifestation of metabolic syndrome, ranging from simple steatosis (NAFL) to steatohepatitis (NASH) and can progress to fibrosis and hepatocellular carcinoma (HCC) (Kim et al. 2021). NAFLD is the most common chronic liver disease and an unmet global public health and medical challenge (Litin & Mayo Clinic. 2009). Inflammation and oxidative stress are hallmarks of NAFLD progression to NASH (Ma et al. 2021). One of the main enzymes involved in oxidative stress is xanthine dehydrogenase (Xdh), which is highly expressed by hepatocytes (Wright et al. 1993) and participates in the hypoxanthine-uric acid pathway producing H_2O_2.

We have generated by Crispr-Cas9 a Xdh-deficient zebrafish line that developed normally and showed classic Mendelian ratio, despite accumulating hypoxanthine and xanthine as early as the larval stage and, consequently, had lower levels of uric acid. We have used this model to address the study of XDH deficiency in NAFLD/NASH but it can be used to study the impact of XDH in different human pathologies, including xanthinuria, as mice deficient in XDH die prematurely due to kidney failure (Piret et al. 2012).

Western type diets (i.e., rich in fat, cholesterol, and sugar) trigger the development of NAFLD and associated comorbidities, such as obesity, type 2 diabetes and cancer. Recently, several groups have established diet-induced NAFLD/NASH models in zebrafish (de Oliveira et al. 2019, Fang et al. 2010, Kulkarni et al. 2022, Ma et al. 2019, Park et al. 2019, Progatzky et al. 2014). We have used a model of NAFLD/NASH induced by HCD and NASH progression was assessed by histologic analysis, whole-larvae Oil Red O (ORO) staining, liver oxidative stress and proteomics. We observed accumulation of lipids and increased ROS production in the liver of larvae fed with HCD, concomitant with liver histological features related with NAFLD/NASH in humans, such as accumulation of lipid droplets and ballooning of hepatocytes. Importantly, Xdh deficiency ameliorated the progression of the disease by decreasing all these pathological alterations associated to NASH progression. Unexpectedly, Xdh-deficient larvae fed with ND showed higher liver ROS levels than wild type, suggesting that Xdh protects the liver from oxidative stress in physiological conditions, while playing an opposite role during NASH

development. This result is of interest from a clinical point of view and requires further investigation.

The role of XDH in the liver is very complex. Despite its ROS generating ability, XDH has a crucial role in the formation and accumulation of uric acid in the liver, which has been associated with hepatocellular steatosis and NASH in a cohort of patients (Fernandez Rodriguez et al. 2019, Mosca et al. 2017). However, in mouse model of obesity, it has been demonstrated that although the specific deletion of *Xdh* in hepatocytes is sufficient to prevent systemic hyperuricemia, it does not improve insulin resistance and dyslipidemia (Harmon et al. 2019). Therefore, although systemic uric acid levels are good biomarkers of the metabolic abnormalities of obesity, they do not appear to cause or affect the progression of this disease.

Proteomic analysis of livers of wild type larvae fed with HCD showed downregulation of several enzymes which participates in the cholesterol and lipids biosynthesis pathway, namely Hmgcs, Mvk, Fdps, Fdft1, Cyp51, Hsd17b7 and Dhcr7, and lipid metabolic pathways, such as fatty acid oxidation, PPAR signaling pathways, cholesterol and lipid biosynthesis, retinol metabolism and BCAA degradation. Conversely, HCD promoted the upregulation in the liver of several proteins previously associated with human NAFLD/NASH, such as Igfsp1, Apoeb, Pltp, Fn1a and Fn1b, Ferritin, Aifm2 and Soat2. All these pathways may be involved in NASH. For example, on the one hand a PPAR defective signaling has been reported as a key regulating factor leading to decreased fatty acid oxidation and accumulation of unoxidized fatty acids produces lipotoxicity and steatohepatitis (Berlanga et al. 2014). On the other hand, an altered retinol metabolism is involved in hepatic fibrosis (Tsuchida & Friedman 2017) and mice models of obesity show reduced hepatic retinol and accumulation of retinyl esters (Berasain & Avila 2021).

Another interesting observation is that the pathway involved in the degradation of valine, leucine and isoleucine amino acids is altered in the liver of larvae fed with HCD, so it is likely an accumulation of this amino acids. This is in agreement with previous studies showing increased levels of BCAA during the transition from steatosis to NASH (Lake et al. 2015). In addition, dietary administration of valine or isoleucine to mouse model of NASH ameliorate liver inflammation and oxidative stress, and hyperinsulinemia (Gart et al. 2022).

We also found increased Apoeb protein levels in the liver of zebrafish larvae fed with HCD. Apoeb is an apolipoprotein that participates in the transport of triglycerides and cholesterol from the liver to peripheral tissues and it has been reported that elevated human serum ApoB levels can predict an increased risk for NAFLD development (Wang et al. 2017). We also found increased levels of fibronectins (Fn1a and Fn1b), which are prognosis biomarkers of fibrosis development in NAFLD/NASH (Baralle & Baralle 2021) and in plasma phospholipid transfer protein (Pltp) which participates in VLDL secretion (Yazdanyar & Jiang 2012). Sterol-O-acetyltransferase (Soat2) was also found to be increased in the liver of larvae fed with HCD and it has been found that diminished production of this enzyme could protect from hepatic steatosis (Ahmed et al. 2019). We also observed in the liver of HCD fed larvae increased ferritin, which has been previously reported as a biomarker of histologic severity and advanced fibrosis in patients with metabolic syndrome and NAFLD (Kowdley et al. 2012, Zelber-Sagi et al. 2007).

One of the most interesting observations of our study is that Xdh deficiency was able to ameliorate NASH progression in larvae fed with HCD and, concomitantly, to promote the downregulation of lipid metabolic pathways, including fatty acid degradation, retinol metabolism and glycerolipid metabolism, and the upregulation of oxidative phosphorylation. One interesting Reactome pathway that we found upregulated in Xdh-deficient larvae fed with HCD was Hsf1 (Heat Shock transcription Factor 1) activation, which has been found to ameliorate NASH by stimulating mitochondrial oxidation in mouse models of obesity (Rao et al. 2022) and to improve biomarkers of NAFLD in patients (Kondo et al. 2021). Another interesting pathway found to be upregulated is sulfonation, which is involved in liver detoxification. Thus, it has been demonstrated in mouse models of NAFLD that the overexpression of sulfotransferase SULT2B1b decreases lipogenesis (Bai et al. 2012) and inhibits hepatic gluconeogenesis and ameliorates metabolic liver disease (Bi et al. 2018). Overall, all these results support that Xdh is involved in NAFLD disease progression, explaining the association found between XDH and NAFLD in several clinical studies, and point out to the relevance of the zebrafish larval model fed with HCD to identify novel signaling pathways associated with NAFLD/NASH in humans.

CONCLUSIONS

1. High *DUOX1* transcript levels are associated with poor prognosis of patients with early-stage melanoma, while *DUOX1* levels are not associated to the prognosis of patients with late-stage melanoma.
2. Although melanocyte Duox1 inhibition does not affect melanocyte transformation and early melanoma progression in zebrafish, Duox1 inhibition reduces in a cell autonomous manner the growth of transplanted melanomas while increasing its metastatic potential.
3. A pharmacological screening identifies 17 potential inhibitors and 3 activators of human DUOX1.
4. Xdh-deficient zebrafish are fertile, viable and show normal Mendelian ratio. The Xdh-deficient zebrafish line is an excellent animal model to study the role of XDH in human diseases, including xanthinuria.
5. Xdh deficiency ameliorates liver pathology in a zebrafish model of HCD-induced NASH. This includes alleviation of liver lipid accumulation, hepatocellular injury, and oxidative stress.
6. The proteomic changes induced by HCD in the liver of zebrafish larvae resembles the ones promoted by Western diets in human.
7. Xdh deficiency results in the downregulation of lipid metabolic pathways, including fatty acid degradation, retinol metabolism and glycerolipid metabolism, in the liver of zebrafish larvae fed with HCD. In addition, it promotes the upregulation of oxidative phosphorylation, Hsf1 activation and sulfonation, which are all involved in liver detoxification and NASH alleviation.

REFERENCES

Ablain J, Xu M, Rothschild H, Jordan RC, Mito JK, Daniels BH, Bell CF, Joseph NM, Wu H, Bastian BC, Zon LI & Yeh I. 2018. Human tumor genomics and zebrafish modeling identify SPRED1 loss as a driver of mucosal melanoma. *Science* 362: 1055-1060. #10.1126/science.aau6509

Agarwal A, Banerjee A & Banerjee UC. 2011. Xanthine oxidoreductase: a journey from purine metabolism to cardiovascular excitation-contraction coupling. *Crit Rev Biotechnol* 31: 264-280. #10.3109/07388551.2010.527823

Aguilan JT, Kulej K & Sidoli S. 2020. Guide for protein fold change and p-value calculation for non-experts in proteomics. *Mol Omics* 16: 573-582. #10.1039/d0mo00087f

Ahmed O, Pramfalk C, Pedrelli M, Olin M, Steffensen KR, Eriksson M & Parini P. 2019. Genetic depletion of Soat2 diminishes hepatic steatosis via genes regulating de novo lipogenesis and by GLUT2 protein in female mice. *Dig Liver Dis* 51: 1016-1022. #10.1016/j.dld.2018.12.007

Allaoui A, Botteaux A, Dumont JE, Hoste C & De Deken X. 2009. Dual oxidases and hydrogen peroxide in a complex dialogue between host mucosae and bacteria. *Trends Mol Med* 15: 571-579. #10.1016/j.molmed.2009.10.003

Alpha-Tocopherol BCCPSG. 1994. The effect of vitamin E and beta carotene on the incidence of lung cancer and other cancers in male smokers. *N Engl J Med* 330: 1029-1035. #10.1056/NEJM199404143301501

Amatruda JF & Patton EE. 2008. Genetic models of cancer in zebrafish. *Int Rev Cell Mol Biol* 271: 1-34. #10.1016/S1937-6448(08)01201-X

Amatruda JF, Shepard JL, Stern HM & Zon LI. 2002. Zebrafish as a cancer model system. *Cancer Cell* 1: 229-231. #10.1016/s1535-6108(02)00052-1

Angulo P. 2002. Nonalcoholic fatty liver disease. *N Engl J Med* 346: 1221-1231. #10.1056/NEJMra011775

Anstee QM, Reeves HL, Kotsiliti E, Govaere O & Heikenwalder M. 2019. From NASH to HCC: current concepts and future challenges. *Nat Rev Gastroenterol Hepatol* 16: 411-428. #10.1038/s41575-019-0145-7

Antonio N, Bonnelykke-Behrndtz ML, Ward LC, Collin J, Christensen IJ, Steiniche T, Schmidt H, Feng Y & Martin P. 2015. The wound inflammatory response exacerbates growth of pre-neoplastic cells and progression to cancer. *EMBO J* 34: 2219-2236. #10.15252/embj.201490147

Aratani Y. 2018. Myeloperoxidase: Its role for host defense, inflammation, and neutrophil function. *Arch Biochem Biophys* 640: 47-52. #10.1016/j.abb.2018.01.004

Arrese M, Cabrera D, Kalergis AM & Feldstein AE. 2016. Innate Immunity and Inflammation in NAFLD/NASH. *Dig Dis Sci* 61: 1294-1303. #10.1007/s10620-016-4049-x

Arroyave-Ospina JC, Wu Z, Geng Y & Moshage H. 2021. Role of Oxidative Stress in the Pathogenesis of Non-Alcoholic Fatty Liver Disease: Implications for Prevention and Therapy. *Antioxidants (Basel)* 10#10.3390/antiox10020174

Athreya K & Xavier MF. 2017. Antioxidants in the Treatment of Cancer. *Nutr Cancer* 69: 1099-1104. #10.1080/01635581.2017.1362445

Baeck C, Wei X, Bartneck M, Fech V, Heymann F, Gassler N, Hittatiya K, Eulberg D, Luedde T, Trautwein C & Tacke F. 2014. Pharmacological inhibition of the chemokine C-C motif chemokine ligand 2 (monocyte chemoattractant protein 1) accelerates liver fibrosis regression by suppressing Ly-6C(+) macrophage infiltration in mice. *Hepatology* 59: 1060-1072. #10.1002/hep.26783

Bai Q, Zhang X, Xu L, Kakiyama G, Heuman D, Sanyal A, Pandak WM, Yin L, Xie W & Ren S. 2012. Oxysterol sulfation by cytosolic sulfotransferase suppresses liver X receptor/sterol regulatory element binding protein-1c signaling pathway and reduces serum and hepatic lipids in mouse models of nonalcoholic fatty liver disease. *Metabolism* 61: 836-845. #10.1016/j.metabol.2011.11.014

Baralle M & Baralle FE. 2021. Alternative splicing and liver disease. *Ann Hepatol* 26: 100534. #10.1016/j.aohep.2021.100534

Bardi GT, Smith MA & Hood JL. 2018. Melanoma exosomes promote mixed M1 and M2 macrophage polarization. *Cytokine* 105: 63-72. #10.1016/j.cyto.2018.02.002

Barriuso J, Nagaraju R & Hurlstone A. 2015. Zebrafish: a new companion for translational research in oncology. *Clin Cancer Res* 21: 969-975. #10.1158/1078-0432.CCR-14-2921

Battelli MG, Bortolotti M, Polito L & Bolognesi A. 2019. Metabolic syndrome and cancer risk: The role of xanthine oxidoreductase. *Redox Biol* 21: 101070. #10.1016/j.redox.2018.101070

Berasain C & Avila MA. 2021. Vitamin A in Nonalcoholic Fatty Liver Disease: A Key Player in an Offside Position? *Cell Mol Gastroenterol Hepatol* 11: 291-293. #10.1016/j.jcmgh.2020.08.007

Berlanga A, Guiu-Jurado E, Porras JA & Auguet T. 2014. Molecular pathways in non-alcoholic fatty liver disease. *Clin Exp Gastroenterol* 7: 221-239. #10.2147/CEG.S62831

Bessone F, Razori MV & Roma MG. 2019. Molecular pathways of nonalcoholic fatty liver disease development and progression. *Cell Mol Life Sci* 76: 99-128. #10.1007/s00018-018-2947-0

Bi Y, Shi X, Zhu J, Guan X, Garbacz WG, Huang Y, Gao L, Yan J, Xu M, Ren S, Ren S, Liu Y, Ma X, Li S & Xie W. 2018. Regulation of Cholesterol Sulfotransferase SULT2B1b by Hepatocyte Nuclear Factor 4alpha Constitutes a Negative Feedback Control of Hepatic Gluconeogenesis. *Mol Cell Biol* 38#10.1128/MCB.00654-17

Brandner JM & Haass NK. 2013. Melanoma's connections to the tumour microenvironment. *Pathology* 45: 443-452. #10.1097/PAT.0b013e328363b3bd

Brar SS, Kennedy TP, Whorton AR, Sturrock AB, Huecksteadt TP, Ghio AJ & Hoidal JR. 2001. Reactive oxygen species from NAD(P)H:quinone oxidoreductase constitutively activate NF-kappaB in malignant melanoma cells. *Am J Physiol Cell Physiol* 280: C659-676. #10.1152/ajpcell.2001.280.3.C659

Britto DD, Wyroba B, Chen W, Lockwood RA, Tran KB, Shepherd PR, Hall CJ, Crosier KE, Crosier PS & Astin JW. 2018. Macrophages enhance Vegfa-driven angiogenesis in an embryonic zebrafish tumour xenograft model. *Dis Model Mech* 11#10.1242/dmm.035998

Brunt EM. 2010. Pathology of nonalcoholic fatty liver disease. *Nat Rev Gastroenterol Hepatol* 7: 195-203. #10.1038/nrgastro.2010.21

Caligiuri A, Gentilini A & Marra F. 2016. Molecular Pathogenesis of NASH. *Int J Mol Sci* 17#10.3390/ijms17091575

Cancer Genome Atlas N. 2015. Genomic Classification of Cutaneous Melanoma. *Cell* 161: 1681-1696. #10.1016/j.cell.2015.05.044

Candel S, de Oliveira S, Lopez-Munoz A, Garcia-Moreno D, Espin-Palazon R, Tyrkalska SD, Cayuela ML, Renshaw SA, Corbalan-Velez R, Vidal-Abarca I, Tsai HJ, Meseguer J, Sepulcre MP & Mulero V. 2014. Tnfa signaling through tnfr2 protects skin against oxidative stress-induced inflammation. *PLoS Biol* 12: e1001855. #10.1371/journal.pbio.1001855

Cannavo SP, Tonacci A, Bertino L, Casciaro M, Borgia F & Gangemi S. 2019. The role of oxidative stress in the biology of melanoma: A systematic review. *Pathol Res Pract* 215: 21-28. #10.1016/j.prp.2018.11.020

Cantu-Medellin N & Kelley EE. 2013a. Xanthine oxidoreductase-catalyzed reactive species generation: A process in critical need of reevaluation. *Redox Biol* 1: 353-358. #10.1016/j.redox.2013.05.002

Cantu-Medellin N & Kelley EE. 2013b. Xanthine oxidoreductase-catalyzed reduction of nitrite to nitric oxide: insights regarding where, when and how. *Nitric Oxide* 34: 19-26. #10.1016/j.niox.2013.02.081

Carvalho DP & Dupuy C. 2017. Thyroid hormone biosynthesis and release. *Mol Cell Endocrinol* 458: 6-15. #10.1016/j.mce.2017.01.038

Casbon AJ, Reynaud D, Park C, Khuc E, Gan DD, Schepers K, Passegue E & Werb Z. 2015. Invasive breast cancer reprograms early myeloid differentiation in the bone marrow to generate

immunosuppressive neutrophils. *Proc Natl Acad Sci U S A* 112: E566-575. #10.1073/pnas.1424927112

Cayuela ML, Claes KBM, Ferreira MG, Henriques CM, van Eeden F, Varga M, Vierstraete J & Mione MC. 2018. The Zebrafish as an Emerging Model to Study DNA Damage in Aging, Cancer and Other Diseases. *Front Cell Dev Biol* 6: 178. #10.3389/fcell.2018.00178

Ceol CJ, Houvras Y, Jane-Valbuena J, Bilodeau S, Orlando DA, Battisti V, Fritsch L, Lin WM, Hollmann TJ, Ferre F, Bourque C, Burke CJ, Turner L, Uong A, Johnson LA, Beroukhim R, Mermel CH, Loda M, Ait-Si-Ali S, Garraway LA, Young RA & Zon LI. 2011. The histone methyltransferase SETDB1 is recurrently amplified in melanoma and accelerates its onset. *Nature* 471: 513-517. #10.1038/nature09806

Charlton M, Sreekumar R, Rasmussen D, Lindor K & Nair KS. 2002. Apolipoprotein synthesis in nonalcoholic steatohepatitis. *Hepatology* 35: 898-904. #10.1053/jhep.2002.32527

Chen JJ, Lin YC, Yao PL, Yuan A, Chen HY, Shun CT, Tsai MF, Chen CH & Yang PC. 2005. Tumor-associated macrophages: the double-edged sword in cancer progression. *J Clin Oncol* 23: 953-964. #10.1200/JCO.2005.12.172

Chen K, Chen X, Xue H, Zhang P, Fang W, Chen X & Ling W. 2019. Coenzyme Q10 attenuates high-fat diet-induced non-alcoholic fatty liver disease through activation of the AMPK pathway. *Food Funct* 10: 814-823. #10.1039/c8fo01236a

Cho JH, Robinson JP, Arave RA, Burnett WJ, Kircher DA, Chen G, Davies MA, Grossmann AH, VanBrocklin MW, McMahon M & Holmen SL. 2015. AKT1 Activation Promotes Development of Melanoma Metastases. *Cell Rep* 13: 898-905. #10.1016/j.celrep.2015.09.057

Choi H, Park JY, Kim HJ, Noh M, Ueyama T, Bae Y, Lee TR & Shin DW. 2014. Hydrogen peroxide generated by DUOX1 regulates the expression levels of specific differentiation markers in normal human keratinocytes. *J Dermatol Sci* 74: 56-63. #10.1016/j.jdermsci.2013.11.011

Ciarletta P, Foret L & Ben Amar M. 2011. The radial growth phase of malignant melanoma: multi-phase modelling, numerical simulations and linear stability analysis. *J R Soc Interface* 8: 345-368. #10.1098/rsif.2010.0285

Cichorek M, Wachulska M & Stasiewicz A. 2013a. Heterogeneity of neural crest-derived melanocytes. *Open Life Sciences* 8: 315-330. #doi:10.2478/s11535-013-0141-1

Cichorek M, Wachulska M, Stasiewicz A & Tyminska A. 2013b. Skin melanocytes: biology and development. *Postepy Dermatol Alergol* 30: 30-41. #10.5114/pdia.2013.33376

Clark WH, Jr., Evans HL, Everett MA, Farmer ER, Graham JH, Mihm MC, Jr., Rosai J, Sagebiel RW & Wick MR. 1991. Early melanoma. Histologic terms. *Am J Dermatopathol* 13: 579-582.

Coffelt SB, Wellenstein MD & de Visser KE. 2016. Neutrophils in cancer: neutral no more. *Nat Rev Cancer* 16: 431-446. #10.1038/nrc.2016.52

Cooper GM. 2000. *The cell : a molecular approach*. Washington, D.C.: ASM Press.

Corkery DP, Dellaire G & Berman JN. 2011. Leukaemia xenotransplantation in zebrafish--chemotherapy response assay in vivo. *Br J Haematol* 153: 786-789. #10.1111/j.1365-2141.2011.08661.x

Costin GE & Hearing VJ. 2007. Human skin pigmentation: melanocytes modulate skin color in response to stress. *FASEB J* 21: 976-994. #10.1096/fj.06-6649rev

Cotter TG & Rinella M. 2020. Nonalcoholic Fatty Liver Disease 2020: The State of the Disease. *Gastroenterology* 158: 1851-1864. #10.1053/j.gastro.2020.01.052

Couillard C, Ruel G, Archer WR, Pomerleau S, Bergeron J, Couture P, Lamarche B & Bergeron N. 2005. Circulating levels of oxidative stress markers and endothelial adhesion molecules in men with abdominal obesity. *J Clin Endocrinol Metab* 90: 6454-6459. #10.1210/jc.2004-2438

Crowson AN, Magro CM & Mihm MC. 2006. Prognosticators of melanoma, the melanoma report, and the sentinel lymph node. *Mod Pathol* 19 Suppl 2: S71-87. #10.1038/modpathol.3800517

D'Mello SA, Finlay GJ, Baguley BC & Askarian-Amiri ME. 2016. Signaling Pathways in Melanogenesis. *Int J Mol Sci* 17#10.3390/ijms17071144

Dai W, Wang K, Zheng X, Chen X, Zhang W, Zhang Y, Hou J & Liu L. 2015. High fat plus high cholesterol diet lead to hepatic steatosis in zebrafish larvae: a novel model for screening anti-hepatic steatosis drugs. *Nutr Metab (Lond)* 12: 42. #10.1186/s12986-015-0036-z

Dang M, Henderson RE, Garraway LA & Zon LI. 2016. Long-term drug administration in the adult zebrafish using oral gavage for cancer preclinical studies. *Dis Model Mech* 9: 811-820. #10.1242/dmm.024166

Day CP & James OF. 1998. Steatohepatitis: a tale of two "hits"? *Gastroenterology* 114: 842-845. #10.1016/s0016-5085(98)70599-2

de Oliveira S, Boudinot P, Calado A & Mulero V. 2015. Duox1-derived H2O2 modulates Cxcl8 expression and neutrophil recruitment via JNK/c-JUN/AP-1 signaling and chromatin modifications. *J Immunol* 194: 1523-1533. #10.4049/jimmunol.1402386

de Oliveira S, Houseright RA, Graves AL, Golenberg N, Korte BG, Miskolci V & Huttenlocher A. 2019. Metformin modulates innate immune-mediated inflammation and early progression of NAFLD-associated hepatocellular carcinoma in zebrafish. *J Hepatol* 70: 710-721. #10.1016/j.jhep.2018.11.034

de Oliveira S, Lopez-Munoz A, Candel S, Pelegrin P, Calado A & Mulero V. 2014. ATP modulates acute inflammation in vivo through dual oxidase 1-derived H2O2 production and NF-kappaB activation. *J Immunol* 192: 5710-5719. #10.4049/jimmunol.1302902

de Oliveira S, Reyes-Aldasoro CC, Candel S, Renshaw SA, Mulero V & Calado A. 2013. Cxcl8 (IL-8) mediates neutrophil recruitment and behavior in the zebrafish inflammatory response. *J Immunol* 190: 4349-4359. #10.4049/jimmunol.1203266

de Sa Junior PL, Camara DAD, Porcacchia AS, Fonseca PMM, Jorge SD, Araldi RP & Ferreira AK. 2017. The Roles of ROS in Cancer Heterogeneity and Therapy. *Oxid Med Cell Longev* 2017: 2467940. #10.1155/2017/2467940

Dee CT, Nagaraju RT, Athanasiadis EI, Gray C, Fernandez Del Ama L, Johnston SA, Secombes CJ, Cvejic A & Hurlstone AF. 2016. CD4-Transgenic Zebrafish Reveal Tissue-Resident Th2- and Regulatory T Cell-like Populations and Diverse Mononuclear Phagocytes. *J Immunol* 197: 3520-3530. #10.4049/jimmunol.1600959

Deghan Manshadi S, Ishiguro L, Sohn KJ, Medline A, Renlund R, Croxford R & Kim YI. 2014. Folic acid supplementation promotes mammary tumor progression in a rat model. *PLoS One* 9: e84635. #10.1371/journal.pone.0084635

Di Carlo E, Forni G, Lollini P, Colombo MP, Modesti A & Musiani P. 2001. The intriguing role of polymorphonuclear neutrophils in antitumor reactions. *Blood* 97: 339-345. #10.1182/blood.v97.2.339

Dinulos JGH. 2021. Nevi and Malignant Melanoma In *Habif's Clinical Dermatology*, ed. Elsevier

Dovey M, White RM & Zon LI. 2009. Oncogenic NRAS cooperates with p53 loss to generate melanoma in zebrafish. *Zebrafish* 6: 397-404. #10.1089/zeb.2009.0606

Ebbing M, Bonaa KH, Nygard O, Arnesen E, Ueland PM, Nordrehaug JE, Rasmussen K, Njolstad I, Refsum H, Nilsen DW, Tverdal A, Meyer K & Vollset SE. 2009. Cancer incidence and mortality after treatment with folic acid and vitamin B12. *JAMA* 302: 2119-2126. #10.1001/jama.2009.1622

Ehrlich P. 1909. Über den jetzigen Stand der Karzinomforschung. *Beiträge zur experimentellen Pathologie und Chemotherapie* 117-164.

Elder D. 1999. Tumor progression, early diagnosis and prognosis of melanoma. *Acta Oncol* 38: 535-547. #10.1080/028418699431113

Ellett F, Pase L, Hayman JW, Andrianopoulos A & Lieschke GJ. 2011. mpeg1 promoter transgenes direct macrophage-lineage expression in zebrafish. *Blood* 117: e49-56. #10.1182/blood-2010-10-314120

Elwood JM & Jopson J. 1997. Melanoma and sun exposure: an overview of published studies. *Int J Cancer* 73: 198-203. #10.1002/(sici)1097-0215(19971009)73:2<198::aid-ijc6>3.0.co;2-r

Fan Y, Mao R & Yang J. 2013. NF-kappaB and STAT3 signaling pathways collaboratively link inflammation to cancer. *Protein Cell* 4: 176-185. #10.1007/s13238-013-2084-3

Fang L, Harkewicz R, Hartvigsen K, Wiesner P, Choi SH, Almazan F, Pattison J, Deer E, Sayaphupha T, Dennis EA, Witztum JL, Tsimikas S & Miller YI. 2010. Oxidized cholesteryl esters and phospholipids in zebrafish larvae fed a high cholesterol diet: macrophage binding and activation. *J Biol Chem* 285: 32343-32351. #10.1074/jbc.M110.137257

Faria CC & Fortunato RS. 2020. The role of dual oxidases in physiology and cancer. *Genet Mol Biol* 43: e20190096. #10.1590/1678-4685/GMB-2019-0096

Fazio M, Ablain J, Chuan Y, Langenau DM & Zon LI. 2020. Zebrafish patient avatars in cancer biology and precision cancer therapy. *Nat Rev Cancer* 20: 263-273. #10.1038/s41568-020-0252-3

Feng H, Stachura DL, White RM, Gutierrez A, Zhang L, Sanda T, Jette CA, Testa JR, Neuberg DS, Langenau DM, Kutok JL, Zon LI, Traver D, Fleming MD, Kanki JP & Look AT. 2010a. T-lymphoblastic lymphoma cells express high levels of BCL2, S1P1, and ICAM1, leading to a blockade of tumor cell intravasation. *Cancer Cell* 18: 353-366. #10.1016/j.ccr.2010.09.009

Feng Y, Renshaw S & Martin P. 2012. Live imaging of tumor initiation in zebrafish larvae reveals a trophic role for leukocyte-derived PGE(2). *Curr Biol* 22: 1253-1259. #10.1016/j.cub.2012.05.010

Feng Y, Santoriello C, Mione M, Hurlstone A & Martin P. 2010b. Live imaging of innate immune cell sensing of transformed cells in zebrafish larvae: parallels between tumor initiation and wound inflammation. *PLoS Biol* 8: e1000562. #10.1371/journal.pbio.1000562

Fernandez Rodriguez CM, Aller R, Gutierrez Garcia ML, Ampuero J, Gomez-Camarero J, Martin-Mateos RMf, Burgos-Santamaria D, Rosales JM, Aspichueta P, Buque X, Latorre M, Andrade RJ, Hernandez-Guerra M & Romero-Gomez M. 2019. Higher levels of serum uric acid influences hepatic damage in patients with non-alcoholic fatty liver disease (NAFLD). *Rev Esp Enferm Dig* 111: 264-269. #10.17235/reed.2019.5965/2018

Fidler IJ. 2003. The pathogenesis of cancer metastasis: the 'seed and soil' hypothesis revisited. *Nat Rev Cancer* 3: 453-458. #10.1038/nrc1098

Fridlender ZG, Sun J, Kim S, Kapoor V, Cheng G, Ling L, Worthen GS & Albelda SM. 2009. Polarization of tumor-associated neutrophil phenotype by TGF-beta: "N1" versus "N2" TAN. *Cancer Cell* 16: 183-194. #10.1016/j.ccr.2009.06.017

Friedman RJ & Rigel DS. 1985. The clinical features of malignant melanoma. *Dermatol Clin* 3: 271-283.

Gabellini C, Gomez-Abenza E, Ibanez-Molero S, Tupone MG, Perez-Oliva AB, de Oliveira S, Del Bufalo D & Mulero V. 2018. Interleukin 8 mediates bcl-xL-induced enhancement of human melanoma cell dissemination and angiogenesis in a zebrafish xenograft model. *Int J Cancer* 142: 584-596. #10.1002/ijc.31075

Galadari S, Rahman A, Pallichankandy S & Thayyullathil F. 2017. Reactive oxygen species and cancer paradox: To promote or to suppress? *Free Radic Biol Med* 104: 144-164. #10.1016/j.freeradbiomed.2017.01.004

Gandini S, Sera F, Cattaruzza MS, Pasquini P, Picconi O, Boyle P & Melchi CF. 2005. Meta-analysis of risk factors for cutaneous melanoma: II. Sun exposure. *Eur J Cancer* 41: 45-60. #10.1016/j.ejca.2004.10.016

Gao B, Ahmad MF, Nagy LE & Tsukamoto H. 2019. Inflammatory pathways in alcoholic steatohepatitis. *J Hepatol* 70: 249-259. #10.1016/j.jhep.2018.10.023

Gao P, Zhang H, Dinavahi R, Li F, Xiang Y, Raman V, Bhujwalla ZM, Felsher DW, Cheng L, Pevsner J, Lee LA, Semenza GL & Dang CV. 2007. HIF-dependent antitumorigenic effect of antioxidants in vivo. *Cancer Cell* 12: 230-238. #10.1016/j.ccr.2007.08.004

Gart E, van Duyvenvoorde W, Caspers MPM, van Trigt N, Snabel J, Menke A, Keijer J, Salic K, Morrison MC & Kleemann R. 2022. Intervention with isoleucine or valine corrects hyperinsulinemia and reduces intrahepatic diacylglycerols, liver steatosis, and inflammation in Ldlr-/-.Leiden mice with manifest obesity-associated NASH. *FASEB J* 36: e22435. #10.1096/fj.202200111R

Giehl K. 2005. Oncogenic Ras in tumour progression and metastasis. *Biol Chem* 386: 193-205. #10.1515/BC.2005.025

Giorgio V, Prono F, Graziano F & Nobili V. 2013. Pediatric non alcoholic fatty liver disease: old and new concepts on development, progression, metabolic insight and potential treatment targets. *BMC Pediatr* 13: 40. #10.1186/1471-2431-13-40

Glasauer A & Chandel NS. 2014. Targeting antioxidants for cancer therapy. *Biochem Pharmacol* 92: 90-101. #10.1016/j.bcp.2014.07.017

Goessling W & Sadler KC. 2015. Zebrafish: an important tool for liver disease research. *Gastroenterology* 149: 1361-1377. #10.1053/j.gastro.2015.08.034

Gomez-Abenza E, Ibanez-Molero S, Garcia-Moreno D, Fuentes I, Zon LI, Mione MC, Cayuela ML, Gabellini C & Mulero V. 2019. Zebrafish modeling reveals that SPINT1 regulates the aggressiveness of skin cutaneous melanoma and its crosstalk with tumor immune microenvironment. *J Exp Clin Cancer Res* 38: 405. #10.1186/s13046-019-1389-3

Goodman GE, Thornquist MD, Balmes J, Cullen MR, Meyskens FL, Jr., Omenn GS, Valanis B & Williams JH, Jr. 2004. The Beta-Carotene and Retinol Efficacy Trial: incidence of lung cancer and cardiovascular disease mortality during 6-year follow-up after stopping beta-carotene and retinol supplements. *J Natl Cancer Inst* 96: 1743-1750. #10.1093/jnci/djh320

Grasberger H & Refetoff S. 2006. Identification of the maturation factor for dual oxidase. Evolution of an eukaryotic operon equivalent. *J Biol Chem* 281: 18269-18272. #10.1074/jbc.C600095200

Guo M, Wei H, Hu J, Sun S, Long J & Wang X. 2015. U0126 inhibits pancreatic cancer progression via the KRAS signaling pathway in a zebrafish xenotransplantation model. *Oncol Rep* 34: 699-706. #10.3892/or.2015.4019

Gupta RK, Patel AK, Shah N, Chaudhary AK, Jha UK, Yadav UC, Gupta PK & Pakuwal U. 2014. Oxidative stress and antioxidants in disease and cancer: a review. *Asian Pac J Cancer Prev* 15: 4405-4409. #10.7314/apjcp.2014.15.11.4405

Haldi M, Ton C, Seng WL & McGrath P. 2006. Human melanoma cells transplanted into zebrafish proliferate, migrate, produce melanin, form masses and stimulate angiogenesis in zebrafish. *Angiogenesis* 9: 139-151. #10.1007/s10456-006-9040-2

Hales CM, Carroll MD, Fryar CD & Ogden CL. 2017. Prevalence of Obesity Among Adults and Youth: United States, 2015-2016. *NCHS Data Brief*: 1-8.

Handy DE & Loscalzo J. 2012. Redox regulation of mitochondrial function. *Antioxid Redox Signal* 16: 1323-1367. #10.1089/ars.2011.4123

Harmon DB, Mandler WK, Sipula IJ, Dedousis N, Lewis SE, Eckels JT, Du J, Wang Y, Huckestein BR, Pagano PJ, Cifuentes-Pagano E, Homanics GE, Van't Erve TJ, Stefanovic-Racic M, Jurczak MJ, O'Doherty RM & Kelley EE. 2019. Hepatocyte-Specific Ablation or Whole-Body Inhibition of Xanthine Oxidoreductase in Mice Corrects Obesity-Induced Systemic Hyperuricemia Without Improving Metabolic Abnormalities. *Diabetes* 68: 1221-1229. #10.2337/db18-1198

Harris AL. 2002. Hypoxia--a key regulatory factor in tumour growth. *Nat Rev Cancer* 2: 38-47. #10.1038/nrc704

Harris IS & DeNicola GM. 2020. The Complex Interplay between Antioxidants and ROS in Cancer. *Trends Cell Biol* 30: 440-451. #10.1016/j.tcb.2020.03.002

Harris IS, Treloar AE, Inoue S, Sasaki M, Gorrini C, Lee KC, Yung KY, Brenner D, Knobbe-Thomsen CB, Cox MA, Elia A, Berger T, Cescon DW, Adeoye A, Brustle A, Molyneux SD, Mason JM, Li WY, Yamamoto K, Wakeham A, Berman HK, Khokha R, Done SJ, Kavanagh TJ, Lam CW

& Mak TW. 2015. Glutathione and thioredoxin antioxidant pathways synergize to drive cancer initiation and progression. *Cancer Cell* 27: 211-222. #10.1016/j.ccell.2014.11.019

Hartman ML & Czyz M. 2015. MITF in melanoma: mechanisms behind its expression and activity. *Cell Mol Life Sci* 72: 1249-1260. #10.1007/s00018-014-1791-0

Hasney C, Butcher RB, 2nd & Amedee RG. 2008. Malignant melanoma of the head and neck: a brief review of pathophysiology, current staging, and management. *Ochsner J* 8: 181-185.

Heusinkveld M, de Vos van Steenwijk PJ, Goedemans R, Ramwadhdoebe TH, Gorter A, Welters MJ, van Hall T & van der Burg SH. 2011. M2 macrophages induced by prostaglandin E2 and IL-6 from cervical carcinoma are switched to activated M1 macrophages by CD4+ Th1 cells. *J Immunol* 187: 1157-1165. #10.4049/jimmunol.1100889

Heusinkveld M & van der Burg SH. 2011. Identification and manipulation of tumor associated macrophages in human cancers. *J Transl Med* 9: 216. #10.1186/1479-5876-9-216

Hirakawa S, Saito R, Ohara H, Okuyama R & Aiba S. 2011. Dual oxidase 1 induced by Th2 cytokines promotes STAT6 phosphorylation via oxidative inactivation of protein tyrosine phosphatase 1B in human epidermal keratinocytes. *J Immunol* 186: 4762-4770. #10.4049/jimmunol.1000791

Hirsova P & Gores GJ. 2015. Death Receptor-Mediated Cell Death and Proinflammatory Signaling in Nonalcoholic Steatohepatitis. *Cell Mol Gastroenterol Hepatol* 1: 17-27. #10.1016/j.jcmgh.2014.11.005

Hirsova P, Ibrahim SH, Krishnan A, Verma VK, Bronk SF, Werneburg NW, Charlton MR, Shah VH, Malhi H & Gores GJ. 2016. Lipid-Induced Signaling Causes Release of Inflammatory Extracellular Vesicles From Hepatocytes. *Gastroenterology* 150: 956-967. #10.1053/j.gastro.2015.12.037

Hooijkaas AI, Gadiot J, van der Valk M, Mooi WJ & Blank CU. 2012. Targeting BRAFV600E in an inducible murine model of melanoma. *Am J Pathol* 181: 785-794. #10.1016/j.ajpath.2012.06.002

Howe K, Clark MD, Torroja CF, Torrance J, Berthelot C, Muffato M, Collins JE, Humphray S, McLaren K, Matthews L, McLaren S, Sealy I, Caccamo M, Churcher C, Scott C, Barrett JC, Koch R, Rauch GJ, White S, Chow W, Kilian B, Quintais LT, Guerra-Assuncao JA, Zhou Y, Gu Y, Yen J, Vogel JH, Eyre T, Redmond S, Banerjee R, Chi J, Fu B, Langley E, Maguire SF, Laird GK, Lloyd D, Kenyon E, Donaldson S, Sehra H, Almeida-King J, Loveland J, Trevanion S, Jones M, Quail M, Willey D, Hunt A, Burton J, Sims S, McLay K, Plumb B, Davis J, Clee C, Oliver K, Clark R, Riddle C, Elliot D, Threadgold G, Harden G, Ware D, Begum S, Mortimore B, Kerry G, Heath P, Phillimore B, Tracey A, Corby N, Dunn M, Johnson C, Wood J, Clark S, Pelan S, Griffiths G, Smith M, Glithero R, Howden P, Barker N, Lloyd C, Stevens C, Harley J, Holt K, Panagiotidis G, Lovell J, Beasley H, Henderson C, Gordon D, Auger K, Wright D, Collins J, Raisen C, Dyer L, Leung K, Robertson L, Ambridge K, Leongamornlert D, McGuire S, Gilderthorp R, Griffiths C, Manthravadi D, Nichol S, Barker G, Whitehead S, Kay M, Brown J, Murnane C, Gray E, Humphries M, Sycamore N, Barker D, Saunders D, Wallis J, Babbage A, Hammond S, Mashreghi-Mohammadi M, Barr L, Martin S, Wray P, Ellington A, Matthews N, Ellwood M, Woodmansey R, Clark G, Cooper J, Tromans A, Grafham D, Skuce C, Pandian R, Andrews R, Harrison E, Kimberley A, Garnett J, Fosker N, Hall R, Garner P, Kelly D, Bird C, Palmer S, Gehring I, Berger A, Dooley CM, Ersan-Urun Z, Eser C, Geiger H, Geisler M, Karotki L, Kirn A, Konantz J, Konantz M, Oberlander M, Rudolph-Geiger S, Teucke M, Lanz C, Raddatz G, Osoegawa K, Zhu B, Rapp A, Widaa S, Langford C, Yang F, Schuster SC, Carter NP, Harrow J, Ning Z, Herrero J, Searle SM, Enright A, Geisler R, Plasterk RH, Lee C, Westerfield M, de Jong PJ, Zon LI, Postlethwait JH, Nusslein-Volhard C, Hubbard TJ, Roest Crollius H, Rogers J & Stemple DL. 2013. The zebrafish reference genome sequence and its relationship to the human genome. *Nature* 496: 498-503. #10.1038/nature12111

Huemer K, Squirrell JM, Swader R, LeBert DC, Huttenlocher A & Eliceiri KW. 2017. zWEDGI: Wounding and Entrapment Device for Imaging Live Zebrafish Larvae. *Zebrafish* 14: 42-50. #10.1089/zeb.2016.1323

Hughes MM & O'Neill LAJ. 2018. Metabolic regulation of NLRP3. *Immunol Rev* 281: 88-98. #10.1111/imr.12608

Hwang S, Yun H, Moon S, Cho YE & Gao B. 2021. Role of Neutrophils in the Pathogenesis of Nonalcoholic Steatohepatitis. *Front Endocrinol (Lausanne)* 12: 751802. #10.3389/fendo.2021.751802

Iida C, Fujii K, Koga E, Washino Y, Kitamura Y, Ichi I, Abe K, Matsura T & Kojo S. 2009. Effect of alpha-tocopherol on carbon tetrachloride intoxication in the rat liver. *Arch Toxicol* 83: 477-483. #10.1007/s00204-008-0394-7

International Agency for Research on Cancer Working Group on artificial ultraviolet l & skin c. 2007. The association of use of sunbeds with cutaneous malignant melanoma and other skin cancers: A systematic review. *Int J Cancer* 120: 1116-1122. #10.1002/ijc.22453

Inzaugarat ME, De Matteo E, Baz P, Lucero D, Garcia CC, Gonzalez Ballerga E, Daruich J, Sorda JA, Wald MR & Chernavsky AC. 2017. New evidence for the therapeutic potential of curcumin to treat nonalcoholic fatty liver disease in humans. *PLoS One* 12: e0172900. #10.1371/journal.pone.0172900

Itoh M, Kato H, Suganami T, Konuma K, Marumoto Y, Terai S, Sakugawa H, Kanai S, Hamaguchi M, Fukaishi T, Aoe S, Akiyoshi K, Komohara Y, Takeya M, Sakaida I & Ogawa Y. 2013. Hepatic crown-like structure: a unique histological feature in non-alcoholic steatohepatitis in mice and humans. *PLoS One* 8: e82163. #10.1371/journal.pone.0082163

Iyengar S, Houvras Y & Ceol CJ. 2012. Screening for melanoma modifiers using a zebrafish autochthonous tumor model. *J Vis Exp*: e50086. #10.3791/50086

Jagannathan-Bogdan M & Zon LI. 2013. Hematopoiesis. *Development* 140: 2463-2467. #10.1242/dev.083147

Jakubczyk K, Dec K, Kaldunska J, Kawczuga D, Kochman J & Janda K. 2020. Reactive oxygen species - sources, functions, oxidative damage. *Pol Merkur Lekarski* 48: 124-127.

Jones MW, Small K, Kashyap S & Deppen JG. 2022. Physiology, Gallbladder In *StatPearls*. Treasure Island (FL)

Kasumov T, Li L, Li M, Gulshan K, Kirwan JP, Liu X, Previs S, Willard B, Smith JD & McCullough A. 2015. Ceramide as a mediator of non-alcoholic Fatty liver disease and associated atherosclerosis. *PLoS One* 10: e0126910. #10.1371/journal.pone.0126910

Kaufman CK, Mosimann C, Fan ZP, Yang S, Thomas AJ, Ablain J, Tan JL, Fogley RD, van Rooijen E, Hagedorn EJ, Ciarlo C, White RM, Matos DA, Puller AC, Santoriello C, Liao EC, Young RA & Zon LI. 2016. A zebrafish melanoma model reveals emergence of neural crest identity during melanoma initiation. *Science* 351: aad2197. #10.1126/science.aad2197

Kawachi Y, Fujishima Y, Nishizawa H, Nakamura T, Akari S, Murase T, Saito T, Miyazaki Y, Nagao H, Fukuda S, Kita S, Katakami N, Doki Y, Maeda N & Shimomura I. 2021. Increased plasma XOR activity induced by NAFLD/NASH and its possible involvement in vascular neointimal proliferation. *JCI Insight* 6#10.1172/jci.insight.144762

Kazankov K, Jorgensen SMD, Thomsen KL, Moller HJ, Vilstrup H, George J, Schuppan D & Gronbaek H. 2019. The role of macrophages in nonalcoholic fatty liver disease and nonalcoholic steatohepatitis. *Nat Rev Gastroenterol Hepatol* 16: 145-159. #10.1038/s41575-018-0082-x

Kelley EE, Hock T, Khoo NK, Richardson GR, Johnson KK, Powell PC, Giles GI, Agarwal A, Lancaster JR, Jr. & Tarpey MM. 2006. Moderate hypoxia induces xanthine oxidoreductase activity in arterial endothelial cells. *Free Radic Biol Med* 40: 952-959. #10.1016/j.freeradbiomed.2005.11.008

Khan H, Reale M, Ullah H, Sureda A, Tejada S, Wang Y, Zhang ZJ & Xiao J. 2020. Anti-cancer effects of polyphenols via targeting p53 signaling pathway: updates and future directions. *Biotechnol Adv* 38: 107385. #10.1016/j.biotechadv.2019.04.007

Khan N, Mahajan NK, Sinha P & Jayandharan GR. 2019. An efficient method to generate xenograft tumor models of acute myeloid leukemia and hepatocellular carcinoma in adult zebrafish. *Blood Cells Mol Dis* 75: 48-55. #10.1016/j.bcmd.2018.12.007

Kim H, Lee DS, An TH, Park HJ, Kim WK, Bae KH & Oh KJ. 2021. Metabolic Spectrum of Liver Failure in Type 2 Diabetes and Obesity: From NAFLD to NASH to HCC. *Int J Mol Sci* 22#10.3390/ijms22094495

Kizil C, Kaslin J, Kroehne V & Brand M. 2012. Adult neurogenesis and brain regeneration in zebrafish. *Dev Neurobiol* 72: 429-461. #10.1002/dneu.20918

Kleiner DE, Brunt EM, Van Natta M, Behling C, Contos MJ, Cummings OW, Ferrell LD, Liu YC, Torbenson MS, Unalp-Arida A, Yeh M, McCullough AJ, Sanyal AJ & Nonalcoholic Steatohepatitis Clinical Research N. 2005. Design and validation of a histological scoring system for nonalcoholic fatty liver disease. *Hepatology* 41: 1313-1321. #10.1002/hep.20701

Knight T & Irving JA. 2014. Ras/Raf/MEK/ERK Pathway Activation in Childhood Acute Lymphoblastic Leukemia and Its Therapeutic Targeting. *Front Oncol* 4: 160. #10.3389/fonc.2014.00160

Ko JS. 2017. The Immunology of Melanoma. *Clin Lab Med* 37: 449-471. #10.1016/j.cll.2017.06.001

Konantz M, Balci TB, Hartwig UF, Dellaire G, Andre MC, Berman JN & Lengerke C. 2012. Zebrafish xenografts as a tool for in vivo studies on human cancer. *Ann N Y Acad Sci* 1266: 124-137. #10.1111/j.1749-6632.2012.06575.x

Kondo T, Miyakawa N, Kitano S, Watanabe T, Goto R, Suico MA, Sato M, Takaki Y, Sakaguchi M, Igata M, Kawashima J, Motoshima H, Matsumura T, Kai H & Araki E. 2021. Activation of heat shock response improves biomarkers of NAFLD in patients with metabolic diseases. *Endocr Connect* 10: 521-533. #10.1530/EC-21-0084

Kousis PC, Henderson BW, Maier PG & Gollnick SO. 2007. Photodynamic therapy enhancement of antitumor immunity is regulated by neutrophils. *Cancer Res* 67: 10501-10510. #10.1158/0008-5472.CAN-07-1778

Kowdley KV, Belt P, Wilson LA, Yeh MM, Neuschwander-Tetri BA, Chalasani N, Sanyal AJ, Nelson JE & Network NCR. 2012. Serum ferritin is an independent predictor of histologic severity and advanced fibrosis in patients with nonalcoholic fatty liver disease. *Hepatology* 55: 77-85. #10.1002/hep.24706

Krenkel O, Puengel T, Govaere O, Abdallah AT, Mossanen JC, Kohlhepp M, Liepelt A, Lefebvre E, Luedde T, Hellerbrand C, Weiskirchen R, Longerich T, Costa IG, Anstee QM, Trautwein C & Tacke F. 2018. Therapeutic inhibition of inflammatory monocyte recruitment reduces steatohepatitis and liver fibrosis. *Hepatology* 67: 1270-1283. #10.1002/hep.29544

Kulkarni A, Ibrahim S, Haider I, Basha A, Montgomery E, Ermis E, Mirmira RG & Anderson RM. 2022. A Novel 2-Hit Zebrafish Model to Study Early Pathogenesis of Non-Alcoholic Fatty Liver Disease. *Biomedicines* 10#10.3390/biomedicines10020479

Kunapuli P, Chitta KS & Cowell JK. 2003. Suppression of the cell proliferation and invasion phenotypes in glioma cells by the LGI1 gene. *Oncogene* 22: 3985-3991. #10.1038/sj.onc.1206584

Kwan KM, Fujimoto E, Grabher C, Mangum BD, Hardy ME, Campbell DS, Parant JM, Yost HJ, Kanki JP & Chien CB. 2007. The Tol2kit: a multisite gateway-based construction kit for Tol2 transposon transgenesis constructs. *Dev Dyn* 236: 3088-3099. #10.1002/dvdy.21343

Lake AD, Novak P, Shipkova P, Aranibar N, Robertson DG, Reily MD, Lehman-McKeeman LD, Vaillancourt RR & Cherrington NJ. 2015. Branched chain amino acid metabolism profiles in progressive human nonalcoholic fatty liver disease. *Amino Acids* 47: 603-615. #10.1007/s00726-014-1894-9

Lam SH, Chua HL, Gong Z, Lam TJ & Sin YM. 2004. Development and maturation of the immune system in zebrafish, Danio rerio: a gene expression profiling, in situ hybridization and immunological study. *Dev Comp Immunol* 28: 9-28. #10.1016/s0145-305x(03)00103-4

Langenau DM, Ferrando AA, Traver D, Kutok JL, Hezel JP, Kanki JP, Zon LI, Look AT & Trede NS. 2004. In vivo tracking of T cell development, ablation, and engraftment in transgenic zebrafish. *Proc Natl Acad Sci U S A* 101: 7369-7374. #10.1073/pnas.0402248101

Lanthier N. 2015. Targeting Kupffer cells in non-alcoholic fatty liver disease/non-alcoholic steatohepatitis: Why and how? *World J Hepatol* 7: 2184-2188. #10.4254/wjh.v7.i19.2184

Lawson ND & Weinstein BM. 2002. In vivo imaging of embryonic vascular development using transgenic zebrafish. *Dev Biol* 248: 307-318. #10.1006/dbio.2002.0711

Lee MC, Velayutham M, Komatsu T, Hille R & Zweier JL. 2014. Measurement and characterization of superoxide generation from xanthine dehydrogenase: a redox-regulated pathway of radical generation in ischemic tissues. *Biochemistry* 53: 6615-6623. #10.1021/bi500582r

Levene AP & Goldin RD. 2012. The epidemiology, pathogenesis and histopathology of fatty liver disease. *Histopathology* 61: 141-152. #10.1111/j.1365-2559.2011.04145.x

Li H, Zhou Y, Wang H, Zhang M, Qiu P, Zhang M, Zhang R, Zhao Q & Liu J. 2020. Crosstalk Between Liver Macrophages and Surrounding Cells in Nonalcoholic Steatohepatitis. *Front Immunol* 11: 1169. #10.3389/fimmu.2020.01169

Li P, White RM & Zon LI. 2011. Transplantation in zebrafish. *Methods Cell Biol* 105: 403-417. #10.1016/B978-0-12-381320-6.00017-5

Li Z, Pang Y, Gara SK, Achyut BR, Heger C, Goldsmith PK, Lonning S & Yang L. 2012. Gr-1+CD11b+ cells are responsible for tumor promoting effect of TGF-beta in breast cancer progression. *Int J Cancer* 131: 2584-2595. #10.1002/ijc.27572

Liang W, Menke AL, Driessen A, Koek GH, Lindeman JH, Stoop R, Havekes LM, Kleemann R & van den Hoek AM. 2014. Establishment of a general NAFLD scoring system for rodent models and comparison to human liver pathology. *PLoS One* 9: e115922. #10.1371/journal.pone.0115922

Lin JY & Fisher DE. 2007. Melanocyte biology and skin pigmentation. *Nature* 445: 843-850. #10.1038/nature05660

Lin Z, Xie YZ, Zhao MC, Hou PP, Tang J & Chen GL. 2021. Xanthine dehydrogenase as a prognostic biomarker related to tumor immunology in hepatocellular carcinoma. *Cancer Cell Int* 21: 475. #10.1186/s12935-021-02173-7

Lister JA, Robertson CP, Lepage T, Johnson SL & Raible DW. 1999. nacre encodes a zebrafish microphthalmia-related protein that regulates neural-crest-derived pigment cell fate. *Development* 126: 3757-3767.

Litin SC & Mayo Clinic. 2009. *Mayo clinic family health book*. Des Moines, IA: Time Inc. 1423 p. pp.

Lopez-Suarez A, Elvira-Gonzalez J, Bascunana-Quirell A, Rosal-Obrador J, Michan-Dona A, Escribano-Serrano J, Benitez-Rodriguez E & Grupo para el Estudio del Riesgo Vascular A. 2006. [Serum urate levels and urinary uric acid excretion in subjects with metabolic syndrome]. *Med Clin (Barc)* 126: 321-324. #10.1157/13085753

Luxen S, Noack D, Frausto M, Davanture S, Torbett BE & Knaus UG. 2009. Heterodimerization controls localization of Duox-DuoxA NADPH oxidases in airway cells. *J Cell Sci* 122: 1238-1247. #10.1242/jcs.044123

Ma J, Yin H, Li M, Deng Y, Ahmad O, Qin G, He Q, Li J, Gao K, Zhu J, Wang B, Wu S, Wang T & Shang J. 2019. A Comprehensive Study of High Cholesterol Diet-Induced Larval Zebrafish Model: A Short-Time In Vivo Screening Method for Non-Alcoholic Fatty Liver Disease Drugs. *Int J Biol Sci* 15: 973-983. #10.7150/ijbs.30013

Ma Y, Lee G, Heo SY & Roh YS. 2021. Oxidative Stress Is a Key Modulator in the Development of Nonalcoholic Fatty Liver Disease. *Antioxidants (Basel)* 11#10.3390/antiox11010091

Machado M, Marques-Vidal P & Cortez-Pinto H. 2006. Hepatic histology in obese patients undergoing bariatric surgery. *J Hepatol* 45: 600-606. #10.1016/j.jhep.2006.06.013

Malhi H & Gores GJ. 2008. Molecular mechanisms of lipotoxicity in nonalcoholic fatty liver disease. *Semin Liver Dis* 28: 360-369. #10.1055/s-0028-1091980

Marelli G, Sica A, Vannucci L & Allavena P. 2017. Inflammation as target in cancer therapy. *Curr Opin Pharmacol* 35: 57-65. #10.1016/j.coph.2017.05.007

Markovic SN, Erickson LA, Flotte TJ, Kottschade LA, McWilliams RR, Jakub JW, Farley DR, Tran NV, Schild SE, Olivier KR, Vuk-Pavlovic S, Sekulic A, Weenig RH, Pulido JS, Quevedo JF, Vile RG, Wiseman GA, Stoian I, Pittelkow MR & Melanoma Study Group of the Mayo Clinic Cancer C. 2009. Metastatic malignant melanoma. *G Ital Dermatol Venereol* 144: 1-26.

Marra F & Tacke F. 2014. Roles for chemokines in liver disease. *Gastroenterology* 147: 577-594 e571. #10.1053/j.gastro.2014.06.043

Masarone M, Rosato V, Dallio M, Gravina AG, Aglitti A, Loguercio C, Federico A & Persico M. 2018. Role of Oxidative Stress in Pathophysiology of Nonalcoholic Fatty Liver Disease. *Oxid Med Cell Longev* 2018: 9547613. #10.1155/2018/9547613

Masucci MT, Minopoli M & Carriero MV. 2019. Tumor Associated Neutrophils. Their Role in Tumorigenesis, Metastasis, Prognosis and Therapy. *Front Oncol* 9: 1146. #10.3389/fonc.2019.01146

Mateos FA, Puig JG, Jimenez ML & Fox IH. 1987. Hereditary xanthinuria. Evidence for enhanced hypoxanthine salvage. *J Clin Invest* 79: 847-852. #10.1172/JCI112893

McConnell AM, Mito JK, Ablain J, Dang M, Formichella L, Fisher DE & Zon LI. 2019. Neural crest state activation in NRAS driven melanoma, but not in NRAS-driven melanocyte expansion. *Dev Biol* 449: 107-114. #10.1016/j.ydbio.2018.05.026

McNally JS, Davis ME, Giddens DP, Saha A, Hwang J, Dikalov S, Jo H & Harrison DG. 2003. Role of xanthine oxidoreductase and NAD(P)H oxidase in endothelial superoxide production in response to oscillatory shear stress. *Am J Physiol Heart Circ Physiol* 285: H2290-2297. #10.1152/ajpheart.00515.2003

Meier F, Schittek B, Busch S, Garbe C, Smalley K, Satyamoorthy K, Li G & Herlyn M. 2005. The RAS/RAF/MEK/ERK and PI3K/AKT signaling pathways present molecular targets for the effective treatment of advanced melanoma. *Front Biosci* 10: 2986-3001. #10.2741/1755

Merlin JPJ, Rupasinghe HPV, Dellaire G & Murphy K. 2021. Role of Dietary Antioxidants in p53-Mediated Cancer Chemoprevention and Tumor Suppression. *Oxid Med Cell Longev* 2021: 9924328. #10.1155/2021/9924328

Meyskens FL, Jr., McNulty SE, Buckmeier JA, Tohidian NB, Spillane TJ, Kahlon RS & Gonzalez RI. 2001. Aberrant redox regulation in human metastatic melanoma cells compared to normal melanocytes. *Free Radic Biol Med* 31: 799-808. #10.1016/s0891-5849(01)00650-5

Meziani L, Gerbe de Thore M, Hamon P, Bockel S, Louzada RA, Clemenson C, Corre R, Liu W, Dupuy C, Mondini M & Deutsch E. 2020. Dual oxidase 1 limits the IFNgamma-associated antitumor effect of macrophages. *J Immunother Cancer* 8#10.1136/jitc-2020-000622

Michael C, Martinez-Navarro FJ & de Oliveira S. 2021. Analysis of Liver Microenvironment during Early Progression of Non-Alcoholic Fatty Liver Disease-Associated Hepatocellular Carcinoma in Zebrafish. *J Vis Exp* #10.3791/62457

Mignogna C, Scali E, Camastra C, Presta I, Zeppa P, Barni T, Donato G, Bottoni U & Di Vito A. 2017. Innate immunity in cutaneous melanoma. *Clin Exp Dermatol* 42: 243-250. #10.1111/ced.13023

Miller AJ & Mihm MC, Jr. 2006. Melanoma. *N Engl J Med* 355: 51-65. #10.1056/NEJMra052166

Mills CD, Kincaid K, Alt JM, Heilman MJ & Hill AM. 2000. M-1/M-2 macrophages and the Th1/Th2 paradigm. *J Immunol* 164: 6166-6173. #10.4049/jimmunol.164.12.6166

Mione MC & Trede NS. 2010. The zebrafish as a model for cancer. *Dis Model Mech* 3: 517-523. #10.1242/dmm.004747

Mohapatra P, Prasad CP & Andersson T. 2019. Combination therapy targeting the elevated interleukin-6 level reduces invasive migration of BRAF inhibitor-resistant melanoma cells. *Mol Oncol* 13: 480-494. #10.1002/1878-0261.12433

Morand S, Ueyama T, Tsujibe S, Saito N, Korzeniowska A & Leto TL. 2009. Duox maturation factors form cell surface complexes with Duox affecting the specificity of reactive oxygen species generation. *FASEB J* 23: 1205-1218. #10.1096/fj.08-120006

Mosca A, Nobili V, De Vito R, Crudele A, Scorletti E, Villani A, Alisi A & Byrne CD. 2017. Serum uric acid concentrations and fructose consumption are independently associated with NASH in children and adolescents. *J Hepatol* 66: 1031-1036. #10.1016/j.jhep.2016.12.025

Moyer VA & Force USPST. 2014. Vitamin, mineral, and multivitamin supplements for the primary prevention of cardiovascular disease and cancer: U.S. Preventive services Task Force recommendation statement. *Ann Intern Med* 160: 558-564. #10.7326/M14-0198

Mraz M, Hurba O, Bartl J, Dolezel Z, Marinaki A, Fairbanks L & Stiburkova B. 2015. Modern diagnostic approach to hereditary xanthinuria. *Urolithiasis* 43: 61-67. #10.1007/s00240-014-0734-4

Nakagawa T, Tuttle KR, Short RA & Johnson RJ. 2005. Hypothesis: fructose-induced hyperuricemia as a causal mechanism for the epidemic of the metabolic syndrome. *Nat Clin Pract Nephrol* 1: 80-86. #10.1038/ncpneph0019

Nappi AJ & Vass E. 1996. Hydrogen peroxide generation associated with the oxidations of the eumelanin precursors 5,6-dihydroxyindole and 5,6-dihydroxyindole-2-carboxylic acid. *Melanoma Res* 6: 341-349. #10.1097/00008390-199610000-00001

Negrin KA, Roth Flach RJ, DiStefano MT, Matevossian A, Friedline RH, Jung D, Kim JK & Czech MP. 2014. IL-1 signaling in obesity-induced hepatic lipogenesis and steatosis. *PLoS One* 9: e107265. #10.1371/journal.pone.0107265

Neuschwander-Tetri BA & Caldwell SH. 2003. Nonalcoholic steatohepatitis: summary of an AASLD Single Topic Conference. *Hepatology* 37: 1202-1219. #10.1053/jhep.2003.50193

Niethammer P, Grabher C, Look AT & Mitchison TJ. 2009. A tissue-scale gradient of hydrogen peroxide mediates rapid wound detection in zebrafish. *Nature* 459: 996-999. #10.1038/nature08119

Norton W & Bally-Cuif L. 2010. Adult zebrafish as a model organism for behavioural genetics. *BMC Neurosci* 11: 90. #10.1186/1471-2202-11-90

Oates JR, McKell MC, Moreno-Fernandez ME, Damen M, Deepe GS, Jr., Qualls JE & Divanovic S. 2019. Macrophage Function in the Pathogenesis of Non-alcoholic Fatty Liver Disease: The Mac Attack. *Front Immunol* 10: 2893. #10.3389/fimmu.2019.02893

Obermajer N, Muthuswamy R, Lesnock J, Edwards RP & Kalinski P. 2011. Positive feedback between PGE2 and COX2 redirects the differentiation of human dendritic cells toward stable myeloid-derived suppressor cells. *Blood* 118: 5498-5505. #10.1182/blood-2011-07-365825

Ogrunc M, Di Micco R, Liontos M, Bombardelli L, Mione M, Fumagalli M, Gorgoulis VG & d'Adda di Fagagna F. 2014. Oncogene-induced reactive oxygen species fuel hyperproliferation and DNA damage response activation. *Cell Death Differ* 21: 998-1012. #10.1038/cdd.2014.16

Ostuni R, Kratochvill F, Murray PJ & Natoli G. 2015. Macrophages and cancer: from mechanisms to therapeutic implications. *Trends Immunol* 36: 229-239. #10.1016/j.it.2015.02.004

Palmieri G, Ombra M, Colombino M, Casula M, Sini M, Manca A, Paliogiannis P, Ascierto PA & Cossu A. 2015. Multiple Molecular Pathways in Melanomagenesis: Characterization of Therapeutic Targets. *Front Oncol* 5: 183. #10.3389/fonc.2015.00183

Palmieri VO, Grattagliano I, Portincasa P & Palasciano G. 2006. Systemic oxidative alterations are associated with visceral adiposity and liver steatosis in patients with metabolic syndrome. *J Nutr* 136: 3022-3026. #10.1093/jn/136.12.3022

Paluncic J, Kovacevic Z, Jansson PJ, Kalinowski D, Merlot AM, Huang ML, Lok HC, Sahni S, Lane DJ & Richardson DR. 2016. Roads to melanoma: Key pathways and emerging players in melanoma progression and oncogenic signaling. *Biochim Biophys Acta* 1863: 770-784. #10.1016/j.bbamcr.2016.01.025

Papaspyridonos M, Matei I, Huang Y, do Rosario Andre M, Brazier-Mitouart H, Waite JC, Chan AS, Kalter J, Ramos I, Wu Q, Williams C, Wolchok JD, Chapman PB, Peinado H, Anandasabapathy N, Ocean AJ, Kaplan RN, Greenfield JP, Bromberg J, Skokos D & Lyden D. 2015. Id1 suppresses anti-tumour immune responses and promotes tumour progression by impairing myeloid cell maturation. *Nat Commun* 6: 6840. #10.1038/ncomms7840

Pardo-Sanchez I, Garcia-Moreno D & Mulero V. 2022. Zebrafish Models to Study the Crosstalk between Inflammation and NADPH Oxidase-Derived Oxidative Stress in Melanoma. *Antioxidants (Basel)* 11#10.3390/antiox11071277

Park HY, Kosmadaki M, Yaar M & Gilchrest BA. 2009. Cellular mechanisms regulating human melanogenesis. *Cell Mol Life Sci* 66: 1493-1506. #10.1007/s00018-009-8703-8

Park KH, Ye ZW, Zhang J & Kim SH. 2019. Palmitic Acid-Enriched Diet Induces Hepatic Steatosis and Injury in Adult Zebrafish. *Zebrafish* 16: 497-504. #10.1089/zeb.2019.1758

Passarelli A, Mannavola F, Stucci LS, Tucci M & Silvestris F. 2017. Immune system and melanoma biology: a balance between immunosurveillance and immune escape. *Oncotarget* 8: 106132-106142. #10.18632/oncotarget.22190

Pathria P, Louis TL & Varner JA. 2019. Targeting Tumor-Associated Macrophages in Cancer. *Trends Immunol* 40: 310-327. #10.1016/j.it.2019.02.003

Patton EE, Widlund HR, Kutok JL, Kopani KR, Amatruda JF, Murphey RD, Berghmans S, Mayhall EA, Traver D, Fletcher CD, Aster JC, Granter SR, Look AT, Lee C, Fisher DE & Zon LI. 2005. BRAF mutations are sufficient to promote nevi formation and cooperate with p53 in the genesis of melanoma. *Curr Biol* 15: 249-254. #10.1016/j.cub.2005.01.031

Pellicoro A, Ramachandran P, Iredale JP & Fallowfield JA. 2014. Liver fibrosis and repair: immune regulation of wound healing in a solid organ. *Nat Rev Immunol* 14: 181-194. #10.1038/nri3623

Pierantonelli I & Svegliati-Baroni G. 2019. Nonalcoholic Fatty Liver Disease: Basic Pathogenetic Mechanisms in the Progression From NAFLD to NASH. *Transplantation* 103: e1-e13. #10.1097/TP.0000000000002480

Piret SE, Esapa CT, Gorvin CM, Head R, Loh NY, Devuyst O, Thomas G, Brown SD, Brown M, Croucher P, Cox R & Thakker RV. 2012. A mouse model of early-onset renal failure due to a xanthine dehydrogenase nonsense mutation. *PLoS One* 7: e45217. #10.1371/journal.pone.0045217

Piscaglia F, Svegliati-Baroni G, Barchetti A, Pecorelli A, Marinelli S, Tiribelli C, Bellentani S & Group H-NIS. 2016. Clinical patterns of hepatocellular carcinoma in nonalcoholic fatty liver disease: A multicenter prospective study. *Hepatology* 63: 827-838. #10.1002/hep.28368

Piskounova E, Agathocleous M, Murphy MM, Hu Z, Huddlestun SE, Zhao Z, Leitch AM, Johnson TM, DeBerardinis RJ & Morrison SJ. 2015. Oxidative stress inhibits distant metastasis by human melanoma cells. *Nature* 527: 186-191. #10.1038/nature15726

Pollard JW. 2004. Tumour-educated macrophages promote tumour progression and metastasis. *Nat Rev Cancer* 4: 71-78. #10.1038/nrc1256

Pratomo IP, Noor DR, Kusmardi K, Rukmana A, Paramita RI, Erlina L, Fadilah F, Gayatri A, Fitriani M, Purnomo TTH, Ariane A, Heryanto R & Tedjo A. 2021. Xanthine Oxidase-Induced Inflammatory Responses in Respiratory Epithelial Cells: A Review in Immunopathology of COVID-19. *Int J Inflam* 2021: 1653392. #10.1155/2021/1653392

Progatzky F, Sangha NJ, Yoshida N, McBrien M, Cheung J, Shia A, Scott J, Marchesi JR, Lamb JR, Bugeon L & Dallman MJ. 2014. Dietary cholesterol directly induces acute

inflammasome-dependent intestinal inflammation. *Nat Commun* 5: 5864. #10.1038/ncomms6864

Qian BZ & Pollard JW. 2010. Macrophage diversity enhances tumor progression and metastasis. *Cell* 141: 39-51. #10.1016/j.cell.2010.03.014

Qiu Y, Chen T, Hu R, Zhu R, Li C, Ruan Y, Xie X & Li Y. 2021. Next frontier in tumor immunotherapy: macrophage-mediated immune evasion. *Biomark Res* 9: 72. #10.1186/s40364-021-00327-3

Rada P, Gonzalez-Rodriguez A, Garcia-Monzon C & Valverde AM. 2020. Understanding lipotoxicity in NAFLD pathogenesis: is CD36 a key driver? *Cell Death Dis* 11: 802. #10.1038/s41419-020-03003-w

Rajput S & Wilber A. 2010. Roles of inflammation in cancer initiation, progression, and metastasis. *Front Biosci (Schol Ed)* 2: 176-183. #10.2741/s55

Rao Y, Li C, Hu YT, Xu YH, Song BB, Guo SY, Jiang Z, Zhao DD, Chen SB, Tan JH, Huang SL, Li QJ, Wang XJ, Zhang YJ, Ye JM & Huang ZS. 2022. A novel HSF1 activator ameliorates non-alcoholic steatohepatitis by stimulating mitochondrial adaptive oxidation. *Br J Pharmacol* 179: 1411-1432. #10.1111/bph.15727

Rashighi M & Harris JE. 2017. Vitiligo Pathogenesis and Emerging Treatments. *Dermatol Clin* 35: 257-265. #10.1016/j.det.2016.11.014

Rastrelli M, Tropea S, Rossi CR & Alaibac M. 2014. Melanoma: epidemiology, risk factors, pathogenesis, diagnosis and classification. *In Vivo* 28: 1005-1011.

Razzell W, Evans IR, Martin P & Wood W. 2013. Calcium flashes orchestrate the wound inflammatory response through DUOX activation and hydrogen peroxide release. *Curr Biol* 23: 424-429. #10.1016/j.cub.2013.01.058

Reczek CR & Chandel NS. 2015. ROS-dependent signal transduction. *Curr Opin Cell Biol* 33: 8-13. #10.1016/j.ceb.2014.09.010

Rensen SS, Bieghs V, Xanthoulea S, Arfianti E, Bakker JA, Shiri-Sverdlov R, Hofker MH, Greve JW & Buurman WA. 2012. Neutrophil-derived myeloperoxidase aggravates non-alcoholic steatohepatitis in low-density lipoprotein receptor-deficient mice. *PLoS One* 7: e52411. #10.1371/journal.pone.0052411

Rensen SS, Slaats Y, Nijhuis J, Jans A, Bieghs V, Driessen A, Malle E, Greve JW & Buurman WA. 2009. Increased hepatic myeloperoxidase activity in obese subjects with nonalcoholic steatohepatitis. *Am J Pathol* 175: 1473-1482. #10.2353/ajpath.2009.080999

Renshaw SA, Loynes CA, Trushell DM, Elworthy S, Ingham PW & Whyte MK. 2006. A transgenic zebrafish model of neutrophilic inflammation. *Blood* 108: 3976-3978. #10.1182/blood-2006-05-024075

Rodriguez-Ruiz L, Lozano-Gil JM, Lachaud C, Mesa-Del-Castillo P, Cayuela ML, Garcia-Moreno D, Perez-Oliva AB & Mulero V. 2020. Zebrafish Models to Study Inflammasome-Mediated Regulation of Hematopoiesis. *Trends Immunol* 41: 1116-1127. #10.1016/j.it.2020.10.006

Rodriguez PC, Quiceno DG, Zabaleta J, Ortiz B, Zea AH, Piazuelo MB, Delgado A, Correa P, Brayer J, Sotomayor EM, Antonia S, Ochoa JB & Ochoa AC. 2004. Arginase I production in the tumor microenvironment by mature myeloid cells inhibits T-cell receptor expression and antigen-specific T-cell responses. *Cancer Res* 64: 5839-5849. #10.1158/0008-5472.CAN-04-0465

Roh-Johnson M, Shah AN, Stonick JA, Poudel KR, Kargl J, Yang GH, di Martino J, Hernandez RE, Gast CE, Zarour LR, Antoku S, Houghton AM, Bravo-Cordero JJ, Wong MH, Condeelis J & Moens CB. 2017. Macrophage-Dependent Cytoplasmic Transfer during Melanoma Invasion In Vivo. *Dev Cell* 43: 549-562 e546. #10.1016/j.devcel.2017.11.003

Ryder M, Ghossein RA, Ricarte-Filho JC, Knauf JA & Fagin JA. 2008. Increased density of tumor-associated macrophages is associated with decreased survival in advanced thyroid cancer. *Endocr Relat Cancer* 15: 1069-1074. #10.1677/ERC-08-0036

Sarwar R, Pierce N & Koppe S. 2018. Obesity and nonalcoholic fatty liver disease: current perspectives. *Diabetes Metab Syndr Obes* 11: 533-542. #10.2147/DMSO.S146339

Sayin VI, Ibrahim MX, Larsson E, Nilsson JA, Lindahl P & Bergo MO. 2014. Antioxidants accelerate lung cancer progression in mice. *Sci Transl Med* 6: 221ra215. #10.1126/scitranslmed.3007653

Scapini P, Lapinet-Vera JA, Gasperini S, Calzetti F, Bazzoni F & Cassatella MA. 2000. The neutrophil as a cellular source of chemokines. *Immunol Rev* 177: 195-203. #10.1034/j.1600-065x.2000.17706.x

Schiaffino MV. 2010. Signaling pathways in melanosome biogenesis and pathology. *Int J Biochem Cell Biol* 42: 1094-1104. #10.1016/j.biocel.2010.03.023

Schmid-Schonbein GW. 2006. Analysis of inflammation. *Annu Rev Biomed Eng* 8: 93-131. #10.1146/annurev.bioeng.8.061505.095708

Schmidt R, Strahle U & Scholpp S. 2013. Neurogenesis in zebrafish - from embryo to adult. *Neural Dev* 8: 3. #10.1186/1749-8104-8-3

Schuster S, Cabrera D, Arrese M & Feldstein AE. 2018. Triggering and resolution of inflammation in NASH. *Nat Rev Gastroenterol Hepatol* 15: 349-364. #10.1038/s41575-018-0009-6

Schwabe RF, Tabas I & Pajvani UB. 2020. Mechanisms of Fibrosis Development in Nonalcoholic Steatohepatitis. *Gastroenterology* 158: 1913-1928. #10.1053/j.gastro.2019.11.311

Scott G. 2014. Selective proliferation of normal human melanocytes in vitro in the presence of phorbol ester and cholera toxin by Eisinger and Marko. *Exp Dermatol* 23: 18-19. #10.1111/exd.12226

Seiji M & Fitzpatrick TB. 1961. The reciprocal relationship between melanization and tyrosinase activity in melanosomes (melanin granules). *J Biochem* 49: 700-706. #10.1093/oxfordjournals.jbchem.a127360

Sekine M, Okamoto K & Ichida K. 2021. Association of Mutations Identified in Xanthinuria with the Function and Inhibition Mechanism of Xanthine Oxidoreductase. *Biomedicines* 9#10.3390/biomedicines9111723

Sen S, Sen S, Kumari MG, Khan S & Singh S. 2021. Oral Malignant Melanoma: A Case Report. *Prague Med Rep* 122: 222-227. #10.14712/23362936.2021.20

Senn JJ, Klover PJ, Nowak IA & Mooney RA. 2002. Interleukin-6 induces cellular insulin resistance in hepatocytes. *Diabetes* 51: 3391-3399. #10.2337/diabetes.51.12.3391

Shain AH & Bastian BC. 2016. From melanocytes to melanomas. *Nat Rev Cancer* 16: 345-358. #10.1038/nrc.2016.37

Sheppard D. 1994. Dominant negative mutants: tools for the study of protein function in vitro and in vivo. *Am J Respir Cell Mol Biol* 11: 1-6. #10.1165/ajrcmb.11.1.8018332

Shors AR, Iwamoto S, Doody DR & Weiss NS. 2002. Relationship of uveal and cutaneous malignant melanoma in persons with multiple primary tumors. *Int J Cancer* 102: 266-268. #10.1002/ijc.10703

Siegel RL, Miller KD, Fuchs HE & Jemal A. 2021. Cancer Statistics, 2021. *CA Cancer J Clin* 71: 7-33. #10.3322/caac.21654

Siegel RL, Miller KD & Jemal A. 2020. Cancer statistics, 2020. *CA Cancer J Clin* 70: 7-30. #10.3322/caac.21590

Sies H. 2017. Hydrogen peroxide as a central redox signaling molecule in physiological oxidative stress: Oxidative eustress. *Redox Biol* 11: 613-619. #10.1016/j.redox.2016.12.035

Silva MT. 2010. When two is better than one: macrophages and neutrophils work in concert in innate immunity as complementary and cooperative partners of a myeloid phagocyte system. *J Leukoc Biol* 87: 93-106. #10.1189/jlb.0809549

Skoyum R, Eide K, Berg K & Rofstad EK. 1997. Energy metabolism in human melanoma cells under hypoxic and acidic conditions in vitro. *Br J Cancer* 76: 421-428. #10.1038/bjc.1997.405

Slominski A, Tobin DJ, Shibahara S & Wortsman J. 2004. Melanin pigmentation in mammalian skin and its hormonal regulation. *Physiol Rev* 84: 1155-1228. #10.1152/physrev.00044.2003

Smith HG, Bagwan I, Board RE, Capper S, Coupland SE, Glen J, Lalondrelle S, Mayberry A, Muneer A, Nugent K, Pathiraja P, Payne M, Peach H, Smith J, Westwell S, Wilson E, Rodwell S, Gore M, Turnbull N & Smith MJF. 2020. Ano-uro-genital mucosal melanoma UK national guidelines. *Eur J Cancer* 135: 22-30. #10.1016/j.ejca.2020.04.030

Sommer L. 2011. Generation of melanocytes from neural crest cells. *Pigment Cell Melanoma Res* 24: 411-421. #10.1111/j.1755-148X.2011.00834.x

Sonthalia S, Daulatabad D & Sarkar R. 2016. Glutathione as a skin whitening agent: Facts, myths, evidence and controversies. *Indian J Dermatol Venereol Leprol* 82: 262-272. #10.4103/0378-6323.179088

Stienstra R, Saudale F, Duval C, Keshtkar S, Groener JE, van Rooijen N, Staels B, Kersten S & Muller M. 2010. Kupffer cells promote hepatic steatosis via interleukin-1beta-dependent suppression of peroxisome proliferator-activated receptor alpha activity. *Hepatology* 51: 511-522. #10.1002/hep.23337

Sulaimon SS & Kitchell BE. 2003. The biology of melanocytes. *Vet Dermatol* 14: 57-65. #10.1046/j.1365-3164.2003.00327.x

Sun G, Cao Y, Qian C, Wan Z, Zhu J, Guo J & Shi L. 2020. Romo1 is involved in the immune response of glioblastoma by regulating the function of macrophages. *Aging (Albany NY)* 12: 1114-1127. #10.18632/aging.102648

Sundin J, Morgan R, Finnoen MH, Dey A, Sarkar K & Jutfelt F. 2019. On the Observation of Wild Zebrafish (Danio rerio) in India. *Zebrafish* 16: 546-553. #10.1089/zeb.2019.1778

Takahashi Y & Fukusato T. 2014. Histopathology of nonalcoholic fatty liver disease/nonalcoholic steatohepatitis. *World J Gastroenterol* 20: 15539-15548. #10.3748/wjg.v20.i42.15539

Teng Y, Xie X, Walker S, White DT, Mumm JS & Cowell JK. 2013. Evaluating human cancer cell metastasis in zebrafish. *BMC Cancer* 13: 453. #10.1186/1471-2407-13-453

Toledo-Ibelles P, Gutierrez-Vidal R, Calixto-Tlacomulco S, Delgado-Coello B & Mas-Oliva J. 2021. Hepatic Accumulation of Hypoxanthine: A Link Between Hyperuricemia and Nonalcoholic Fatty Liver Disease. *Arch Med Res* 52: 692-702. #10.1016/j.arcmed.2021.04.005

Traver D, Herbomel P, Patton EE, Murphey RD, Yoder JA, Litman GW, Catic A, Amemiya CT, Zon LI & Trede NS. 2003. The zebrafish as a model organism to study development of the immune system. *Adv Immunol* 81: 253-330.

Trede NS, Langenau DM, Traver D, Look AT & Zon LI. 2004. The use of zebrafish to understand immunity. *Immunity* 20: 367-379. #10.1016/s1074-7613(04)00084-6

Trefts E, Gannon M & Wasserman DH. 2017. The liver. *Curr Biol* 27: R1147-R1151. #10.1016/j.cub.2017.09.019

Tsuchida T & Friedman SL. 2017. Mechanisms of hepatic stellate cell activation. *Nat Rev Gastroenterol Hepatol* 14: 397-411. #10.1038/nrgastro.2017.38

Tvinnereim AR, Hamilton SE & Harty JT. 2004. Neutrophil involvement in cross-priming CD8+ T cell responses to bacterial antigens. *J Immunol* 173: 1994-2002. #10.4049/jimmunol.173.3.1994

van Rooijen E, Fazio M & Zon LI. 2017. From fish bowl to bedside: The power of zebrafish to unravel melanoma pathogenesis and discover new therapeutics. *Pigment Cell Melanoma Res* 30: 402-412. #10.1111/pcmr.12592

Varshney GK, Sood R & Burgess SM. 2015. Understanding and Editing the Zebrafish Genome. *Adv Genet* 92: 1-52. #10.1016/bs.adgen.2015.09.002

Vatner DF, Majumdar SK, Kumashiro N, Petersen MC, Rahimi Y, Gattu AK, Bears M, Camporez JP, Cline GW, Jurczak MJ, Samuel VT & Shulman GI. 2015. Insulin-independent regulation of hepatic triglyceride synthesis by fatty acids. *Proc Natl Acad Sci U S A* 112: 1143-1148. #10.1073/pnas.1423952112

Vernon G, Baranova A & Younossi ZM. 2011. Systematic review: the epidemiology and natural history of non-alcoholic fatty liver disease and non-alcoholic steatohepatitis in adults. *Aliment Pharmacol Ther* 34: 274-285. #10.1111/j.1365-2036.2011.04724.x

Waight JD, Hu Q, Miller A, Liu S & Abrams SI. 2011. Tumor-derived G-CSF facilitates neoplastic growth through a granulocytic myeloid-derived suppressor cell-dependent mechanism. *PLoS One* 6: e27690. #10.1371/journal.pone.0027690

Walton EM, Cronan MR, Beerman RW & Tobin DM. 2015. The Macrophage-Specific Promoter mfap4 Allows Live, Long-Term Analysis of Macrophage Behavior during Mycobacterial Infection in Zebrafish. *PLoS One* 10: e0138949. #10.1371/journal.pone.0138949

Wang J, Zhu W, Huang S, Xu L, Miao M, Wu C, Yu C, Li Y & Xu C. 2017. Serum apoB levels independently predict the development of non-alcoholic fatty liver disease: A 7-year prospective study. *Liver Int* 37: 1202-1208. #10.1111/liv.13363

Wang K, Tan W, Liu X, Deng L, Huang L, Wang X & Gao X. 2021. New insight and potential therapy for NAFLD: CYP2E1 and flavonoids. *Biomed Pharmacother* 137: 111326. #10.1016/j.biopha.2021.111326

Weiss JM, Hunter MV, Cruz NM, Baggiolini A, Tagore M, Ma Y, Misale S, Marasco M, Simon-Vermot T, Campbell NR, Newell F, Wilmott JS, Johansson PA, Thompson JF, Long GV, Pearson JV, Mann GJ, Scolyer RA, Waddell N, Montal ED, Huang TH, Jonsson P, Donoghue MTA, Harris CC, Taylor BS, Xu T, Chaligne R, Shliaha PV, Hendrickson R, Jungbluth AA, Lezcano C, Koche R, Studer L, Ariyan CE, Solit DB, Wolchok JD, Merghoub T, Rosen N, Hayward NK & White RM. 2022. Anatomic position determines oncogenic specificity in melanoma. *Nature* 604: 354-361. #10.1038/s41586-022-04584-6

Westerfield M & Streisinger G. 1994. *The zebrafish book : a guide for the laboratory use of zebrafish (Brachydanio rerio)*. Eugene: Oregon University Press.

White RM, Cech J, Ratanasirintrawoot S, Lin CY, Rahl PB, Burke CJ, Langdon E, Tomlinson ML, Mosher J, Kaufman C, Chen F, Long HK, Kramer M, Datta S, Neuberg D, Granter S, Young RA, Morrison S, Wheeler GN & Zon LI. 2011. DHODH modulates transcriptional elongation in the neural crest and melanoma. *Nature* 471: 518-522. #10.1038/nature09882

White RM, Sessa A, Burke C, Bowman T, LeBlanc J, Ceol C, Bourque C, Dovey M, Goessling W, Burns CE & Zon LI. 2008. Transparent adult zebrafish as a tool for in vivo transplantation analysis. *Cell Stem Cell* 2: 183-189. #10.1016/j.stem.2007.11.002

Wittgen HG & van Kempen LC. 2007. Reactive oxygen species in melanoma and its therapeutic implications. *Melanoma Res* 17: 400-409. #10.1097/CMR.0b013e3282f1d312

Wright RM, Vaitaitis GM, Wilson CM, Repine TB, Terada LS & Repine JE. 1993. cDNA cloning, characterization, and tissue-specific expression of human xanthine dehydrogenase/xanthine oxidase. *Proc Natl Acad Sci U S A* 90: 10690-10694. #10.1073/pnas.90.22.10690

Wu L, Gao X, Guo Q, Li J, Yao J, Yan K, Xu Y, Jiang X, Ye D & Guo J. 2020. The role of neutrophils in innate immunity-driven nonalcoholic steatohepatitis: lessons learned and future promise. *Hepatol Int* 14: 652-666. #10.1007/s12072-020-10081-7

Xue D, Zhou X & Qiu J. 2020. Emerging role of NRF2 in ROS-mediated tumor chemoresistance. *Biomed Pharmacother* 131: 110676. #10.1016/j.biopha.2020.110676

Yajima I, Kumasaka MY, Thang ND, Goto Y, Takeda K, Iida M, Ohgami N, Tamura H, Yamanoshita O, Kawamoto Y, Furukawa K & Kato M. 2011. Molecular Network Associated with MITF in Skin Melanoma Development and Progression. *J Skin Cancer* 2011: 730170. #10.1155/2011/730170

Yan C, Brunson DC, Tang Q, Do D, Iftimia NA, Moore JC, Hayes MN, Welker AM, Garcia EG, Dubash TD, Hong X, Drapkin BJ, Myers DT, Phat S, Volorio A, Marvin DL, Ligorio M, Dershowitz L, McCarthy KM, Karabacak MN, Fletcher JA, Sgroi DC, Iafrate JA, Maheswaran S, Dyson NJ, Haber DA, Rawls JF & Langenau DM. 2019. Visualizing

Engrafted Human Cancer and Therapy Responses in Immunodeficient Zebrafish. *Cell* 177: 1903-1914 e1914. #10.1016/j.cell.2019.04.004

Yasueda A, Urushima H & Ito T. 2016. Efficacy and Interaction of Antioxidant Supplements as Adjuvant Therapy in Cancer Treatment: A Systematic Review. *Integr Cancer Ther* 15: 17-39. #10.1177/1534735415610427

Yazdanyar A & Jiang XC. 2012. Liver phospholipid transfer protein (PLTP) expression with a PLTP-null background promotes very low-density lipoprotein production in mice. *Hepatology* 56: 576-584. #10.1002/hep.25648

Yilmaz Y. 2012. Review article: is non-alcoholic fatty liver disease a spectrum, or are steatosis and non-alcoholic steatohepatitis distinct conditions? *Aliment Pharmacol Ther* 36: 815-823. #10.1111/apt.12046

Younossi ZM, Koenig AB, Abdelatif D, Fazel Y, Henry L & Wymer M. 2016. Global epidemiology of nonalcoholic fatty liver disease-Meta-analytic assessment of prevalence, incidence, and outcomes. *Hepatology* 64: 73-84. #10.1002/hep.28431

Zaidi MR, Day CP & Merlino G. 2008. From UVs to metastases: modeling melanoma initiation and progression in the mouse. *J Invest Dermatol* 128: 2381-2391. #10.1038/jid.2008.177

Zelber-Sagi S, Nitzan-Kaluski D, Halpern Z & Oren R. 2007. NAFLD and hyperinsulinemia are major determinants of serum ferritin levels. *J Hepatol* 46: 700-707. #10.1016/j.jhep.2006.09.018

Zhu H, Jia Z, Trush MA & Li YR. 2016. A Highly Sensitive Chemiluminometric Assay for Real-Time Detection of Biological Hydrogen Peroxide Formation. *React Oxyg Species (Apex)* 1: 216-227. #10.20455/ros.2016.841

Zhu XD, Zhang JB, Zhuang PY, Zhu HG, Zhang W, Xiong YQ, Wu WZ, Wang L, Tang ZY & Sun HC. 2008. High expression of macrophage colony-stimulating factor in peritumoral liver tissue is associated with poor survival after curative resection of hepatocellular carcinoma. *J Clin Oncol* 26: 2707-2716. #10.1200/JCO.2007.15.6521

Zito PM & Scharf R. 2022. Melanoma Of The Head And Neck In *StatPearls*. Treasure Island (FL)

RESUMEN EN CASTELLANO

Durante el desarrollo de esta tesis doctoral se ha abordado el estudio de la relevancia de Duox1 y Xdh, dos enzimas implicadas en el estrés oxidativo, en la progresión del melanoma y la esteatohepatitis.

El melanoma es el quinto tipo de cáncer más común y el cáncer de piel más peligroso. La incidencia del melanoma maligno ha ido en aumento y aunque es más común en adultos a partir de los 65 años también afecta a la población más joven (Siegel et al. 2021). La causa del melanoma es la transformación maligna de los melanocitos, un tipo celular de la piel que produce melanina como protección contra los rayos ultravioleta. La exposición solar está considerada junto a la susceptibilidad genética uno de los principales factores de riesgo para desarrollar melanoma (Elwood & Jopson 1997, Gandini et al. 2005, Rastrelli et al. 2014).

El melanoma comienza como una proliferación de melanocitos normales para formar un nevus, en este nivel los melanocitos aún están confinados a la epidermis. Posteriormente, el nevus puede adquirir un crecimiento atípico y se desarrolla un nevus displásico. Luego, comienza un crecimiento radial ilimitado, seguido de una fase de crecimiento vertical, atraviesa la membrana basal formando un tumor y, finalmente, se disemina con éxito por todo el cuerpo como tumores metastásicos (Clark et al. 1991).

Recientemente, se ha estudiado el estrés oxidativo como un factor clave involucrado en el desarrollo de varias enfermedades crónicas, en la transformación y progresión de muchos tipos de cáncer, incluido el melanoma. En particular, se ha demostrado una compleja relación entre el estrés oxidativo y las respuestas inflamatorias e inmunitarias (Cannavo et al. 2019). La respuesta inflamatoria induce el reclutamiento de células inmunitarias innatas y adaptativas al tumor que, a su vez, pueden inducir estrés oxidativo que está involucrado en muchos pasos del desarrollo del melanoma, como daño en el ADN y mutación de genes asociados con el melanoma, metabolismo celular, respuesta a hipoxia, inmunidad tumoral y metástasis (Wittgen & van Kempen 2007). El papel que las ROS juegan en el desarrollo temprano, la progresión o la supresión en muchos tipos de cáncer ha sido ampliamente estudiado. En este trabajo, nos hemos centrado en el papel de DUOX1, una importante NADPH oxidasa expresada en piel (Candel et al. 2014).

Además, por otro lado, se ha estudiado la contribución de la inflamación y el estrés oxidativo durante la progresión de la enfermedad de hígado graso, donde ambas son características clave. La enfermedad del hígado graso no alcohólico (NAFLD) es la manifestación hepática del síndrome metabólico, que va desde la esteatosis simple (NAFL) hasta la esteatohepatitis (NASH) y puede progresar a fibrosis y carcinoma hepatocelular (HCC). Las dietas de tipo occidental (es decir, ricas en grasas, colesterol y azúcar) desencadenan el desarrollo de NAFLD y las comorbilidades asociadas, como la obesidad, la diabetes tipo 2 y el cáncer.

Day y James (Day & James 1998) desarrollaron una teoría de "dos golpes" para proporcionar una base teórica para la progresión de NAFLD a NASH. El “primer golpe” se manifiesta por esteatosis hepática simple. La ingesta de ácidos grasos libres aumenta la biosíntesis de triglicéridos, y esto conduce a la acumulación de grasa en los hepatocitos y al consiguiente aumento de la resistencia a la insulina. Además, la eficiencia de exportación de ácidos grasos libres, TG y colesterol se reduce drásticamentte.

El estrés oxidativo es el iniciador del "segundo golpe" (Ma et al. 2019). La eliminación del exceso de ROS es esencial para aliviar la acumulación de lípidos en los hepatocitos dañados. Además, el estrés oxidativo media la apoptosis de los hepatocitos y la muerte celular (Ma et al. 2021). El exceso de ácidos grasos en las células hepáticas, su agotamiento energético y la consecuente disfunción mitocondrial conducen a un aumento de los niveles de estrés oxidativo y, finalmente, al daño celular (Couillard et al. 2005) que favorece el progreso de NAFLD de esteatosis a esteatohepatitis (NASH), fibrosis y cirrosis o HCC.

La progresión de NAFLD parece implicar la aparición de varias lesiones simultáneas, como disfunción mitocondrial inducida por estrés oxidativo, liberación de citocinas inflamatorias, estrés del retículo endoplásmico y aumento de hierro, entre muchas otras. Estos factores son responsables de la activación de una serie de cascadas de señalización que conducen a la inflamación, la muerte celular y la fibrosis características importantes del desarrollo de NASH (Yilmaz 2012). Para clasificar a los pacientes con NAFLD/NASH, se identificaron como componentes necesarios: esteatosis, inflamación lobular y “ballooning” hepatocelular. La fibrosis

no es una característica necesaria para el diagnóstico de NASH, aunque si suele estar presente (Takahashi & Fukusato 2014).

Una de las principales enzimas implicadas en el estrés oxidativo en el hígado es la xantina deshidrogenasa (Xdh). Esta está mayoritariamente expresada por los hepatocitos y participa en la vía hipoxantina-ácido úrico produciendo H_2O_2.

Los **objetivos** específicos que se plantean en esta tesis doctoral son:

1. Estudiar el papel de DUOX1 en la progresión temprana, agresividad y capacidad de hacer metástasis del melanoma cutáneo.
2. Identificar inhibidores específicos contra DUOX1.
3. Generar un mutante deficiente para la enzima Xdh en pez cebra para estudiar el papel de esta proteína en la esteatohepatitis no alcohólica.
4. Caracterizar el papel de Xdh en esta enfermedad hepática.

Para estudiar el papel de DUOX1 en el diagnóstico de melanoma se utilizaron datos de expresión génica y supervivencia de pacientes disponibles en la base de datos TCGA (The Cancer Genome Atlas). Este análisis mostró que la alta expresión de *DUOX1*, pero no la baja expresión, en estadíos tempranos de melanoma se correlacionaba con una menor supervivencia de los pacientes. Mientras que no se observaron diferencias estadísticamente significativas en estadíos tardíos. La expresión de *DUOX1* en muestras de melanoma metastásico fue menor que en melanoma primario. Además, se encontraron alteradas rutas relacionadas con el sistema inmune, activación del complemento y rechazo de alotransplante en los melanomas que expresan bajos niveles de *DUOX1*. Esto sugiere la importancia del equilibrio del estrés oxidativo en la progresión del melanoma y la importancia de la desregulación de los ROS derivados de DUOX1 en el pronóstico del paciente con melanoma. Las ROS tienen un papel dual en cáncer, pueden promover el daño en el ADN y la activación de oncogenes o inactivación de antioncogenes que facilitan la progresión tumoral (Galadari et al. 2017). Además, las ROS pueden atraer células inmunes y promover así un microambiente tumoral inflamatorio que ayude a la proliferación tumoral (Pollard 2004, Rajput & Wilber 2010). Pero, por otro lado, las células de melanoma en la sangre experimentan un aumento del estrés oxidativo que limita las metástasis de las células de melanoma *in vivo* (Piskounova et al. 2015).

Estos resultados son consistentes con la baja supervivencia de pacientes con melanoma con alta expresión de DUOX1 en melanomas en estadíos tempranos y con la regulación a la baja de DUOX1 en melanomas metastásicos. Además, sugieren que DUOX1 juega un papel dual en el melanoma, como se confirmó con nuestro modelo de pez cebra con inhibición de Duox1 en células de melanoma. Aunque no encontramos ningún efecto significativo de esta enzima en la transformación de los melanocitos y la progresión temprana del melanoma, los experimentos de alotrasplante en peces cebra previamente irradiados, es decir, inmunocomprometidos, revelaron que las células de melanoma deficientes en Duox1 muestran una disminución del crecimiento, pero paradójicamente, tuvieron una mayor incidencia de metástasis que el control. Por lo tanto, las ROS derivadas de Duox1 pueden facilitar el crecimiento del melanoma primario, pero limitar la metástasis a distancia, como se ha demostrado con líneas celulares de melanoma humano xenotrasplantadas en ratones inmunocomprometidos (Piskounova et al. 2015).

Para buscar fármacos que inhibieran DUOX1 de forma específica desarrollamos una línea celular de melanoma que sobreexpresa tanto DUOX1 como su activador DUOXA1, mediante un método basado en la peroxidasa y luminol se probaron 256 compuestos encontrando 17 potenciales inhibidores y 3 activadores que deberán ser testados más específicamente.

Por otro lado, generamos un pez cebra deficiente en Xdh que se desarrolla normalmente y muestra una relación mendeliana clásica. El impacto de la mutación Xdh en NAFLD se estudió utilizando un modelo NASH de pez cebra inducido por dieta alta en colesterol y la progresión de NAFLD se evaluó mediante análisis histológico, tinción de Oil Red O (ORO) de larvas completas, medidas de estrés oxidativo hepático, y análisis proteómico.

Descubrimos que la mutación Xdh redujo notablemente las características histológicas de NASH, la acumulación de lípidos y el estrés oxidativo en las larvas con NASH. El análisis proteómico de hígados de larvas alimentadas con dieta alta en grasas muestra una regulación negativa de las vías metabólicas de los lípidos (p. ej., biosíntesis de colesterol y lípidos (Hmgcs, Mvk, Fdps, Fdft1, Cyp51, Hsd17b7 and Dhcr7), y otras vías de metabolismo de lípidos como la oxidación de ácidos grasos,

metabolismo del retinol y degradación de valina, leucina e isoleucina (BCAA). Además, se observó una regulación positiva de varias proteínas previamente asociadas con NAFLD/NASH humano (Igfsp1, Apoeb, Pltp, Fn1a and Fn1b, Ferritin, Aifm2 y Soat2). Curiosamente, la mutación Xdh pudo rescatar las larvas de NASH y promover la regulación negativa de las vías metabólicas de los lípidos (por ejemplo, la degradación de los ácidos grasos, el metabolismo del retinol, el metabolismo de los glicerolípidos), así como la regulación positiva de la fosforilación oxidativa, Además, se encontraron reguladas positivamente la ruta de activación de Hsf1 (Heat Shock transcription Factor 1), que estimula la oxidación mitocondrial y ha sido previamente asociada tanto a una mejora de NASH al en modelos de obesidad en ratones (Rao et al. 2022), como a una mejora en biomarcadores de NAFLD en humanos (Kondo et al. 2021). Otra vía interesante regulada al alza en larvas deficientes en Xdh alimentadas con dieta alta en colesterol es la sulfonación, una vía muy involucrada en la desintoxicación del hígado. En trabajos previos en modelos de NAFLD en ratones se demostró que la sobreexpresión de la sulfotransferasa SULT2B1b disminuye la lipogénesis (Bai et al. 2012) e inhibe la gluconeogénesis mejorando la enfermedad metabólica hepática (Bi et al. 2018).

En general, estos resultados respaldan que Xdh está involucrado en la progresión de la enfermedad NAFLD, lo que explica la asociación encontrada entre XDH y NAFLD en varios estudios clínicos, y señala la relevancia del modelo de larva de pez cebra alimentado con HCD para identificar nuevas vías de señalización asociadas con NAFLD/NASH en humanos.

Los resultados obtenidos en este trabajo condujeron a las siguientes **conclusiones**:

1. La alta expresión de DUOX1, pero no la baja expresión, en estadíos tempranos de melanoma se correlacionaba con una menor supervivencia de los pacientes. Mientras que no se observaron diferencias estadísticamente significativas en estadíos tardíos.
2. Aunque la inhibición de Duox1 en los melanocitos no afecta la transformación de estos melanocitos ni a la progresión temprana del melanoma en el pez cebra, la inhibición de Duox1 reduce el crecimiento de

los melanomas trasplantados al tiempo que aumenta su potencial metastásico.

3. Mediante un cribado farmacológico se identificaron 17 posibles inhibidores y 3 activadores de la enzima DUOX1 humana.
4. El pez cebra con deficiencia de Xdh es fértil, viable y muestra una relación mendeliana normal. La línea de pez cebra deficiente en Xdh es un excelente modelo animal para estudiar el papel de XDH en enfermedades humanas, incluida la xantinuria.
5. La deficiencia de Xdh mejora la patología hepática en un modelo de pez cebra de NASH inducido por dieta alta en colesterol. Esto incluye una disminución en la acumulación de lípidos en el hígado, la lesión hepatocelular y el estrés oxidativo.
6. Los cambios proteómicos inducidos por dieta alta en colesterol en el hígado de las larvas de pez cebra se asemejan a los que promueven las dietas occidentales en humanos.
7. La deficiencia de Xdh da como resultado la regulación a la baja de las vías metabólicas de los lípidos, incluida la degradación de los ácidos grasos, el metabolismo del retinol y el metabolismo de los glicerolípidos, en el hígado de las larvas de pez cebra alimentadas con dieta alta en colesterol. Además, promueve la regulación positiva de la fosforilación oxidativa, la activación y la sulfonación de Hsf1, que están involucrados en la desintoxicación del hígado y la mejora de NASH.

ANNEXE I: PUBLICATION CONTRIBUTION DURING THE PhD

Publications derived from the thesis

Pardo-Sanchez I, Garcia-Moreno D & Mulero V. 2022. Zebrafish Models to Study the Crosstalk between Inflammation and NADPH Oxidase-Derived Oxidative Stress in Melanoma. Antioxidants (Basel) 11(7):1277
DOI: 10.3390/antiox11071277
IF: 7.675

Pardo-Sanchez I, Sofia Ibañez-Molero, Garcia-Moreno D & Mulero V. 2023. Dual role of DUOX1-derived reactive oxygen species in melanoma. Under review.

Other publications non-related to the thesis

Martinez-Navarro FJ, Martinez-Morcillo FJ, Lopez-Munoz A, **Pardo-Sanchez I**, Martinez-Menchon T, Corbalan-Velez R, Cayuela ML, Perez-Oliva AB, Garcia-Moreno D & Mulero V. 2020. The vitamin B6-regulated enzymes PYGL and G6PD fuel NADPH oxidases to promote skin inflammation. Dev Comp Immunol 108: 103666.
DOI: 10.1016/j.dci.2020.103666
IF: 3.636

Tyrkalska SD, Perez-Oliva AB, Rodriguez-Ruiz L, Martinez-Morcillo FJ, Alcaraz-Perez F, Martinez-Navarro FJ, Lachaud C, Ahmed N, Schroeder T, **Pardo-Sanchez I**, Candel S, Lopez-Munoz A, Choudhuri A, Rossmann MP, Zon LI, Cayuela ML, Garcia-Moreno D & Mulero V. 2019. Inflammasome Regulates Hematopoiesis through Cleavage of the Master Erythroid Transcription Factor GATA1. Immunity 51: 50-63 e55.
DOI: 10.1016/j.immuni.2019.05.005
IF: 22.553

Maria Carmen Rodenas, Julia Peñas-Martínez, **Irene Pardo-Sánchez**, David Zaragoza-Huesca, Carmen Ortega-Sabater, Jorge Peña-García, Salvador Espín, Guillermo Ricote, Sofía Montenegro, Francisco Ayala de la Peña, Ginés Luengo-Gil, Andrés Nieto, Francisco García-Molina, Vicente Vicente, Francesco Bernardi, Maria Luisa Lozano, Victoriano Mulero, Horacio Pérez-Sánchez, Alberto Carmona-

Bayonas, Irene Martínez-Martínez. 2023. Pro-tumor and prothrombotic activities of hepsin in colorectal cancer cells and suppression by venetoclax. Biorxiv
DOI: 10.1101/2022.10.01.510038

ANNEXE II: CONTRIBUTION TO SCIENTIFIC CONFERENCES DURING THE PhD

Contribution to scientific conferences during PhD

Irene Pardo Sánchez, Victoriano Mulero Méndez, Isabel Cabas Sánchez, Alfonsa García Ayala. Role of the estrogen receptor gper1 in the immune system. III Jornadas Científicas del IMIB-Arrixaca. Murcia (Spain). 2018. Poster.

Ana Belen Perez Oliva, Lola Rodríguez Ruiz, Sylwia Tyrkalska, Francisco Juan Martínez Navarro, Francisco Javier Martínez Morcillo, **Irene Pardo Sánchez**, Francisca Alcaraz Perez, Maria Luisa Cayuela Fuentes, Diana García Moreno, Victoriano Mulero Méndez. III Jornadas Científicas del IMIB-Arrixaca. Murcia (Spain). 2018. Oral Communication.

A.B. Pérez-Oliva, S.D. Tyrkalska, F.J. Martínez-Navarro, F.J. Martínez-Morcillo, L. Rodríguez-Ruiz, **I. Pardo-Sánchez**, F. Alcaraz-Pérez, S. Candel, A. Lopez-Muñoz, A. Choudhuri, M.P. Rossmann, L.I. Zon, D. García-Moreno, M.L. Cayuela, V. Mulero. Pharmacological inhibition of the inflammasome for anemia of chronic disease treatment. Zebrafish Disease Model 11. Leiden (Netherland). 2018. Poster.

I. Pardo-Sánchez, D. García-Moreno, V. Mulero. Impact of Oxidative Stress in Melanoma. V Jornadas Doctorales EIDUM. Murcia (Spain). 2019. Oral Communication.

I. Pardo-Sánchez, A.B. Pérez-Oliva, D. García-Moreno, M.L. Cayuela, V. Mulero. Modeling the role of DUOX1 and XDH in melanoma aggressiveness and its crosstalk with the immune microenvironment. IV Jornadas Científicas del IMIB-Arrixaca Murcia (Spain). 2019. Communication online.

I. Pardo-Sánchez, I. Cabas-Sánchez, M.L. Cayuela, A.B. Pérez-Oliva, D. García-Moreno, V. Mulero. DUOX1-derived reactive oxygen species in melanoma: friend or foe? V Jornadas Científicas del IMIB-Arrixaca Murcia (Spain). 2020. Poster.

Azucena López Muñoz, **Irene Pardo Sánchez**, Maria Teresa Martínez Menchon, Antonio Raúl Corbalán Vélez, Maria Luisa Cayuela Fuentes, Ana Belén Pérez Oliva, Diana García Moreno, Victoriano Mulero Méndez. The role of vitamin B6-dependent enzymes pygl and g6pd in skin inflammation. V Jornadas Científicas del IMIB-Arrixaca Murcia (Spain). 2020. Poster

I. Pardo-Sánchez, D. García-Moreno, V. Mulero. DUOX1-derived reactive oxygen species in melanoma: friend or foe? Defence is The Best Attack - ImmunoOncology Breackthroughs EACR. (online). 2021. Oral Communication.

I. Pardo-Sánchez, D. García-Moreno, V. Mulero. DUOX1-derived reactive oxygen species in melanoma: friend or foe? Biotechnology Anual Congress 2021 (online). 2021. Poster.

I. Pardo-Sánchez, D. García-Moreno, V. Mulero. Xanthine dehydrogenase contributes to diet-induced Non-Alcoholic Steatohepatitis. VII Jornadas Científicas del IMIB-Arrixaca Murcia (Spain). 2022. Oral Communication.

I. Pardo-Sánchez, D. García-Moreno, V. Mulero. Xanthine dehydrogenase contributes to diet-induced Non-Alcoholic Steatohepatitis. 44 Congreso Nacional de la Sociedad Española de Bioquímica y Biología Molecular (SEBBM), Málaga (Spain). 2022. Oral Communication.

ANNEXE III: RESEARCH STAY IN OTHER LABORATORIES DURING THE PhD

Short stay at international research center

Host institution: **Albert Einstein College of Medicine, Montefiore**
Department/Centre: **Department of Developmental & Molecular Biology, Department of Medicine (Hepatology)/ Albert Einstein Cancer College**
Country: **New York, USA.**

Responsible person in the Host: **Dra. Sofia de Oliveira**

Stay period: **1st September 2021 – 1st March 2022**